Author:
Lee, Yeseul

Title:
Functional study of Kainate receptors in the mossy fibre pathway in the hippocampus

Functional study of Kainate receptors in the mossy fibre pathway in the hippocampus

Yeseul Lee

A dissertation submitted to the University of Bristol in accordance with the requirements for award of the degree of Doctor of Philosophy in the faculty of Life Science

School of Physiology, Pharmacology and Neuroscience
March.2019

36,335 words

Abstract

Mossy fiber synapses have properties that are fundamentally different from CA1 synapses. Frequency dependent facilitation and expression of an NMDAR-independent form of LTP are examples of the unique physiology of MF synapses. Presynaptic KARs have been shown to trigger these striking features of MF synapses. However, which KAR subunits are mainly responsible for these features has been under intense debate. Previous pharmacological studies emphasised the role of GluK1 whereas genetic studies demonstrated a role for GluK2. Therefore, we investigated the role of GluK1 and GluK2 subunits on MF characteristics with a combination of genetic and pharmacological tools.

We observed that GluK1 antagonism did not block LFF, PTP and LTP in the MF in Wistar rats, regardless of DCG-IV sensitivity. Next, we generated global GluK1 KO animals and validated them using the GluK1 specific agonist ATPA. In KOs, the degree of HFF and MF-LTP were comparable to WT confirming that in these conditions GluK1 is not involved in triggering these forms of plasticity. However, ACET did reduce the amplitude of the 5th response during HFF in WT, but not in KO implying the GluK1 subunit does contribute to this phenomenon.

GluK2 antagonism of kynurenic acid-derivatives, UBP2002 and UBP2038, were tested on MF function in global GluK1 KO mice to preclude any confounding actions at GluK1. In the presence of UBP2002, we did not observe MF-LTP and the degree of PTP was comparable to WT. In addition, UBP2002 and UBP2038 significantly reduced the amplitude of the 5th response during HFF in a reversible manner and the degree of LFF after drug washing out was significantly increased. To clarify the role of presynaptic GluK1, DG-GluK1 KOs were generated, however, validation by ATPA was unsuccessful. Taken together, our results indicate that GluK1 plays a minor role whereas GluK2 contributes substantially to MF function.

Acknowledgements

Firstly, I would like to express my deepest thanks to my supervisors. Zuner, I appreciate all the support you have provided for me whenever, whatever and wherever. You were always there when I needed you. Graham, you guided me into the field of science. Your insightful advice always inspires and encourages me to be a better scientist. I shall try my best to follow your example.

I would also like to thank past and present members that I met in ZAB and GLC lab. I enjoyed being accompanied by everyone for serious discussion or casual beer time. Being surrounded by great colleagues has been such a fortune for me.

I would like to thank my husband Tom, as the partner of my life and for scientific discussions, I have gone through every stage with you. It would have not been possible without you. Also, I would like to thank my little boy Louhee, this thesis started and completed with you.

I dedicate this dissertation to my family for their endless love and support.

Author’s Declaration

I declare that the work in this dissertation was carried out in accordance with the requirements of the University's Regulations and Code of Practice for Research Degree Programmes and that it has not been submitted for any other academic award. Except where indicated by specific reference in the text, the work is the candidate's own work. Work done in collaboration with, or with the assistance of, others, is indicated as such. Any views expressed in the dissertation are those of the author.

SIGNED: ..... DATE: .....

Table of Contents

List of figures

Abbreviations

A/C – associational / commissural fibers

ABP – AMPA receptor binding protein

AC – adenylyl cyclase

aCSF – artificial cerebrospinal fluid

AMPARs – α-amino-3-hydroxy-5-methyl-4-isoxazolepropionic acid receptors

AP – action potential

ATD – amino terminal domain

CA – cornu ammonis

cAMP – cyclic adenosine monophosphate

CFC – contextual fear conditioning

CV – coefficient variance

DG – dentate gyrus

DKO – double knock out

EPSCs – excitatory postsynaptic currents

ER – endoplasmic reticulum

fEPSPs – field excitatory postsynaptic potentials

FRT – flippase recognition target

GABA – γ-aminobutyric acid

GAD – glutamate decarboxylase

GC – granule cell

GRIP – glutamate receptor interacting protein

HFF – high frequency facilitation

HFS – high frequency stimulation

IMF – infrapyramidal mossy fiber

I-W – *(S)*-5-Iodowilladiine

KA – kainic acid, kainate

KARs – kainate receptors

LBD – ligand binding domain

LFF – low frequency facilitation

LFS – low frequency stimulation

LTD – long term depression

LTP – long term potentiation

MF-LTP – mossy fiber LTP

mGluRs – metabotropic glutamate receptors

MWM – Morris water maze

Neto – neuropilin and tolloid-like

NMDARs – N-methyl-d-aspartate receptors

NSF – N-ethylmaleimide-sensitive fusion protein

PhTx – philanthotoxin

PICK1 – proteins with interacting with C kinase 1

PKA – protein kinase A

PKC – protein kinase C

POMC – pro-opiomelanocortin

PPF – paired pulse facilitation

PSD – postsynaptic density

PTP – post tetanic potentiation

PTx – pertussis toxin

sAHP – slow afterhyperpolarization current

SAP – synapse associated protein

SMF – suprapyramidal mossy fiber

STP – short term plasticity

TMD – transmembrane domain

VGCCs – voltage-gated calcium channels

Chapter 1. Introduction

1.1. The hippocampal formation

The hippocampal formation is a group of brain structures that lie deep in the medial temporal lobe of the brain. It consists of the dentate gyrus (DG), the hippocampus, the subiculum, the presubiculum, the parasubiculum and the entorhinal cortex. The structure of hippocampal formation was firstly described by Ramon y Cajal with the Golgi staining method (Ramón y Cajal et al 1909, 1911, 1995) and the basic structure is shared in all mammals (**Fig 1-1 a**, drawing taken from Andersen et al 2007). In the rat brain, the hippocampus is a three-dimensional c-shape. This elongated structure begins close to the septal nuclei and finishes near temporal lobe. The hippocampus consists of two major sectors, fascia dentate (*area dentate*, Dentate gyrus, DG) and the hippocampus proper (*Cornu ammonis,* CA) (Andersen et al 2007)

1.1.1. Anatomy of Hippocampus

Dentate Gyrus

Granule cells are the principal neurons of the DG. The DG has three layers; the cell body of the granule cell is located in the granule cell layer. To one side of them is the molecular layer where dendrites of the granule cell lies, and to the other side is the polymorphic layer in the hilus which contains granule cell axons and other types of neurons. While the DG of the human and monkey is more U-shaped, rat's DG is V-shaped (**Figure 1-1 a**). The hilus area in between the upper blade (suprapyramidal blade) and the lower blade (infrapyramidal blade) is highly heterogeneous (Amaral et al 2007). GABAergic interneurons and hilar mossy cells are located in this area in a disorganised manner without a densely packed somatic layer (Soriano & Frotscher 1994, Wenzel et al 1997). Interestingly, axon terminals of these hilar mossy cells back project to the molecular layer. In addition, they also give rise to associational/commissural fibers (A/C) and are thought to be important for inhibitory basket cell function in the CA3 area.

The fiber projection of the granule cell is called the mossy fiber (**Figure 1-1 b**). This unmyelinated axon is the major way to convey information from DG to CA3. The efferent projection of the GC terminates on the dendrites in the stratum lucidum of CA3. These connections are called mossy fiber synapses. The detailed anatomy and function of this synapse will be discussed later in the introduction (**section 1.3.**).

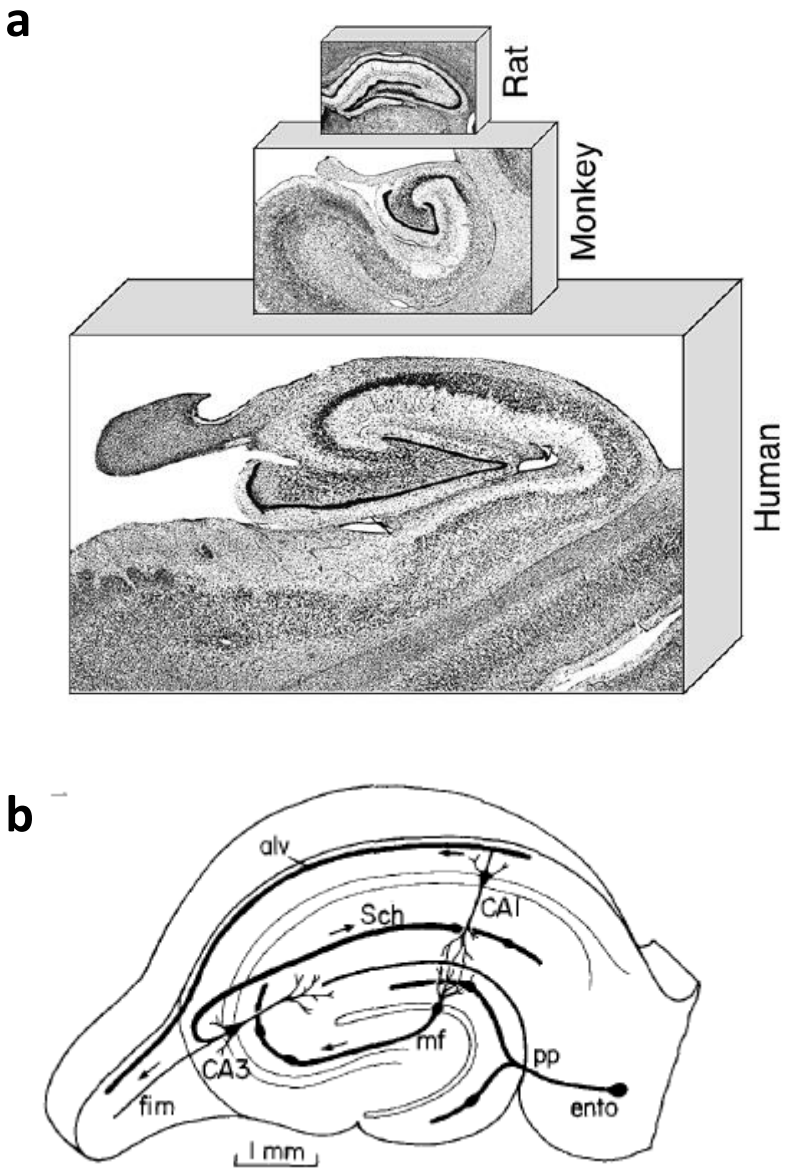

Figure 1-1. Anatomy of the hippocampal formation
a. Nissl-stained sections showing hippocampal formation in different species (taken from Andersen et al., 2007).
b. A drawing of hippocampal slice showing intrinsic connections of hippocampus (taken from Andersen et al., 1971).

Hippocampus proper: Ammon's horn, Cornu Ammonis (CA)

The arched appearance of the hippocampus resulted in it being named 'Ammon's horn (cornu ammonis)' which was the name of an Egyptian god. Although, hippocampus is acknowledged as the standard term now, subregions of the hippocampus are still referred to by the abbreviation of cornu ammonis (CA).

When histological sections of the hippocampus are taken, the shape of the CA region and the DG appear as two interlocking Cs. The pyramidal cell layer starts in the hilus region of the DG, and bend over the DG reaching the subiculum (**Figure 1-1 b**). The hippocampus proper can be divided into four subregions, CA1-CA4 according to cell morphology and fiber projection (Lorente De Nó 1934, Ramón y Cajal et al 1909, 1911, 1995). CA4 is closest to the DG. CA4 is a polymorphic region where cell bodies are not packed but still receive an input from the MF. It is categorized as an area where cells have pyramidal-like characteristics but do not receive inputs from interneurons such as basket cells. In CA3, generally cells are bigger, and they receive inputs from the DG (the MF) and from the entorhinal cortex (the perforant pathway). CA2 is often considered as a transition zone between CA1 and CA3. A recent study showed that somata of pyramidal neurons here are bigger than those in CA1 and CA3 (Mercer et al 2007) and possess uniquely patterned apical dendrite (Bartesaghi & Ravasi 1999). CA2 is designated as the area which does not receive MF input (Lorente De Nó 1934). The boundary between CA2 and CA1 can be distinguished by a neurochemical marker since pyramidal cells in CA2 express Purkinje cell protein 4 (PCP4) while cells in CA1 and CA3 region do not (Lein et al 2005, San Antonio et al 2014). CA1 is located farthest from the DG, closest to the subiculum. Pyramidal cells in CA1 are smaller than CA3 in size and more densely packed in rodents. In human and monkey, CA1 cells are not so densely packed and the pyramidal layer is broader. As the subiculum does not receive a CA3 projection, this feature is used as a criterion to distinguish it from CA1.

Hippocampus proper is tri-laminate. The somata of pyramidal cells are packed in the stratum pyramidal (pyramidal layer). The stratum oriens contains the basal dendrite of pyramidal cells. The area which contains the apical dendrites can be further divided into two layers. The stratum radiatum is where proximal apical dendrites are located, and the other layer is stratum moleculare-lacunosum where distal apical dendrites are located. As pyramidal cells in CA all have the same orientation, each layer contains certain parts of the pyramidal cell and receive separate input.

1.1.2. Intrinsic connections in the hippocampus

Inputs that come into the hippocampus are processed through the trisynaptic pathway, which consist of entorhinal cortex – DG – CA3 – CA1 (Andersen et al 1971). Layer II of the entorhinal cortex sends axons to the molecular layer of the DG through the perforant pathway (Amaral & Witter 1989, Lorente De Nó 1934). There are two functional branches of the perforant pathway. The major branch perforates hippocampal fissure and makes contacts with granule cells of DG and the minor branch provides contacts to CA3 and CA1 neurons. The first step of the trisynaptic pathway is this perforant pathway that excites granule cells in the DG. In turn, granule cells excite the proximal apical dendrite of CA3 pyramidal neurons in stratum lucidum which is the second step. Lastly, CA3 neurons connect to CA1 via the Schaffer collateral axon (third synapse). Following these structures, the trisynaptic circuit is completed and information goes back to layer V of the entorhinal cortex (**Figure 1-1 b**).

The striking feature of the hippocampus compared to other cortical areas emerges from this trisynaptic pathway. Synaptic inputs that go through the hippocampal formation are processed unidirectionally. The entorhinal cortex sends inputs to the DG but there is no axon that back projects from the DG to the entorhinal cortex. Similarly, the axons from the DG and CA3 unilaterally send axons to CA3 and CA1 respectively. In addition, neurons have similar orientations leading to no overlap between field. Neurons that are located in the same region receive the same input and summation of these inputs creates strong field potentials.

1.1.3. Function of hippocampus

Originally, it was assumed that brain function to form a new memory is spread over many brain regions and processed through the entire brain. However, later studies of the human patient Henry Molaison (H.M.) (Scoville & Milner 1957) demonstrated the unique function of the hippocampus to form episodic memory (autobiographical memory). H.M. developed epilepsy at an early age and at the age of 27 in 1953, he received bilateral temporal lobectomy to remove the hippocampal formation and adjacent structures in the brain. This surgical procedure was taken to reduce epilepsy and actually resulted in the partial success of controlling epilepsy. However, H.M. also developed severe anterograde amnesia which meant he could not form new memories. As there was no intellectual disability or loss of perceptual function that accompanied the inability to form long term memory, scientists began to recognize memory as a distinct cerebral function and the hippocampus as a pivotal part that is responsible for the

process. Following these studies, the role of the hippocampus in learning and memory processes has been studied intensively.

1.2. Ionotropic glutamate receptors

1.2.1. Kainate receptors (KARs)

An analogue of glutamate, kainic acid (Kainate, KA) was first discovered and extracted from seaweed that kill intestinal worms in 1953 (Moloney 1998). Kainate is very potent neurotoxic amino acid. By binding its receptor, kainate receptors, it overexcites neurons causing cell death. Because of its neurotoxicity and ability to induce epileptic activity, it has been intensively studied in animal models of temporal lobe epilepsy and neurotoxicity-induced cell death (reviewed in Ben-Ari 1985, Nadler 1981).

Originally, kainate receptors were categorized as 'non-NMDA' receptors, together with α-amino-3-hydroxy-5-methyl-4-isoxazolepropionic acid receptors (AMPA receptors, AMPARs), as there was a lack of selective pharmacological tool to differentiate between KARs and AMPARs. In 1981, Evans and Watkins speculated that KARs are different from AMPARs (Watkins & Evans 1981). This was proved by Lerma and colleagues in that they showed functional KARs differ from AMPARs expressed on hippocampal neurons as when they rapidly changed AMPA-containing solution to KA-containing solution the evoked synaptic responses had different kinetics (Lerma et al 1993). Soon after, GYKI 53655 (but also see Perrais et al 2009) and GYKI 52466 which antagonise AMPAR activity while leaving KAR intact was discovered (Paternain et al 1995, Wilding & Huettner 1995) opening up new opportunities for research on the role and function of KARs.

KARs are tetrameric ion channels that have five subunits (GluK1-5). GluK1, GluK2 and GluK3 (also called GluR5, GluR6 and GluR7 respectively) are subunits which response to kainate in the range 50-100 nM and are therefore called 'low affinity' subunits. 'High affinity' subunits, GluK4 and GluK5 (also called KA1, KA2) react to 5-15 nM of kainate. Homology between low affinity and high affinity subunit is about 45%. Low affinity subunits have 78-80% homology and they can form a functional homomeric receptors by themselves (Egebjerg et al 1991, Schiffer et al 1997, Sommer et al 1992). On the other hand, high affinity subunits have 68% homology and must assemble with low affinity subunits to form functional receptors (Herb et al 1992, Werner et al 1991).

Like other ionotropic glutamate receptors, KARs are tetramers and their assembly involves two KAR subunit dimers making a pair to form a tetramer. Each subunit consists four distinctive domains, an amino terminal domain (ATD), a ligand binding domain (LBD), a transmembrane domain (TMD) and a carboxyl terminal domain (CTD). The ATD plays an important role in receptor assembly, trafficking and functional regulation. The LBD carries the polypeptide sequences S1 and S2 which form a clamshell shape. Agonist and antagonist bind to this domain to regulating receptor activity. The TMD forms the channel pore. When agonist binds to the LBD, a conformational change causes opening of the channel pore, allowing ions to pass through. The CTD is responsible for receptor localization, trafficking and surface expression (Sobolevsky 2013).

1.2.1.1. Alternative splicing variants of KAR

KARs go through alternative splicing processes. These processes make several isoforms of each KAR subunit. Alternative splicing of GluK1 at the extracellular N-terminal (**Figure 1-2 a**) generates GluK1-1 and GluK1-2 that differ by 15 amino acid which is present only in GluK1-1 (**Figure 1-2 b**) (Bettler et al 1990). Other splicing variant points are located on the cytoplasmic C-terminal (**Figure 1-2 a**). As the C-terminal is important for its trafficking, delivery to the synaptic membrane and stabilization, different isoforms affect expression and physiological function of receptors. In case of GluK1, alternative slicing on GluK1 C-terminal produces GluK1a, GluK1b and GluK1c (**Figure 1-2 b**) (Sommer et al 1992). In addition, humans uniquely express an extra variant called GluK1d (Gregor et al 1993). GluK1a and GluK1b are expressed on the plasma membrane at a low level, however GluK1c is entirely retained in endoplasmic reticulum (ER) (Jaskolski et al 2004).

In the case of GluK2, splicing results in GluK2a and GluK2b and again humans uniquely express another isoform, GluK2c (Barbon et al 2001). GluK2a and GluK2b are expressed on the plasma membrane, where GluK2a is expressed at higher levels. There is no difference found in the functional properties between the two variants. They have been observed to co-assemble *in vitro* and *in vivo* (Coussen et al 2005).

GluK3 have two isoforms, GluK3a and GluK3b (**Figure 1-2 b**). GluK3a is highly expressed on plasma membrane and GluK3b is retained in ER (Jaskolski et al 2005). GluK2a and GluK3a assemble with other subunits and are known to increase change of surface expression of the heteromeric receptors (Jaskolski et al 2004, Jaskolski et al 2005). Different from GluK1-3, no alternative splicing occurs for GluK4 and GluK5.

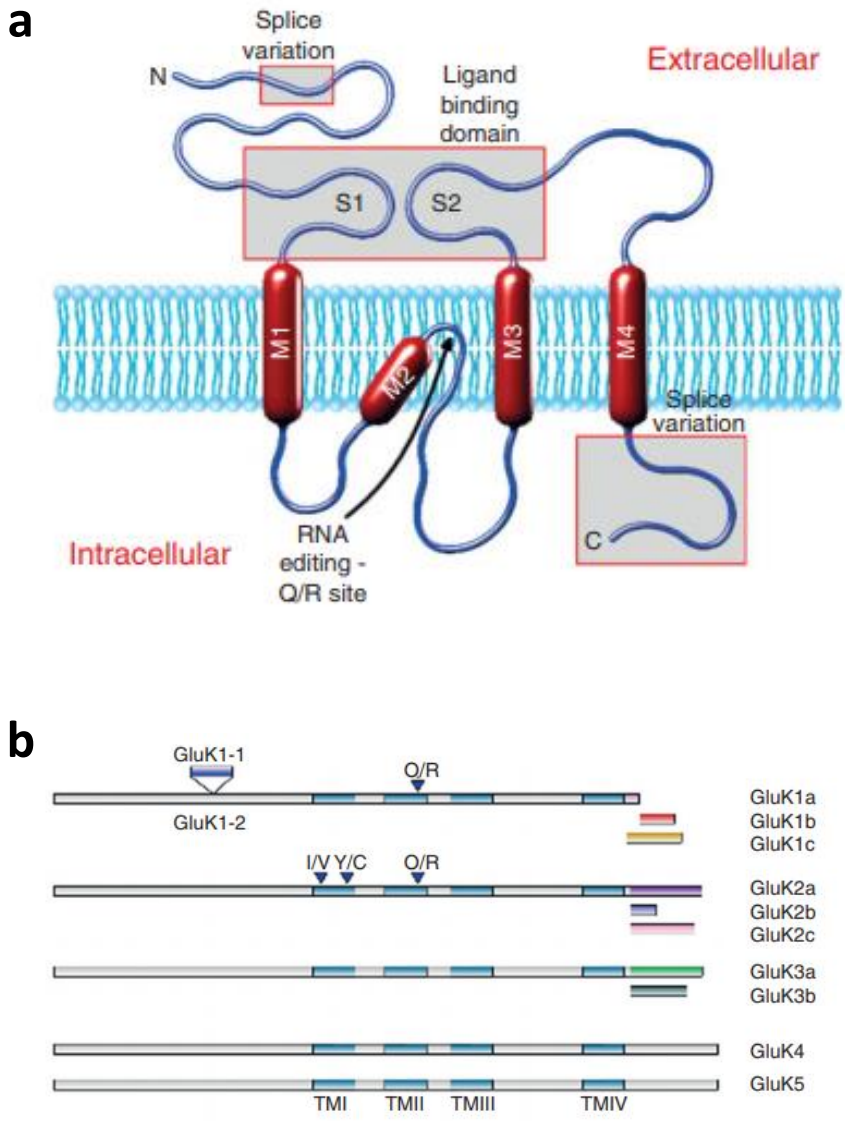

Figure 1-2. Topology of the KARs
a. An Illustration displaying sites for splice variants, ligand binding domains and Q/R RNA editing sites.
b. A schematic drawing that shows sites for splice variants and RNA editing according to subunit isoform. (a and b taken from Gonzalez-Gonzalez et al., 2012)

GluK1 and GluK2 also undergo another post-transcriptional modification such as mRNA editing (**Figure 1-2 a**). In the transmembrane segment, TM2, glutamine / arginine (Q/R) site of GluK1 and GluK2 can be edited. When receptors have unedited version (glutamine), receptors are Ca^{2+} permeable. When glutamine is changed to arginine, it reduces single channel conductance nearly 25 times lower making receptor impermeable to Ca^{2+} ion (Burnashev et al 1995, Swanson et al 1996). Therefore, this process can change property of receptors. As mRNA editing occurs at different rate depending on brain region and developmental stage, physiological property of receptor also changes according to brain region and development. In case of GluK1 subunit, major editing happens during postnatal development. It is most vigorous in peripheral nerve system such as dorsal root ganglia; hippocampus shows robust mRNA editing until postnatal day 4 (P4). In adult animals, > 50% of GluK1 subunits have (R) form (Bernard et al 1999). Editing for GluK2 initiates earlier and occurs more prevalently compared to GluK1 subunit. From E14 of embryonic stage, robust editing takes place and by birth 70% of receptors show edited version. In mature animals, 80-90% of GluK2 subunit have (R) form (Bernard et al 1999, Paschen et al 1995, Schmitt et al 1996).

Q/R editing changes expression of KARs on plasma membrane. GluK2 (Q) is likely to form tetramers and exit from ER and expressed on cell surface while GluK2 (R) is retained in ER as monomer/dimer state (Ball et al 2010). Q/R editing can also affect synaptic plasticity. Impairment of Q/R editing of GluK2 in mutant mice showed NMDAR-independent form of long term plasticity (LTP) at pp-DG synapses which is not seen in WT demonstrating GluK2 (Q) may enable synaptic plasticity (Vissel et al 2001). Although physiological property of receptor is altered by Q/R editing, no substantial behavioural changes have been observed. Lack of mRNA editing of GluK1 did not affect ability to learn spatial information (Sailer et al 1999) and mutant mice with GluK2 editing deficiency showed normal contextual fear memory (Vissel et al 2001).

In addition to Q/R site in TM2, GluK2 subunit has two extra editing sites located in TM1 (**Figure 1-2 b**). One is isoleucine/valine site (I/V site) and the other one is tyrosine / cysteine site (Y/C site). Ca^{2+} permeability also depends on these two sites. When receptor has V and C form in TM1 as well as Q form in TM2, receptor is Ca^{2+} permeable (Kohler et al 1993), in other cases, receptor stays Ca^{2+} impermeable. In native tissue, fully edited GluK2 (R/V/C) are expressed mostly, therefore, it is assumed that majority of GluK2 subunits have low Ca^{2+} permeability (Kohler et al 1993).

1.2.1.2. KAR expression and assembly

Early studies used radioligand binding to find the expression pattern of native KARs. Monaghan and Cotman (1982) demonstrated that [^{3}H]KA binding is spread throughout the CNS; but is highly enriched in hippocampal CA3. Another radioligand binding study showed that KARs reach the peak expression in hippocampus around postnatal week 3 and remain strong until adulthood (Miller et al 1990).

In situ hybridization was also used to demonstrate the distribution of mRNA of KARs (Bahn et al 1994, Wisden & Seeburg 1993). Localization of the different KAR subunit differs according to region. mRNA of GluK1 is enriched in the subiculum, hippocampal CA1 and cerebellar Purkinje cell layer (Bettler et al 1990). GluK2 is expressed strongly in the DG and CA3 region in the hippocampus and also the caudate putamen and the cerebellar granule cell layer. Low levels of GluK3 are widespread throughout the brain and GluK4 is highly expressed in the amygdala, hippocampus and entorhinal cortex. GluK5 is expressed in cerebral cortex, Caudate putamen, hippocampus, entorhinal cortex and cerebellar granule cell layer (Bahn et al 1994, Wisden & Seeburg 1993).

In the hippocampus, low levels of KARs mRNA is detected as early as E14 and levels increase over embryonic development so that after birth robust gene expression takes place. GluK1 is expressed in DG at relatively low levels at all developmental stage. mRNA of GluK2 is found in DG and CA3 at early developmental stages and progressively increases until adulthood. GluK3 reaches its peak around the first postnatal week in DG and decreases as animals age. GluK4 is highly enriched in the DG and CA3 pyramidal cells and its expression level does not change throughout development. GluK5 is found in DG, CA3 and CA1 at very high level at all developmental stages (Bahn et al 1994, Wisden & Seeburg 1993).

Although subunit specific distribution of KARs can be revealed by *in situ* hybridization, pinning down the precise cellular localization, whether it is pre- or postsynaptic, was difficult to achieve using this method. Lesion studies using toxins such as KA or colchicine were a more successful strategy to determine cellular localization of KARs. Injection of KA or colchicine in the DG GC layer led to a reduced high affinity kainate binding signals in the CA3 region where GCs make MF synapses with CA3 pyramidal cells. This demonstrates that high affinity KARs are located in presynaptic terminals (Monaghan & Cotman 1982, Represa et al 1987).

Immunohistology using GluK2/3 and GluK5 antibodies has found that they are located in the CA3 region (Petralia et al 1994) and immunoblotting found that all subunits were found in the

presynaptic active zone (Pinheiro et al 2005). All other subunits except for GluK4 were found on the postsynaptic density (PSD) (Pinheiro et al 2005, Pinheiro et al 2007). Detailed localization of GluK4 and GluK5, determined using immunogold labelling, found that although both GluK4 and GluK5 subunits are found at synaptic contacts, GluK4 is enriched at the presynapse whereas GluK5 is more enriched at the postsynapse (Darstein et al 2003).

Although GluK1-3 subunits can assemble as homomers by themselves, they have preferential assembly partners (Bahn et al 1994, Jaskolski et al 2004). In the hippocampus, genetic knock out of GluK2 resulted in reduced GluK5 protein confirmed by western blotting (Straub et al 2011). Furthermore, the expression pattern of GluK5 was disrupted in GluK2 KO animals, but not in GluK1 KO animals demonstrating GluK2 is the main assembly partner for GluK5 (Ball et al 2010). Both GluK4 and GluK5 subunits coimmunoprecipitated with GluK2 subunit also suggesting they co-assemble with GluK2 subunit (Darstein et al 2003).

1.2.1.3. Synapse trafficking and targeting of KARs

Newly assembled KARs exit ER and are delivered to the cell membrane for surface expression. Splice variant of KAR in cytoplasmic C-terminal affects expression level which differs according to subunits. GluK1a, GluK1b, GluK2b and GluK3b are expressed at low level while GluK2a and GluK3a are highly expressed on the plasma membrane. GluK2a works as the key subunit for high surface expression when assembled with other subunits. Forward trafficking motif in the C-terminal domain of KAR is also required for plasma membrane expression (Jaskolski et al 2004, Jaskolski et al 2005). Although it has been found to be possible that GluK5 subunit forms homomers, but it is not trafficked to the surface and retained in ER. It is because GluK5 has arginine-rich motif which leads ER retention as well as di-leucine sequence which promotes internalization of receptor (Gallyas et al 2003, Hayes et al 2003, Ren et al 2003).

The extracellular domain of KARs also modulates receptor trafficking to the surface. Signal sequences located at the N-terminal of newly made proteins facilitate the insertion of the proteins into the ER membrane. These sequences, that consist of 15-50 amino acid residues, are then cleaved by signal peptidase to produce a free peptide (Martoglio & Dobberstein 1998). A recent study found that the cleaved signal peptide of KARs binds to their ATD as a ligand and this suppresses the surface expression of the GluK1 subunit (Duan et al 2018).

Ligand binding domain of KAR also affects surface expression. A mutation at the ligand binding domain, S1 and S2 domain, eliminated glutamate binding affinity resulting in reduced surface

expression and degradation of receptor (Mah et al 2005, Valluru et al 2005). This indicates that ligand binding is required for receptor trafficking to plasma membrane which serve as a point of quality check.

Interaction between pre- and postsynaptic cell has been found to regulate GluK2 and GluK4 expression. At MF-CA3 synapses, C1ql2 and C1ql3 protein (complement component like protein important for innate immune system) are released from presynaptic side. These proteins bind to N-terminal of postsynaptic GluK2 and GluK4 subunits promoting recruitment of receptor to synaptic site (Matsuda et al 2016). C1ql2 null mice do not show postsynaptic KAR currents confirming a deficiency of functional KARs.

Neuropilin and tolloid like 1 (Neto1) and 2 (Neto2), auxiliary protein of KAR, assist trafficking and synapse targeting of GluK1, not GluK2 (Sheng et al 2015, Sheng et al 2017) (The role of Neto1 and Neto2 will be discussed in more detail in **section 1.2.1.6.**). CaMKII activation leads phosphorylation of Neto2 at ser-409 resulting in decreased GluK1 expression (Lomash et al 2017).

1.2.1.4. Kinetics of KARs

In the hippocampus, KAR-mediated currents have been observed in postsynaptic CA3 pyramidal neurons (Castillo et al 1997b, Cossart et al 2002, Vignes & Collingridge 1997) as well as CA1 interneurons (Frerking et al 1998, Frerking & Ohliger-Frerking 2002).

KAR-meditated currents have distinctively small amplitudes and slow kinetics. Activated KARs display slow rise time (5-10 ms) and slow decay (30-150 ms time constant) (Castillo et al 1997b, Cossart et al 2002, Kidd & Isaac 1999). Compared to AMPA-EPSCs which constitute the majority of the postsynaptic current, KAR-EPSCs contribute only the 10% of peak amplitude at best (Pinhero 2007). The slow desensitization of KARs enables temporal summation during repetitive stimulations (Frerking & Ohliger-Frerking 2002). Also, this feature is thought to contribute to the generation of temporal lobe epilepsy (Artinian et al 2011). The reported kinetics of recombinant KARs are slightly different from that of native KARs. So far, faster desensitization and deactivation of receptor currents have been observed from recombinant KARs compared to native KARs (Contractor et al 2011, Heckmann et al 1996, Swanson et al 2002). It has been demonstrated that a membrane associated protein, synapse associated protein 90 (SAP90), binds to GluK2/5 heteromers and changes their desensitization kinetics (Garcia et al 1998).

Subunit-specific kinetics have been investigated in recombinant KARs. Early studies on GluK1 and GluK2 homomers demonstrated that KAR subunits display different kinetics depending on the agonist used, domoate, kainate and L-glutamate (also discussed in **section 1.2.1.7.**) (Kohler et al 1993, Sommer et al 1992, Swanson et al 1997a). Direct comparison showed homomeric GluK1 receptors exhibit slower desensitization compared to GluK2 when activated with various agonists (Swanson et al 1997a). Genetically engineered mice lacking GluK2 subunit showed reduced sensitivity to kainate demonstrating importance of GluK2 subunit for KAR activation (Mulle et al 1998). Also, KAR-EPSCs are partially reduced in GluK4 KO animals and almost lost in GluK4/5 heteromer KOs suggesting an important role of high affinity receptors for its ionotropic action (Fernandes et al 2009). GluK3 homomers, once thought to be non-functional, require a high concentration of glutamate for their activation and it also desensitizes rapidly (Pinheiro et al 2007, Schiffer et al 1997). Genetic deletion of GluK4 led to a slow decay of KAR currents and GluK5 KOs showed faster decay kinetics compared to WT (Contractor et al 2003, Copits & Swanson 2012). In a simulation model, it was proposed that the decay time of GluK2/5 heteromeric receptors, which is slower than GluK2 homomers, is similar to the KAR-mediated current seen in native tissue (Barberis et al 2008).

The properties and functions of KARs are altered by interaction with auxiliary proteins. One of most studied proteins that affect KAR function is the Neto protein (also discussed in **section 1.2.1.6.**). At MF-CA3 synapses of Neto1 KO animals KAR currents and their decay time are remarkedly reduced, however, this is not the case in Neto2 KOs (Tang et al 2011). Loss of distinctively slow kinetics was also confirmed by another group using Neto1 KO animals who also shared a reduced sensitivity to kainate (Straub et al 2011). Neto1 also accelerates desensitization of homomeric GluK1 receptors while Neto2 decelerates it (Copits et al 2011). Neto2 reduced desensitization and deactivation rate of GluK2 subunits and also increased the open probability of KARs resulting in bigger currents (Zhang et al 2009).

SAP90 and SAP102, PSD-95 family members which help clustering of KARs are also found to affect properties of KARs. GluK2 and GluK5 subunits directly bind to SAP90 and when co-expressed, it reduces desensitization of GluK2 currents (Garcia et al 1998). In addition, PSD-95 aids recovery of GluK2 from desensitization (Bowie et al 2003).

Another neuronal protein, KAR interacting protein for GluR6 (KRIP6) binds to the C-terminal domain of GluK2 and co-localises with GluK2 in hippocampal neurons. Peak amplitude is reduced

but amplitude during steady state is increased without significant changes in decay kinetics when they are co-expressed (Laezza et al 2007).

1.2.1.5. General role of KARs

Ionotropic action

It is well known that activation of KARs regulates excitatory and inhibitory synaptic transmission in a bidirectional manner. Excitatory synaptic transmission can be enhanced or reduced by KAR activation depending on the concentration of agonist. With a low dose of agonist (≤ 50 nM of KA) NMDAR- and AMPAR-mediated EPSCs are enhanced (Rodriguez-Moreno & Sihra 2004, Schmitz et al 2001b). A high dose of agonist (> 200 nM of KA or > 1 μM of ATPA) depresses synaptic transmission (Schmitz et al 2001b, Vignes et al 1998).

In MF synapses, repetitive stimulation at a broad range of frequency (0.5 Hz to 100 Hz) can induce robust enhancement of synaptic response (frequency facilitation, discussed in more detail in **section 1.3.2.3.**) (Salin et al 1996). Frequency facilitation is an example of enhanced synaptic transmission caused by KAR activation. This regulation is believed to be due to the ionotropic action of KARs because enhancement of current is seen within a 10 milliseconds time scale, which is too fast for the G-protein coupled second messenger pathway. In addition, activation of KARs depolarized the presynaptic terminal at MF synapses allowing Ca^{2+} ions to pass through the receptors (Kamiya 2002, Kamiya et al 2002). The Ca^{2+} permeable receptor blocker, philanthotoxin (PhTx), blocks synaptic facilitation demonstrating that influx of Ca^{2+} through KARs as well as internal Ca^{2+} sources are important for the facilitation (Lauri et al 2003, Liang et al 2002). For downstream of KARs, activation of the AC-cAMP-PKA pathway has been suggested to be activated, as activation of AC by forskolin occluded KAR-mediated synaptic facilitation (Rodriguez-Moreno & Sihra 2004). Specific KAR subunits also contribute to frequency facilitation, but it will be discussed in detail later in this chapter with the properties of MF synapses.

Metabotropic action

KARs have been shown to be coupled with G-proteins in hippocampal membrane (Cunha et al 1999). The first metabotropic action of KARs was demonstrated in inhibitory synapses. In hippocampal synaptosomes, GABA release was reduced by application of KA and domoate. This effect was blocked by an AMPA/KAR antagonist, CNQX, but not with a specific antagonist for AMPA, GYKI 53466, demonstrating activation of KARs is responsible for the reduction (Cunha et

al 1997). Similar observations have been made more directly in hippocampal CA1 synapses. KAR activation reduces amplitude of eIPSPs which also indicates GABAergic synaptic transmission is regulated by KARs (Clarke et al 1997), probably through GluK1-containing KARs (Christensen et al 2004) as the effect was mimicked by GluK1 specific agonist ATPA (Clarke et al 1997). This modulatory effect was independent of ion channel action and blocked by a PKC inhibitor suggesting it is the metabotropic action of KAR that is responsible (Cunha et al 2000, Rodriguez-Moreno & Lerma 1998).

In addition, Frerking et al (2001) proposed that depression of excitatory synaptic transmission is due to metabotropic action of KARs as the G-protein inhibitor pertussis toxin (PTx) prevented synaptic depression caused by KAR activation. This inhibitory action on synaptic transmission through metabotropic action is most robust during early developmental stages. At CA3-CA1 synapses, tonic activation of KARs depresses excitatory transmission in a G-protein dependent way (Lauri et al 2006, Sallert et al 2007). This indicates that metabotropic action of KARs in early development is responsible of maturation of the synapses and shaping the network.

The metabotropic action of KARs also affect excitability of cells. In CA1 pyramidal neurons, KAR activation reduces the amplitude of the slow afterhyperpolarization current (sAHP). Reduction of the sAHP consequently increases membrane excitability resulting in higher spiking number during depolarizing stimulation. As this modulatory effect is blocked by a PKC inhibitor, but not altered by ATPA, it is likely that the metabotropic action of KARs is important for membrane excitability independent of the GluK1 subunit (Melyan et al 2004, Melyan et al 2002). Indeed, inhibition of sAHP caused by KAR activation is lost in GluK2 KO animals not in GluK1 KO animals (Fisahn et al 2005). In addition to GluK2, another study showed that a lack of GluK5 subunit also led an impaired reduction of the sAHP when KARs were activated with a low concentration of KA (50 nM) (Ruiz et al 2005). However, not all studies agree on the role of high affinity KAR subunits as GluK5 KOs as well as GluK4 and GluK4/5 DKOs showed unaltered KA-induced inhibition on the sAHP (Fernandes et al 2009). Therefore, which subunit is responsible for metabotropic action of KAR regulating I_{sAHP} needs further investigation.

1.2.1.6. KAR auxiliary protein

Neto proteins are single transmembrane proteins which work as auxiliary subunits for KARs. They affect receptor properties and trafficking when co-assembled with KARs. Neto has two subunits, Neto1 and Neto2 that are 50% homologous overall and share similar structure.

Neto2 is distributed throughout the brain, but in the hippocampus, it is rather poorly expressed (Straub et al 2011). Expression is detected in CA1 and CA3 pyramidal cells, not in the DG. mRNA of Neto2 is abundant by postnatal week 3 and this level stays until adulthood (Michishita et al 2004). Compared to Neto2, expression level of Neto1 is higher in the CNS. In the hippocampus, expression of mRNA of Neto1 starts from embryonic stages and steadily increase until postnatal week 3. Neto1 is highly enriched in CA3 region (Michishita et al 2003, Ng et al 2009), especially in stratum lucidum of CA3 where MF synapses are formed (Straub et al 2011, Tang et al 2011).

Intensive studies on Neto protein and KAR interactions revealed that biophysiological properties of KARs are regulated by Neto protein. In addition, one of the roles of Neto protein on KARs is to regulate their trafficking (Ng et al 2009, Straub et al 2011, Tang et al 2011, Zhang et al 2009). There is controversy over whether Neto also regulates surface expression of KARs. For example, Straub and colleagues found that surface expression of GluK2/3 and GluK5 were unchanged in Neto1 KO mice (Straub et al 2011). On the other hand, another group showed levels of GluK2/3 at CA3 postsynaptic neurons was reduced in Neto null mice as well as Neto1 KO (Wyeth et al 2014) suggesting importance of Neto1 on KAR surface expression. Surface expression of GluK2 was not altered by Neto2 on oocytes (Zhang et al 2009) but GluK1 was increased in hippocampal neurons by Neto2 (Copits et al 2011). Also, studies have shown that both Neto2 and Neto1 can drive GluK1 into synapses and can increase their surface expression and trafficking (Sheng et al 2015, Sheng et al 2017). Recently, a group suggested a possible downstream mechanism of how Neto regulates synaptic targeting of KARs. In this study the authors showed that phosphorylation of Ser-409 of Neto2 inhibit synaptic targeting of the GluK1 subunit (Lomash et al 2017).

Another role of Neto which is well studied and established is to regulate KAR channel properties. Neto1 and 2 increase agonist sensitivity of GluK1 and increase peak current coming through the channel (Fisher 2015). Neto slows deactivation and desensitization of KARs and slows onset to desensitization (Copits et al 2011, Fisher & Mott 2013, Sheng et al 2015, Straub et al 2011, Zhang et al 2009).

In Straub et al (2011), slow decay of KAR-mediated EPSCs was eliminated in Neto1 KOs suggesting Neto1 is important for KAR kinetics. This was also confirmed by Tang et al (2011) which demonstrated the amplitude of KAR-mediated EPSCs were reduced and decayed more rapidly in Neto1 null mice. Wyeth et al (2014) demonstrated that metabotropic action as well as ionotropic action of KAR was affected. KAR activation leads to a reduced inhibitory slow

afterhyperpolarization current (I_{sAHP}) amplitude, which is known to be a metabotropic function of KARs. In Neto1 and Neto1/2 DKO mice, this depressant effect of KA was abolished, which suggest not only ionotropic action of KARs is affected but also metabotropic action of KARs could be regulated by Neto (Wyeth et al 2014).

Recently, a study revealed that Neto regulates axonal delivery of GluK1 in the immature brain. They showed that presynaptic GluK1 activity, which leads to inhibition of glutamate release by tonic activation of KARs is lacking in Neto1 KO mice. This causes disturbed synaptogenesis and synchronization of neurons in CA3 and CA1 (Orav et al 2017). As GluK1 activity is important for normal development (Lauri et al 2005, Lauri et al 2006), cooperation of Neto proteins and GluK1 is likely to play an important role on synapse maturation.

1.2.1.7. KAR pharmacology

Early compounds

Distinguishing KARs from AMPARs was greatly hampered for a long time due to the lack of selective pharmacological tools. Antagonists that were used as KAR antagonist, such as CNQX, have poor selectivity between AMPARs and KARs, making it difficult to observe an effect that is 'purely KAR'. Since NBQX is 100 times more sensitive to AMPARs compared to KARs (Mayer et al 2006), it was used to dissect KARs from AMPAs in early studies, however as this compound still affected KARs (Mayer et al 2006, Randle et al 1992) the selectivity needed to be improved. Development of GYKI 53655 with improved selectivity toward AMPARs made it possible to distinguish KARs from AMPARs (Bleakman et al 1996, Paternain et al 1995, Wilding & Huettner 1995). Soon after, it was used in native tissue and KAR-mediated synaptic currents were successfully isolated (Castillo et al 1997b, Vignes & Collingridge 1997).

KAR agonists

Along with KA, AMPA and glutamate, domoate (also called domoic acid) were used as an agonist for KARs in the initial studies (Alt et al 2004, Sommer et al 1992). It has a very similar structure to KA and is a very potent agonist at KARs. However, it also has agonistic activity at AMPARs and does not distinguish between subunits of KAR (Donevan et al 1998). Compared to domoate, SYM2081 is very selective to KARs (Donevan et al 1998, Jones et al 1997, Wilding & Huettner 1997) but it also does not have selective agonistic activity at specific KAR subunits (Donevan et al 1998).

A small number of subunit selective agonists have been developed which mainly target the GluK1 subunit. One of most potent GluK1-containing KARs antagonist, ATPA, was synthesised as an agonist for AMPARs originally. While it has agonistic activity at AMPARs (Lauridsen et al 1985, Stensbol et al 1999), it was found to be more potent toward GluK1-containing KARs (Alt et al 2004). Since it has no effect on GluK2-containing KARs, ATPA has been used as a specific and potent agonist for GluK1 in physiological conditions (Clarke et al 1997). In parallel, (*S*)-5-Iodowilladiine (I-W) was also synthesised (Jane et al 1997, Wong et al 1994). Like ATPA, it is very potent toward GluK1-containing receptors (Swanson et al 1998). Although ATPA and I-W are most potent at GluK1-containing KARs, they also work as a partial agonist at GluK2/5 heteromers at high concentration (> 100 μM for ATPA, > 30 μM for I-W) (Alt et al 2004, Swanson et al 1998). LY339434 also has agonistic activity specifically at GluK1 (Small et al 1998).

KAR antagonists

Some of the willardiine derivatives show antagonistic activity at KARs. UBP301 (More et al 2004), UBP304 (Dolman et al 2007), UBP296 (More et al 2004) and its (*S*) enantiomer UBP302 have been found to be specific for KARs, in particular, GluK1-containing KARs (More et al 2004). LY382884 is an antagonist of GluK1-containing KARs (Alt et al 2004, Christensen et al 2004). Recently, ACET was synthesised and found to be the most potent and selective antagonist for GluK1-containing receptors (Dargan et al 2009, Dolman et al 2007). However, a study using recombinant GluK3 receptors revealed that UBP302, UBP310 and ACET also antagonize GluK3 homomers (Perrais et al 2009). UBP310 was also found to antagonise GluK2/5 heteromers (Pinheiro et al 2013). In addition, a potent and selective AMPAR antagonist GYKI 53655 was found to antagonise GluK2/3 heteromers as well as GluK3 homomers at higher concentration (Perrais et al 2009).

In the case of NS3763, it does not affect GluK1-containing KARs but antagonizes homomeric GluK1 exclusively (Christensen et al 2004). Other than GluK1 specific antagonists, LU97175 has been found to be selective at low affinity KARs, especially GluK3 (Loscher et al 1999).

1.2.2. NMDA receptors

NMDA receptors are the ligand gated ionotropic channels. Cations such as Na^+, K^+ and Ca^{2+} to flow through the cell membrane. They are named after the selective agonist *N*-Methyl-D-aspartic acid (NMDA). Binding of both agonist and co-agonist are necessary to activate NMDARs. Glycine

was identified as a co-agonist first and later it was found that D-serine also works as a co-agonist (Johnson & Ascher 1987, Kleckner & Dingledine 1988, Mothet et al 2000, Wolosker 2007). Recently, glycine and D-serine were revealed to be localized differently and that D-serine works at synaptic sites whereas glycine works at extrasynaptic sites (Papouin et al 2012).

NMDARs are regulated by Mg^{2+} in addition to binding of ligand. Extracellular Mg^{2+} binds a specific site on the receptor blocking the ion pore. When enough current comes into the cell through AMPARs, intracellular voltage increases causing the cell to depolarize. Depolarization of the cell detaches Mg^{2+} from NMDARs allowing Na^{+}, Ca^{2+} and K^{+} flow through the channel.

NMDARs have 7 major subunits including NR1 (Moriyoshi et al 1991), NR2A-D (Ishii et al 1993, Monyer et al 1992) and NR3A, B (Chatterton et al 2002, Ciabarra et al 1995). Even though it has been reported that NR1 can form a functional homomeric receptor in *Xenopus* oocytes, it is believed that heteromeric assemblies containing an essential NR1 subunit with NR2 subunits are likely to be the main form of NMDARs in mammalian cells (McIlhinney et al 1998, McIlhinney et al 1996, Moriyoshi et al 1991, Sheng et al 1994). As the glycine binding site is located in NR1 and the glutamate binding site in NR2, this may explain why heteromeric assembly of NR1 and NR2 are the main form of functional NMDARs expressed on native tissues (Laube et al 1997, Wafford et al 1995). While the NR1/NR2 combination is involved in physiological functions, NR1 with NR3A or NR3B combination works very differently from NR1/NR2 heteromers. NR1/NR3 heteromers are Ca^{2+} impermeable receptors with reduced current. They do not respond to glutamate or NMDA but are activated by glycine (Chatterton et al 2002, reviewed in Pachernegg et al 2012).

mRNA of NR1 is expressed spontaneously from the embryonic stage throughout the brain. Especially the hippocampus, the cerebral cortex and the cerebellum have abundant expression of the NR1 subunit (Monyer et al 1994, Moriyoshi et al 1991). mRNA of NR2A-D subunits is expressed differently depending on brain region and developmental stage. NR2B and NR2D start to be expressed from E17 while NR2A and NR2C only start to be expressed after birth. In the hippocampal formation, NR1, NR2A and NR2B are present at high level and NR2C and NR2D are detected on interneurons (Ishii et al 1993, Monyer et al 1994). The last member of the NMDAR family, NR3A and NR3B are again differently expressed. Protein and mRNA of NR3A are detected postnatally reaching peak expression in the hippocampus in the first postnatal week. After the peak, gradually decrease to adult. NR3B is found at low levels in the hippocampus (Ciabarra et al 1995, Matsuda et al 2002, Sasaki et al 2002).

NR1 undergoes post-transcriptional splicing modification generating 8 variants (Zukin & Bennett 1995) and these can be categorised into two group according to their conductance (Hollmann et al 1993).

Physiological importance of NMDARs

In Schaffer collateral-CA1 synapses, a repetitive stimulation at high or low frequency results in increased or decreased synaptic strength. For example, a tetanus (100 pulses at 100 Hz for 1 s) can induce LTP and prolonged low frequency (900 pulses at 1 Hz for 15 min) can induce long term depression (LTD). There are two mandatory components for LTP to occur, sufficient depolarization of postsynaptic cell and activation of NMDARs. In this sense, NMDARs work as the synaptic co-incident detector. NMDARs are activated only when presynaptic glutamate release and postsynaptic depolarization occur at the same time. Na^+ entry into the postsynaptic cell via AMPARs raises the membrane voltage and detaches Mg^{2+} from NMDARs. Activated NMDARs are highly permeable to Ca^{2+} (Mayer & Westbrook 1987). The influx of Ca^{2+} reaches maximal level with repetitive stimulation and it triggers intracellular signalling which results in long lasting modification of synapses. The importance of NMDAR activation was confirmed by a study that showed a selective NMDAR antagonist AP5 blocked LTP at Schaffer collateral-CA1 synapses (Collingridge et al 1983).

In the CA3 region of the hippocampus, NMDARs have been found to be expressed at a very low level (Monaghan & Cotman 1985, Watanabe et al 1998). This observation corresponds to the finding that MF synapses exhibit an NMDAR independent form of LTP (Harris & Cotman 1986).

1.2.3. AMPA receptors

AMPA receptors were originally called ‘quisqualate receptors’ as the naturally occurring agonist quisqualate binds to them. Later, they were renamed as ‘AMPA receptor’ after the agonist, α-amino-3-hydroxy-5-methyl-4-isoxazolepropionic acid (AMPA). AMPARs are expressed on almost all excitatory neurons mediating fast postsynaptic currents. Glutamate released from the presynaptic cell binds to AMPARs to activate the channel. Although Na^+ is the major cation that flows in through the channel, also efflux of K^+ can happen in depolarized states. AMPARs have fast binding kinetics and high opening probability.

There are four main subunits of AMPARs, GluA1-4 (also called GluR1-4 respectively). Four subunits are 70-73% homologous and assemble is tetramers as dimer of dimers (Boulter et al

1990, Hollmann et al 1989, Keinanen et al 1990). The hippocampus expresses high level of GluA1, GluA2 and GluA3 mRNA. GluA4 is also expressed but at low level in the DG (Keinanen et al 1990). The major form of functional AMPARs consist of GluA1/2 and GluA2/3 heteromers. GluA1/3 is also present at a lower level and GluA1 homomers make up ~8% of total AMPARs (Wenthold et al 1996). GluA1 and GluA2/3 are localized on the postsynaptic side of dendrite spine (Craig et al 1993).

Post transcriptional modification of AMPARs

All AMPAR subunits contain a domain which is comprised of 115bp that encodes 38 amino acids between TM3 and TM4. Alternative splicing at this domain produce flip/flop variants. Flip/flop forms differ by 9-11 amino acid only. However, this modification alters the desensitization kinetics and the pharmacological properties of AMPARs (Sommer et al 1990). When flop forms are expressed, receptors are rapidly desensitized after activation by agonists such as glutamate (Mosbacher et al 1994, Partin et al 1995). Recently, Pei et al (2009) confirmed that flip/flop variants do not change the opening rate of the channel but shorten the closing rate. They also found GluA1 subunits are unaffected in flip/flop variants unlike previous findings (Pei et al 2009).

GluA2 has extra splice variants which have C-terminal tails of different length. There is a short (50 amino acids) and a long form (68 amino acids) (Kohler et al 1994). Despite the very low expression of GluA2 (long), it has been shown that trafficking of GluA2 (long) version is important for AMPAR-mediated currents and a GluA1 independent form of LTP in juvenile hippocampus (Kolleker et al 2003).

A crucial role of GluA2 lies with its ability to regulate Ca^{2+} permeability. Simply put, GluA2-lacking AMPARs are Ca^{2+} permeable whereas GluA2-containing AMPARs are Ca^{2+} impermeable (Swanson et al 1997b). Ca^{2+} impermeability of GluA2 is a result of mRNA Q/R editing at TM2 near the ion pore of the receptor. When glutamine (Q) which has a neutral charge, sits in this place, receptor is Ca^{2+} permeable. However, if a positively charged arginine (R) sits in this place the receptor become Ca^{2+} impermeable. The major form expressed in the CNS is the Ca^{2+} impermeable GluA2 (R) form. A study showed that GluA2 (R)-deficiency generates spontaneous seizures and leads to complete lethality by postnatal week 3, suggesting importance of the correct regulation of Ca^{2+} permeability of AMPARs for normal synaptic function (Brusa et al 1995). Conversely, Ca^{2+} permeable AMPARs are required for PKA-dependent LTP (Park et al 2016).

Protein-protein interaction of AMPARs

AMPARs have binding sites to interact with various scaffolding proteins in their C-terminal, such as PDZ and NSF/AP2 binding sites. Examples of PDZ containing proteins include glutamate receptor interacting protein (GRIP), AMPA receptor binding protein (ABP), proteins with interacting with C kinase (PICK1) and synapse-associated protein 97 (SAP97). As AMPAR subunits differ in their C-terminal sequence, interactions with intracellular scaffolding proteins are also different for each subunit. For example, GluA1 binds to SAP97 (Leonard et al 1998), whereas GluA2 and GluA3 bind to PICK1 as well as ABP/GRIP (Dev et al 1999, Dong et al 1997, Srivastava et al 1998, Xia et al 1999).

AMPAR interacting proteins that have PDZ domains are important for membrane fusion, regulation of the actin cytoskeleton, synaptic trafficking, targeting and membrane stabilization of AMPARs. They have, therefore, been studied intensively. The PICK1-AMPAR interaction promotes AMPAR clustering at the postsynaptic compartment of excitatory synapses (Dong et al 1997, Xia et al 1999) and regulates the insertion of AMPARs (Daw et al 2000). Interaction with ABP/GRIP is important for stabilization of GluA2 once it is internalized (Braithwaite et al 2002). Interestingly, ABP/GRIP and PICK1 bind to the GluA2 subunit at the same site, and the interaction of ABP/GRIP or PICK1 proteins with GluA2 is regulated by phosphorylation state of Ser880 residue of the receptor. When PKC phosphorylates ser-880, the ability of GluA2 to bind to ABP/GRIP site gets weaker but it does not affect its ability to bind PICK1 (Chung et al 2000, Matsuda et al 1999). In fact, Lu and Ziff (2005) demonstrated that PICK1 and ABP/GRIP also interact intramolecularly, controlling GluA2 trafficking. Disruption of this interaction cause a reduction of GluA2 surface expression and recycling of internalized GluA2 (Lu & Ziff 2005).

SAP97, which interacts with AMPARs by binding the GluA1 subunit (Leonard et al 1998), works as a linkage protein between AMPARs and the actin-dependent motor protein myosin VI (Wu et al 2002). The SAP97-GluA2 interaction promotes trafficking of GluA2 from the ER to the synapse (Greger et al 2002, Sans et al 2001, Xia et al 1999). As trafficking of SAP97 into dendritic spines can be modulated by CaMKII activation, there is a possibility that SAP97 can regulate movement of GluA1-containing AMPARs into dendritic spines (Mauceri et al 2004).

An additional important interaction is with N-ethylmaleimide-sensitive fusion protein (NSF), which is an ATPase which is involved in the fusion of membranes. It dissociates SNARE complexes allowing SNARE proteins to be recycled and reused (May et al 2001). GluA2 and GluA4c subunit interact with NSF.

1.3. Studying MF synapses_What is so special about MF?

1.3.1. Unique anatomical structure of MF

In the dentate gyrus of the hippocampus, about 1 million granule cells are closely packed in the granule cell layer (Boss et al 1985, Rapp & Gallagher 1996, West et al 1991). They send out unmyelinated axons which together are called the mossy fiber. Cajal firstly used the name 'mossy fiber' for these axons because their appearance is similar to the mossy fiber found in cerebellum (Ramón y Cajal et al 1909, 1911, 1995). The mossy fiber pathway can be divided into the suprapyramidal and the infrapyramidal MF. Axons from GCs in the suprapyramidal layer pass through stratum radiatum and make contacts with apical dendrite of CA3 pyramidal neurons in stratum lucidum in the CA3 (suprapyramidal mossy fiber, SMF) (Claiborne et al 1986). Infrapyramidal layer GCs send out axons to distal CA3 to make synapses with basilar dendrites of CA3 pyramidal neurons (infrapyramidal mossy fiber, IMF) (West 1983). CA3 is segmented into three parts, CA3a, CA3b and CA3c (Lorente De Nó 1934). The part closer to CA1, distal to DG is designated as CA3a and the closest to DG is CA3c. There are more short transverse projections running from GC for CA3b and CA3c. On the contrary, there are mainly longitudinal projections from DG to CA3a (Acsády et al. 1998). There are more granule cells in the septal hippocampus and the number is reduced in the temporal hippocampus (Gaarskjaer 1978). Axons from GCs also make synapses with hilar mossy cells, however, it will not be discussed as it is outside of the scope of this study.

The MF has three types of terminal which are morphologically distinctive: large Giant boutons (MFBs), filopodial extensions and small *en passant* boutons. CA3 postsynaptic cells exhibit complex and irregular dendrites called thorny excrescences. These postsynaptic structures are innervated by giant boutons making MF synapses in the stratum lucidum of CA3 (Blackstad & Kjaerheim 1961, Hamlyn 1962, Ishizuka et al 1995). Numerous active zones are concentrated at each terminal. It has been reported that one GC can make connections with 11-18 CA3 pyramidal cells (Acsady et al 1998, Claiborne et al 1986) and single MFB can have up to 35 active zones (Chicurel & Harris 1992). This means that single GC can have over 600 active zones that can be associated with CA3 postsynaptic neurons. Because of this anatomical structure, the MF synapse is called a 'teacher' or 'detonator' synapse as they can excite CA3 cells with a strong driving force (McNaughton & Morris 1987). Also, this explains how sparse firing of GCs can produce a strong excitatory drive to CA3 (Jung & McNaughton 1993). In addition, there is a compelling evidence

demonstrating that the MF helps the formation and postnatal development of thorny excrescence (Amaral & Dent 1981, Represa et al 1991, Robain et al 1994).

On the contrary, filopodial extensions and small *en passant* boutons innervate dendrite of GABAergic interneurons in stratum lucidum (Acsady et al 1998). These synapses have single or very few release sites. GABAergic interneurons in turn make inputs to the CA3 region providing feedforward inhibition that regulate MF activity and excitability (Lawrence & McBain 2003). Although these two types of synapses have few release sites at the terminal, they make ten times as many synapses as MFBs (Acsady et al 1998). Therefore, strong CA3 input is expected to bring about net inhibition. When only a subpopulation of CA3 pyramidal neurons are activated, this net inhibition effect can increase the signal to noise ratio, emphasising those that are activated.

1.3.2. Physiology of MF synapses

1.3.2.1. Complexity of studying MF

Pyramidal cells in CA3 receives input from two main sources, the MF and the A/C pathway, as well as from other minor sources (please see below). Although MF synapses perform a critical role within trisynaptic pathway, the connection between the GCs and CA3 is in fact very sparse. Among the many excitatory inputs one CA3 neuron receives, the input from the MF is an extremely small portion (< 1%) (Amaral et al 1990, Claiborne et al 1986). Most of the synaptic input to CA3 comes from the A/C pathway (Ishizuka et al 1990, Ramón y Cajal et al 1909, 1911, 1995, Swanson et al 1978). Because the MF connection is so sparse, to evoke an observable postsynaptic response via this pathway strong stimulation is required. However, strong stimulation can result in other neurons being activated leading di- or multisynaptic responses.

Apart from the monosynaptic MF input, CA3 neurons can receive three other inputs. First, strong MF stimulation can cause CA3 neurons themselves to fire, and as many CA3 neurons project within CA3 to other CA3 neurons (associational connections) this firing will result in additional EPSPs. Second, strong stimulation in DG can directly activate the hilar projecting collateral axon of CA3 neurons. These two inputs can result in 'non-MF' response. Lastly, the collateral of GCs in the hilar region can be activated. APs travel antidromically reaching the soma and propagate orthodromically to CA3 cells, the so called anti-orthodromic sequence. Although it is not direct, this still evokes synaptic response that exhibit characteristics of 'pure' MF. However, as APs

travel longer distance in this way, synaptic delay is often observed (Henze et al 1997, Langdon et al 1993).

Due to the complexity of the CA3 region, an appropriate degree of caution needs to be taken when recording the MF synaptic response. Sensitivity to group II mGluR agonist has been used as a criterion as to whether a MF response is being recorded as the A/C pathway does not express group II mGluRs (discussed in **section 1.3.2.2.**). In addition, NMDARs are highly enriched in the recurrent pathway but at very low levels in MF synapses (Weisskopf & Nicoll 1995).

Despite these difficulties, polysynaptic contamination can be minimised by making a few experimental manipulations. A low dose of AMPAR antagonist can be used to suppress activity in the A/C pathway. Also, a high concentration of divalent cation (e.g. 4 mM of Ca^{2+} and Mg^{2+}) can be added into the recording solution as activation of NMDARs would be suppressed at all other pathways apart from the MF.

1.3.2.2. DCG-IV sensitivity

The type of mGluR expressed in the MF varies according to species, however, group II mGluRs are thought to be present in MFs regardless of species (Doherty et al 2004, Toth et al 2000) (Doherty et al 2004, Toth et al 2000). *In situ* hybridization studies revealed that mRNA of mGluR2/3 is found in GC of the DG, not in CA3 (Tanabe et al 1992, Tanabe et al 1993) suggesting mGluR2/3 are expressed in the presynaptic terminal of MF synapses (Petralia et al 1996, Shigemoto et al 1997, Yokoi et al 1996). This unique localization of mGluR2/3 was soon found to have a role in regulating glutamate release. Activation of group II mGluRs by their agonists, DCG-IV and AP-4, suppressed excitatory synaptic transmission at hippocampal MF synapses (Kamiya et al 1996, Yoshino et al 1996). Because synaptically released glutamate can activate mGluR2/3s, this suggests synaptic transmission can be regulated by group II mGluR activation in physiological conditions (Min et al 1998, Scanziani et al 1997). Since A/C synapses do not express mGluR2/3 receptors, this inhibitory feedback is used as a criterion to distinguish MF response from A/C responses. A pure MF response is thought to be completely blocked with mGluR2/3 agonist. To verify synaptic responses are coming from the MF, group II mGluR-selective agonist, DCG-IV at low concentration (≤ 2 μM) is used at the end of experiments (reviewed in Nicoll and Schmitz 2005).

However, it has been found that in some conditions DCG-IV sensitivity can vary according to slice preparation (Sherwood et al 2012). In this study, the authors prepared hippocampal slices in two

different orientations, parasagittal and transverse. Synaptic facilitation caused by high frequency stimulation was observed in both slices, although the degree of facilitation from parasagittal slices was a lot less compared to transverse slices. Also, in parasagittal slices, MF response were not suppressed by DCG-IV and antagonists of GluK1 blocked the induction of MF-LTP. In contrast, MF responses from transverse slices were reduced by DCG-IV and GluK1 antagonist were ineffective at blocking the induction of MF-LTP. Therefore, it was suggested that there is a subpopulation of CA3 neurons that are resistant to group II mGluR activation and that are also responsible for MF-LTP that involve GluK1-KARs. Further investigation is needed to see whether this is the case, however, it is well accepted that mGluRs play a pivotal role in synaptic transmission and plasticity at MF synapses.

1.3.2.3. Frequency dependent facilitation

There are several differences between short term plasticity (STP) observed in CA3 compared to CA1. Examples of STP at MF include post tetanic potentiation (PTP), high frequency facilitation (HFF) and low frequency facilitation (LFF). PTP is the synaptic potentiation commonly observed after a tetanus. It only lasts a few minutes and decays quickly in CA1 synapses, however, MF display very high PTP which decays more slowly compared to CA1 (Griffith 1990, Langdon et al 1995).

Another striking feature of MF STP is that it displays robust frequency dependent facilitation. Synaptic facilitation is seen in response to stimulation with a broad range of frequency from 0.025 Hz to 100 Hz. Paired pulse facilitation (PPF) with a short interstimulus interval (< 400 ms) (Salin et al 1996) and trains given at high frequency (usually 5 trains at 25-50 Hz) are used to investigate HFF. After two or more stimuli at high frequency, MFs exhibit enhanced synaptic responses many fold larger than the initial response. This robust enhancement is observed only in MF synapses, not in neighbouring A/C synapses (Salin et al 1996). So far, KARs acting as an autoreceptor have been found to play role in HFF (Lauri et al 2001b).

Not only high frequency stimulation, but also low frequency stimulation can induce facilitation at MFs (LFF). Increases in basal stimulation frequency for example, 0.05 Hz to 0.2 Hz (Salin et al 1996) or 0.033 Hz to 1 Hz (Moore et al 2003) induce synaptic facilitation with a slow onset (Salin et al 1996, reviewed in Henze et al 2000, Nicoll & Schmitz 2005,). In Regehr et al (1994), the authors demonstrated that the presynaptic Ca^{2+} level increase is closely related to the degree of LFF and also that the Ca^{2+} chelator EGTA reduces the magnitude of facilitation. It was therefore suggested that presynaptic Ca^{2+} plays an important role (Regehr et al 1994). LFF is also

dependent on presynaptic CaMKII, indicating facilitation may be expressed through the Calmodulin-AC activation pathway (Salin et al 1996).

As discussed earlier in section 1.3.2.2., activation of mGluRs can regulate synaptic transmission at MF synapses. Scanziani et al (1997) showed that application of the mGluR antagonist, MCPG, enhances LFF induced by 1 Hz. mGluRs are located away from the synaptic terminal but they are thought to be activated by repetitive stimulation such as 30 pulses at 1 Hz. Blockade of these receptors resulting in enhanced LFF indicates that activation of mGluRs in normal conditions suppresses release of glutamate. This idea is in line with the study that showed that a low dose of DCG-IV (0.1 μM) indeed increased PPF, which indicates that probability of release is reduced (Kamiya et al 1996). Therefore, activation of mGluRs in the presynaptic terminal provide negative feedback.

1.3.2.4. NMDAR-independency of MF-LTP

Unique aspect of MF-LTP

Induction of conventional forms of LTP in many excitatory synapses is dependent on NMDAR activation. Ca^{2+} influx through NMDA receptors in the postsynaptic cell activates downstream mechanisms modulating AMPARs (Malenka & Bear 2004). Potentiated AMPAR-mediated transmission by AMPAR trafficking or insertion into the synaptic membrane is thought to be the underlying mechanism of NMDA-LTP (Bredt & Nicoll 2003, Collingridge et al 2004).

MF-CA3 synapses also exhibit long term plasticity. Classical tetanic stimulation (100 Hz for 1 s) that elicits LTP at CA1 can induce LTP at MF synapses as well, however, its induction and expression are very different from CA1 synapses. Firstly, MF-LTP is NMDAR-independent. The first observation of this NMDAR-independent form of LTP was recorded in guinea pig slices (Harris & Cotman 1986, Zalutsky & Nicoll 1990). In this study, the authors demonstrated that the NMDAR antagonist, D-AP5 (50 μM) had no effect on MF-LTP whilst confirming it completely blocked in LTP in A/C synapses (Harris & Cotman 1986). This result corresponds to the very sparse expression pattern of NMDAR in CA3 region (Monaghan & Cotman 1985, Watanabe et al 1998). Although an NMDAR-mediated current was observed in CA3 neurons demonstrating the existence of a functional receptor (Weisskopf & Nicoll 1995). The NMDAR-independency of MF-LTP is observed regardless of species and also can be seen *in vivo* (Henze et al 2000, Wallis et al 2015). Later, Kakegawa et al (2004) showed that GluA1 trafficking onto the postsynaptic membrane caused by CaMKII activation is not detected at MF synapses, demonstrating the NMDAR-mediated downstream mechanism is indeed absent.

Presynaptic or postsynaptic?

Regarding the locus of MF-LTP induction and expression, there still remains controversy. NMDAR-independency of MF-LTP is often used as the basis to support the idea that MF-LTP is presynaptically induced. The idea that MF-LTP is expressed presynaptically was proposed by Zalutsky and Nicoll (1990). The authors observed reduced PPF during MF-LTP which indicates increased probability of neurotransmitter release from the presynaptic terminal. This hypothesis was supported by many other studies, for example a postsynaptic Ca^{2+} rise is not observed in MF-LTP and voltage dependent Ca^{2+} channel blockers do not affect MF-LTP (Castillo et al 1994, Langdon et al 1995, Mellor & Nicoll 2001, Tong et al 1996). In addition, a Ca^{2+} chelator in the presynaptic terminal blocked MF-LTP (Tong et al 1996). In addition to increased presynaptic Ca^{2+} levels, presynaptic changes such as increases in integrated multivesicular release and recruitment of additional release site have been reported to increase glutamate release (Chamberland et al 2014). Recently, more direct evidence has been reported by visualizing presynaptic vesicles using a combination of electrophysiology and total internal reflection fluorescence (TIRF) microscopy (Midorikawa & Sakaba 2017). In this study, tighter coupling between Ca^{2+} channels and release ready synaptic vesicles increases release probability, leading to more exocytosis of neurotransmitter during cAMP-induced LTP (chemically induced LTP, Chem-LTP). This also supports presynaptic locus of MF-LTP expression.

On the contrary, there is also evidence which argues against the idea. MF-LTP induced by brief HFS (B-HFS, 8 trains of 6-10 pulses at 100 Hz, 5 s interval) requires depolarization of postsynaptic CA3 cells (Jaffe & Johnston 1990). Similarly, inhibition of Ca^{2+} rise in the postsynaptic CA3 pyramidal neuron was found to block MF-LTP in some studies (Williams & Johnston 1989, Yeckel et al 1999). In addition, Kwon and Castillo (2008a) observed a novel form of LTP in which only NMDAR-EPSCs are potentiated. These studies suggest a postsynaptic involvement in MF-LTP induction.

Differences between the results obtained in these studies could be due to the stimulation protocols used as a relatively weaker stimulation (e.g. B-HFS) requires postsynaptic component whereas stronger stimulation (3 x 100 pulse at 100 Hz with 10 - 20 s interval, long HFS, L-HFS) does not (Jaffe & Johnston 1990, Kapur et al 1998, Urban & Barrionuevo 1996). This demonstrates that depending on the intensity and frequency of the stimulation, pre- and postsynaptic mechanism can be involved in induction of MF-LTP. Although conflicting observations exists with dynamic underlying mechanism, it is generally agreed that increased release probability is the main factor that elicit and maintain MF-LTP.

cAMP-PKA pathway

If one accepts that MF-LTP is presynaptically expressed, what is the underlying mechanism for it? Many studies consistently find that activation of AC-cAMP-PKA pathway is a key mechanism for MF-LTP. It has been shown that presynaptic Ca^{2+} is critical for MF-LTP induction (Tong 1996, Castillo 1994). R-type (Breustedt et al 2003, Dietrich et al 2003) and L-type (Lauri et al 2003) Ca^{2+} channels as well as Ca^{2+} permeable KARs (Andrade-Talavera et al 2012, Kamiya et al 2002) have been suggested as a gate of external Ca^{2+} entry. Increased levels of cytosolic Ca^{2+} from Ca^{2+} entry though these channels as well as from release from internal Ca^{2+} stores (Lauri et al 2003, Liang et al 2002, but also see Carter et al 2002) binds calmodulin to form Ca^{2+}/Calmodulin (CaM) (Andrade-Talavera et al 2012) initiating the AC-cAMP-PKA pathway. Indeed, the AC isoform that is activated by Ca^{2+}/CaM, AC1, is highly enriched in GC layer (Glatt & Snyder 1993). It catalyses the synthesis of cAMP which in turn increases the activity of PKA. In MF synapses it has been shown that elevated PKA activity can induce chemical MF-LTP. For example, this process can be mimicked by the AC activator forskolin (Huang et al 1994, Tong et al 1996, Weisskopf et al 1994) accompanied by reduced PPF (Weisskopf et al 1994) confirming that presynaptically increased PKA activity is critical for MF-LTP. In reverse, chemical MF-LTP was blocked by bath application of a PKA inhibitor (Tong et al 1996, Weisskopf et al 1994). Not only pharmacological studies but also studies with genetically engineered mice models have confirmed the importance of cAMP-PKA pathway in MF-LTP. Out of the AC family members, AC1 and AC8 are activated by Ca^{2+}/CaM (reviewed in Wang & Storm 2003). In AC1 null mice, MF-LTP was significantly, but not completely, reduced (Villacres et al 1998). It was suggested that a residual degree of MF-LTP in AC1 KO could be blocked by knocking out AC8. However, AC8 and AC1/AC8 DKO animals showed a comparable degree of MF-LTP to in AC1 KO animals indicating AC1/AC8 is not the exclusive mechanism (Wang et al 2003). Downstream of AC and cAMP, genetic ablation of the PKA catalytic subunit Cβ1 and the regulatory subunit RIβ impaired MF-LTP (Huang et al 1995).

As a substrate of PKA, Rab3A (a vesicle associative protein) and RIM1α (an active zone protein) are required for MF-LTP as genetic ablation of each protein led to impairment of MF-LTP (Castillo et al 1997a, Castillo et al 2002). Since forskolin still induced chemical MF-LTP in these KO models, there may be other PKA dependent mechanism that bypass Rab3A and RIM1α.

Expression of MF-LTP

The NMDAR-dependent form of LTP can be divided into two phases, early-LTP and late-LTP. Late-LTP requires protein synthesis and gene transcription while early-LTP does not. Huang et al (1994)

showed that MF-LTP also expresses early and late phases. Strong repeated tetanus (3 trains at 100 Hz for 1 s, 5 min interval) induced long lasting MF-LTP which lasted ≤ 6 h (Huang et al 1994). The protein synthesis inhibitor anisomycin and RNA synthesis inhibitor actinomycin D significantly reduced the late phase of MF-LTP demonstrating it also requires protein synthesis. As well as activity-dependent protein synthesis, axonal transport to MF terminals was found to be necessary for stable expression of MF-LTP (Barnes et al 2010). In parallel, the PPF ratio was decreased during the early phase but recovered during the late phase (> 3 h) indicating a role of increased release probability only in the early phase (Huang et al 1994).

There is evidence that the early phase of MF-LTP is expressed not only by increased probability of release but also by turning on silent synapses (Reid et al 2004, Tong et al 1996). Visualization of Ca^{2+} transient in CA3 cells showed that MF-LTP is expressed by a reduction in failure rate of transmitter release (increased probability release) and activation of silent synapses (Reid et al 2004).

1.3.2.5. Other forms of plasticity

LTP that involves NMDAR

NMDAR independency is a key feature of MF-LTP, however, MFs also exhibit LTP which involves NMDARs. A brief tetanus of 24 stimuli at 25 Hz enhances NMDAR-mediated EPSCs while it does not affect KAR-EPSCs and AMPAR-EPSCs (Kwon & Castillo 2008a). Another group also induced a similar form of LTP (potentiation of NMDAR-EPSCs) with 60 stimuli at 50 Hz (Rebola et al 2008). In both studies, this form of LTP (LTP of NMDAR-EPSCs) required coactivation of NMDARs and mGluR5 and a postsynaptic Ca^{2+} increase from an internal Ca^{2+} source. In a more recent study, it was found that LTP of NMDAR-EPSCs is a form of metaplasticity which is NMDAR-dependent at MF. Spike timing-dependent plasticity (STDP) and depolarization-pairing protocols induce NMDAR-dependent LTP in CA1 but not in the MF. However, these protocols can elicit NMDAR-dependent MF-LTP if they are preceded by induction of LTP of NMDAR-EPSCs (Rebola et al 2011). This indicates that LTP of NMDARs at the MF can lead to LTP of AMPARs by acting as a metaplastic switch at MF. Synaptic plasticity at MF is therefore more diverse than we thought.

Long term depression

Prolonged stimulation at low frequency (1 Hz for 15 min) induces MF-LTD (Kobayashi et al 1996, Tzounopoulos et al 1998). Similar to MF-LTP, induction of MF-LTD is also presynaptic and independent of NMDAR activation as D-AP5 does not block the induction (Kobayashi et al 1996,

Tzounopoulos et al 1998). In MF-LTD, a postsynaptic Ca^{2+} rise is not required for its induction, instead, activation of mGluRs plays a crucial role. The broad spectrum mGluR antagonist MCPG either partially (Kobayashi et al 1996) or fully (Tzounopoulos et al 1998) impaired MF-LTD. Among many groups of mGluRs, group II mGluRs have been suggested to be the critical subunits that modulate synaptic plasticity in the MF. This idea is supported by genetic mouse models that lack mGluR2 (Yokoi et al 1996) or mGluR2/3 (Lyon et al 2011) as they show an attenuated degree of MF-LTD (Lyon et al 2011, Yokoi et al 1996). Later it was shown that the modulatory action of mGluR2 is via the inhibitory G_{α} subunit (Nicholls et al 2006). Although mGluR activation is important, mGluR2/3 agonist alone cannot induce MF-LTD as they must be accompanied by synaptic stimulation for the induction of MF-LTD to be successful (Kobayashi et al 1996, Tzounopoulos et al 1998). Chen et al (2001) proposed a downstream mechanism in which activation of mGluRs reduces the activity of AC via G-protein coupling, in turn, reduced cAMP activity leads to LTD. This suggests that MF-LTD expression is dependent on the same mechanism as MF-LTP but driven in the opposite direction.

On the other hand, there is also MF-LTD that is not modulated by mGluRs (Lei et al 2003). Postsynaptic depolarization from -60 to -10 mV for a brief period depresses postsynaptic response at MF synapses (depolarization induced-LTD). This form of LTD does not require NMDARs, mGluRs and synaptic stimulation, but requires a postsynaptic Ca^{2+} rise through VGCC and internal Ca^{2+} stores. Indeed, PPF and coefficient variation (CV) were not affected in this form of plasticity indicating it is expressed via postsynaptic changes. Depolarization induced-LTD did not occlude LTD that is induced by LFS and vice versa, suggesting there are two separate mechanisms that coexist to produce MF-LTD.

In young animals (P6 - P14), another form of LTD that can be induced by HFS has been observed (Battistin & Cherubini 1994, Domenici et al 1998). Interestingly, this was NMDAR- and mGluR-independent, but, required a postsynaptic Ca^{2+} increase. HFS-induced LTD did not occlude LFS-induced LTD and vice versa, showing these two forms of LTD also do not share the same expression mechanism (Domenici et al 1998).

Coexistence of multiple forms of LTD with distinctive downstream mechanisms suggests that the MF expresses highly diverse plasticity. Indeed, elevated levels of postsynaptic Ca^{2+} induced by photolysis was found to elicit both potentiation and depression (Wang et al 2004). This demonstrates that the similar downstream signalling can cause diverse effect.

1.4. Big questions about the role of KARs in MF function

1.4.1. Which subunit of KARs is important for MF function?

1.4.1.1. GluK1 vs GluK2

Because KARs are localized to the DG and CA3 and are found to be highly expressed in these places (Wisden & Seeburg 1993), the role of KARs on MF function has been studied intensively. An initial study found that KAR-mediated current was observed only in MF synapses, not in A/C synapses (Castillo et al 1997b, Vignes & Collingridge 1997). In addition, it was found that activation of KARs modulates synaptic transmission at the MF in a bi-directional manner. A low dose of KA (≤ 50 nM) activates presynaptic KARs resulting in enhanced NMDAR currents, whereas a high dose (> 500 nM) depresses synaptic transmission (Schmitz et al 2001b). In addition, as detailed above, KARs have been found to play a critical role in synaptic plasticity at the MF.

As discussed earlier in the section 1.3.2.3., MF exhibits distinctive features such as frequency dependent facilitation (HFF and LFF) and NMDAR-independent LTP. The main role of presynaptic KARs in the MF is to work as an autoreceptor (Chittajallu et al 1996, Kamiya 2002, Kamiya et al 2002, Schmitz et al 2001a). A brief HFS induces robust facilitation (HFF) in the presence of AMPAR and NMDAR antagonists and is blocked by CNQX, demonstrating HFF is mediated by KARs (Vignes & Collingridge 1997).

It is well agreed that the NMDAR-independent form of LTP in the MF is presynaptically expressed and that KARs play a role in the induction process. Many pharmacological and genetic studies have been carried out that indicate this. ATPA is a selective and potent GluK1 agonist and activation of GluK1 by ATPA has been shown to depress inhibitory (Clarke et al 1997) and excitatory synaptic transmission (Lauri et al 2001b, Vignes et al 1998). LY382884 is a specific GluK1 antagonist (Bortolotto et al 1999, Breustedt & Schmitz 2004) and its application has been shown to reduce HFF induced by 5 trains over a broad range of frequency from 25 to 100 Hz (Bortolotto et al 2003, Lauri et al 2001b). Because blockade of GluK1 by LY382884 during KA application prevented synaptic depression and ATPA itself depressed transmission, GluK1 was thought to be responsible for KAR-mediated regulation of synaptic transmission (Bortolotto et al 2003). In addition, application of LY382884 prior to a tetanus readily blocked the induction of MF-LTP indicating plasticity at MF is regulated by the GluK1 subunit (Bortolotto et al 1999). In addition, it was found that co-activation of mGluR1/5 and GluK1 can induce chemical MF-LTP.

In this form of LTP, Ca^{2+} released from intracellular Ca^{2+} stores and PKA activity were required (Nistico et al 2011).

However, not every study agrees with this role for the GluK1 subunit. Several studies using mouse models that lack GluK2 propose that GluK2 is the key subunit for KAR-mediated MF function. Firstly, KAR-EPSCs in postsynaptic cells were absent and sensitivity to KA was greatly reduced in GluK2 KOs (Mulle et al 1998). In further reports reduced sensitivity to KA was confirmed as a low or a high dose of KA application did not enhance (Breustedt & Schmitz 2004) or reduce (Contractor et al 2000) synaptic responses respectively in GluK2 KOs. This indicates that the GluK2 subunit is responsible for bi-directional modulation of synaptic transmission caused by KAR activation. Furthermore, the degree of MF-LTP in GluK2 KOs was significantly reduced while GluK1 KOs exhibited a comparable magnitude of MF-LTP to WT (Contractor et al 2001). STP such as PPF, HFF and LFF were greatly decreased in GluK2 KO animals (Breustedt & Schmitz 2004, Contractor et al 2001). Based on these findings it was argued that GluK2 and not GluK1 is important for MF function.

The opposing reports on the role of GluK1 and GluK2 also suggested different underlying mechanisms for MF-LTP. In the mechanism in which the GluK1 subunit is involved, it was suggested that Ca^{2+} enters through GluK1-containing KARs. Increased intracellular Ca^{2+} in turn triggers Ca^{2+} dependent Ca^{2+} release from internal stores which is required for MF induction (Bortolotto et al 2005, Lauri et al 2003, Liang et al 2002). In addition, a high Ca^{2+} concentration in the recording media (3 - 4 mM) can bypass GluK1-mediated mechanisms in that Ca^{2+} entry occurs via L-type Ca^{2+} channel (Bortolotto et al 2005, Lauri et al 2003). On the other hand, in studies where GluK2 was found to be important, Ca^{2+} entry would occur through α1E-containing R-type Ca^{2+} channel (Breustedt et al 2003). These findings may suggest that there is more than a single mechanism involved in KAR-mediated synaptic plasticity. Although these contradicting results indicate different mechanisms, it is generally agreed that downstream of increased Ca^{2+} the AC-cAMP-PKA pathway is activated.

In an attempt to resolve the contradicting results obtained from pharmacological compared to genetic studies, another specific and potent antagonist of GluK1 has been developed (Dolman et al 2007) and tested against MF function (Dargan et al 2009). This strategy produced more direct evidence that changes in Ca^{2+} transients in the presynaptic terminal are due to GluK1-containing KARs. It was shown that HFS induced presynaptic Ca^{2+} transients were reduced following application of 200 nM ACET, indicating they are due to that action of GluK1 subunits

(Dargan et al 2009). Another study using two-photon microscopy revealed that localized application of UBP302, a GluK1 antagonist (More et al 2004), to giant MF boutons also decreases Ca^{2+} transient induced during HFF (Scott et al 2008). More recently, it was suggested that parasagittal/transverse slices could contain different percentages of giant MF boutons; a higher proportion of MF giant boutons were found in parasagittal than in transverse slices (Sherwood et al 2012). In this paper, parasagittal slices showed DCG-IV insensitivity and GluK1 antagonists blocked MF-LTP whereas GluK1 antagonism did not affect LTP and synaptic responses were readily depressed by DCG-IV in transverse slices (Sherwood et al 2012).

Despite the controversy over the detailed underlying mechanisms, all the previously mentioned reports agree on the role of KARs at MF synapses. However, some evidence has also been found that KARs may not be necessary for NMDAR-independent LTP. MF-LTP elicited by weak stimulation protocol (24 pulses at 25 Hz) was blocked by CNQX while MF-LTP induced by a stronger protocol (48 pulses at 25 Hz) was readily induced even in the presence of CNQX. They found that blockade of KARs lowers the threshold for LTP to occur and impairment of LTP in GluK2 KO was rescued by strong stimulation (Schmitz et al 2003). In line with this study, another group found that KARs are not responsible for MF function. Observation of the NMDAR current in the presence of an AMPAR antagonist revealed KARs do not contribute to HFF and LFF (Kwon & Castillo 2008b). Here it was suggested that the previously reported impairment of PPF, HFF and LFF in GluK2 KO and GluK3 KOs can be mimicked by reduced excitability, therefore, frequency dependent facilitation is not KARs-dependent, but it is caused by overexcitation of the CA3 network (Kwon & Castillo 2008b).

1.4.1.2. GluK3

mRNA of GluK3 has been found only in the presynaptic terminal in MF synapses. A mouse model that lacks the GluK3 subunit demonstrated disrupted MF function such as reduced HFF, LFF and impaired MF-LTP (Pinheiro et al 2007). Antagonists including UBP302, UBP310 and ACET, previously known for its specificity for GluK1 subunit was found to have antagonistic effects on GluK3. Another potent and specific AMPAR antagonist, GYKI 53655 also exhibited antagonistic activity on GluK3 homomers and GluK2/3 heteromer in Perrais et al (2009). These antagonists were tested on HFF and LFF and it was revealed that GYKI 53655 at a high dose (50 μM) could attenuate the degree of LFF probably via heteromeric GluK2/3 receptors demonstrating a role of GluK3 on synaptic plasticity (Perrais et al 2009).

1.4.1.3. GluK4 and GluK5

GluK4 expression is restricted to CA3 region where its expression level is very high (Werner et al 1991), while GluK5 is widely dispersed throughout the brain (Herb et al 1992). Aller et al (2015) generated a mouse model that overexpresses the *GRIK4* gene (Aller et al 2015). In this study, the PPF ratio was greatly reduced and the frequency of mEPSC was increased in the mutant mice indicating release probability is increased. In line with this study, ablation of GluK4 resulted in a smaller enhancement in amplitude of the fiber volley following KA application compared to WT, demonstrating excitability of MF axon is reduced (Catches et al 2012). MF-LTP was also impaired in GluK4 KO (Catches et al 2012) and KAR-mediated EPSCs and HFF were significantly reduced (Fernandes et al 2009). GluK5 KOs showed intact monosynaptic MF-LTP but impaired heterosynaptic MF-LTP which can be elicited by activating the A/C (Contractor et al 2003). A mouse model that lacks both of high affinity KARs, a GluK4/5 DKO, showed that KAR-mediated EPSCs and HFF were absent. This animal did not respond to KA and domoate indicating their ionotropic action is severely affected (Fernandes et al 2009).

1.4.2. Other factors that affect MF-LTP

1.4.2.1. mGluR in MF-LTP

As discussed earlier (**section 1.3.2.2.**), mGluRs regulate synaptic transmission in MF synapses. Whether they affect synaptic plasticity has also been investigated using pharmacological and genetic approaches. Ibotenate, an mGluR agonist has been shown to induce LTP in the presence of NMDAR, AMPAR and KAR antagonists (Ito & Sugiyama 1991). MF-LTP was blocked by the mGluR1 antagonists AIDA and CPCCOEt (Yeckel et al 1999) as well as the broad mGluR antagonist MCPG (Bashir et al 1993). However, these three antagonists have also been found to be ineffective at blocking MF-LTP in another study (Mellor & Nicoll 2001). A further study found a partial effect; CPCCOEt did not block the induction but rather attenuated the expression of MF-LTP (Contractor 2001).

Among the mGluR groups, evidence has been produced that implicates group I mGluRs in LTP induction, however again, there are some inconsistencies between studies performed in different labs. Genetic ablation of mGluR1 has produced contradictory results as MF-LTP in mGluR1 KO was intact in one study (Hsia et al 1995) but disrupted in another (Conquet et al 1994). In the case of mGluR5, induction of MF-LTP *in vivo* was prevented with the mGluR5 antagonist MPEP (Hagena & Manahan-Vaughan 2015). Partially consistent with this study, co-

inhibition of mGluR1 and mGluR5 was shown to efficiently block MF-LTP *in vitro* (Nistico et al 2011) and *in vivo* (Wallis et al 2015). Interestingly, activation of group I mGluRs together with GluK1 resulted in chemical LTP suggesting mGluR1/5 and GluK1 have synergistic effects on MF-LTP (Nistico et al 2011). Although it is not clear how mGluRs play role in synaptic plasticity at the MF, they appear to be involved in regulating the induction process. Further studies will be needed to elucidate their role in MF function.

1.4.2.2. Zinc

Zinc is an endogenous neurotransmitter that is highly enriched in the presynaptic terminal of MF synapses (Haug 1967, Slomianka 1992). When MFs are synaptically stimulated by HFS such as by a tetanus, it is co-released with glutamate into the synaptic cleft (Qian & Noebels 2005) and enters postsynaptic neurons via Zn^{2+} permeable channels such as NMDARs, Ca^{2+} permeable AMPAR/KARs and VGCCs (Atar et al 1995, Jia et al 2002, Sensi et al 1997).

Although it seems evident Zn^{2+} is present at high density for a reason, maybe playing an important role on MF function, not every study agrees with its impact on synaptic plasticity. For example, a high dose of CaEDTA (7.5-10 mM), a Zn^{2+} chelator, during HFS completely blocks MF-LTP induction in some studies (Huang et al 2008, Li et al 2001) but not in all (Vogt et al 2000). In addition, mocha animals that express reduced amount of Zn^{2+} in the MF terminal also showed a comparable degree of MF-LTP to WT (Vogt et al 2000). Not only Zn^{2+} deficiency undermines synaptic plasticity, but also excessive Zn^{2+} is neurotoxic. Direct application of Zn^{2+} also attenuate the degree of MF-LTP (Ando et al 2010, Takeda et al 2008) and diminishes LTP already established (Xie & Smart 1994).

The mechanism by which Zn^{2+} affects synaptic plasticity is not clear. It has been suggested that when synaptic stimulation occurs, extracellular Zn^{2+} is taken up presynaptically. In turn, Zn^{2+} inhibits AC activity resulting in reduced chemical MF-LTP (Ando et al 2010). In another study, vesicular Zn^{2+} increases probability of release promoting presynaptic expression of LTP while inhibiting postsynaptic LTP (Pan et al 2011).

1.4.3. Behavioural aspect of MF function

There is some evidence that shows that MF-LTP is involved in hippocampus-dependent behaviour such as spatial or contextual learning. However, contradictory results have also been reported. Early studies that used mouse models with mutated PKA catalytic subunit $C\beta_1$, or the regulatory subunit isoform R1β, have been tested in the Morris water maze (MWM) and

contextual fear conditioning (CFC) test. Although these animals showed impaired MF-LTP, their performance in MWM and CFC was comparable to WT suggesting MF-LTP may not play important role in spatial and contextual learning (Huang et al 1995). However, not every study agrees with this finding. mRNA of AC1 is abundantly expressed in the DG GC layer and CA3 (Glatt & Snyder 1993, Xia et al 1991) and activation of AC1 caused by Ca^{2+}/CaM lead to activation of the cAMP/PKA pathway which is important for MF-LTP (reviewed in Wang & Storm 2003). Disruptions to the AC1 gene resulted in impaired MF-LTP (Villacres et al 1998) and a deficit in spatial memory in the MWM (Wu et al 1995). A more recent study using GluK4 KOs also showed similar results. It was reported that GluK4 KO animals express a similar degree of HFF (Fernandes et al 2009), but impaired MF-LTP (Catches et al 2012). These animals showed a deficit in spatial memory seen as reduced time spent in the target quadrant (Lowry et al 2013). GluK2 KO animals that showed impaired MF-LTP (Contractor et al 2001) exhibited normal performance in MWM but showed impaired spatial flexibility as well as social behaviour (Micheau et al 2014).

GCs usually display low average firing rate (≤ 2 Hz) (Jung & McNaughton 1993). However, it has been shown that GC can exhibit bursting firing activity during a behavioural task. An example of such a firing pattern observed *in vivo* (elevation of firing frequency from low basal frequency to high bursting) when applied to an acute slice *in vitro*, results in MF-LTP being readily induced (Mistry et al 2011). This demonstrates that MF-LTP can occur in response to physiological firing patterns. Also, subthreshold stimulation which does not normally induce MF-LTP, will induce MF-LTP (and LTP at the AC - CA3 pathway) *in vivo* if it is paired with exploration of a novel space (Hagena & Manahan-Vaughan 2011). LTP in CA3 is therefore likely to be relevant to encoding of novel spatial information as it occurs more easily in behavioural contexts where this would be useful.

1.5. The role of KARs in other brain regions

KARs regulate synaptic transmission, long-term and short-term plasticity in several brain regions other than the hippocampus (**Table 1-1**).

Thalamocortical synapses

The receptors that mediate synaptic transmission in thalamocortical neurons change from KARs to AMPARs during the first postnatal week (Bannister et al 2005, Kidd & Isaac 1999). Although the KAR-mediated component of synaptic transmission is reduced in the mature brain, KARs on thalamocortical neurons can still regulate synaptic transmission and plasticity at these synapses.

Bi-directional regulation of KARs has been reported as a low dose of KA (3 μM) increases glutamate release whereas a high dose (10 μM) reduces it (Andrade-Talavera et al 2013, Jouhanneau et al 2011) Also, frequency dependent depression in thalamocortical synapses can be alleviated by GluK1 activation (Kidd et al 2002).

Amygdala

In the lateral nucleus of amygdala (LA) synaptic transmission is regulated by KAR activation. 1 μM of KA depresses the amplitude of NMDA-EPSCs and this effect is blocked by application of the GluK1 antagonist UBP296 (Negrete-Diaz et al 2012). Activation specifically of the GluK1 subunit by ATPA (10 μM) mimicked the depressant effect, again in an UBP296 dependent way (Negrete-Diaz et al 2012). Another study used paired pulses (50 ms interval at 2 Hz for 2 min) to induce LTP in LA that is abolished by UBP296 (Shin et al 2010). ATPA induces a similar potentiation in the LA which is again blocked by UBP296. Taken together, these demonstrate GluK1 containing receptors regulate synaptic transmission as well as long term plasticity in LA.

In Li and Rogawski (1998), synaptic facilitation induced by HFS (5 - 8 pulses at 50 - 100 Hz) was used to investigate KAR-mediated currents in the basolateral amygdala (BLA). The facilitation was abolished by a GluK1 antagonist LY293558, demonstrating GluK1-containing KARs regulate HFF in BLA. In addition, prolonged LFS (1 Hz for 15 min) has been reported to induce heterosynaptic facilitation in BLA. This form of LTP is mimicked by direct activation of GluK1 and blocked by a GluK1 antagonist LY377770 (Li et al 2001) indicating GluK1 is important for long term plasticity in BLA. Both of findings are consistent with the high level of GluK1 mRNA expression in the BLA (Li et al 2001). Along with GluK1, mRNA of GluK2 and 5 have been detected, however, their role has not been investigated yet.

Striatum

The existence of functional KARs has been reported in the dorsal striatum (Chergui et al 2000). Neurons that contain substance P and enkephalin co-express GluK2, indicating GluK2 is located in GABAergic neurons. Consistent with this finding, activation of KARs with domoate increased the frequency of sIPSCs and decreased the amplitude of eIPSCs. In GluK2 KO animals, the depressant effect of domoate on eIPSCs was absent indicating GABAergic inhibitory transmission is mediated by GluK2 subunit in dorsal striatum (Chergui et al 2000).

In the nucleus accumbens, a part of the ventral striatum, activation of KARs with 1 μM KA depresses synaptic transmission. When 1 μM KA is applied in the presence of AMPAR and GABAB

blockers, PPF of NMDA-EPSCs is increased, indicating that presynaptic KARs can affect probability of release (Crowder & Weiner 2002).

Neocortex

In neocortex layer II/III, a low dose of KA (500 nM) increases transmission and a high dose (3 µM) decreases the amplitude of EPSCs, indicating a bi-directional effect of KARs (Campbell et al 2007). As application of ATPA mimicked the effect of presynaptic KAR activation, it was suggested that GluK1-containing KARs are responsible for a modulatory effect at these synapses (Campbell et al 2007). Later, a study using synaptosomes obtained from neocortex suggested that the regulatory effect of KARs acts through activation of the AC-cAMP-PKA pathway (Rodriguez-Moreno & Sihra 2013).

Olfactory bulb

In the olfactory bulb, AMPARs/KARs are involved in controlling the excitatory input from mitral cells to granule cells (Schoppa 2006) that is important for synchronization of the granule cell. In a later study it was shown that GluK1-containing KARs located near synaptic terminals modulates fast synaptic transmission whereas perisynaptic GluK2/3 is activated by glutamate spill over (Davila et al 2007). A recent study found that KARs including the GluK1 subunit can modulate not only excitatory but also inhibitory synaptic transmission (Blakemore et al 2018).

Cerebellum

In the cerebellum cerebellar granule cells express moderate levels of GluK1 and high levels of GluK2/5 subunits (Bahn et al 1994, Bettler et al 1990, Petralia et al 1994). In GluK2 KO animals, it was demonstrated that synaptic transmission at Golgi cell-Purkinje cell synapses was greatly reduced, indicating GluK2 is important for synaptic transmission (Bureau et al 2000). Facilitatory effects of KAR activation on postsynaptic currents at these synapses was also observed in a later study (Falcon-Moya et al 2018). In this later study, they reported that the KAR-dependent facilitation effect is dependent on Ca^{2+} permeable KARs as well as internal Ca^{2+} stores. Ca^{2+}/CaM pathway was suggested to be downstream (Falcon-Moya et al 2018).

Cerebellar granule cells form synapses not only with excitatory cells such as Golgi cells and Purkinje cells, but they also make excitatory synapses with inhibitory neurons such as stellate and Basket cells (Palay & Chan-Palay 1974). At both type of synapses, frequency dependent facilitation is observed and regulated by KARs. At granule cell-Purkinje synapses, frequency dependent facilitation is alleviated by NBQX at various frequency ranges (10 - 100 Hz, LFF and

HFF) (Delaney & Jahr 2002). On the other hand, at synapses between granule cells and inhibitory neurons, NBQX reduces facilitation only at low frequency but augment facilitation at high frequency. This indicates that KARs have differential modulatory roles on different types of neurons depending on the pattern of stimulation (Delaney & Jahr 2002).

Region	Subunit involved	Role	Reference
Thalamocortical synapses			
Barrel cortex	KAR	- mediates synaptic transmission during early development	Bannister et al 2005, Kidd & Isaac 1999
	GluK1	- modulates frequency-dependent depression	Kidd et al 2002
	GluK2/3	- modulates synaptic transmission during early development	Jouhanneau et al 2011
synaptosome	KAR	- modulates synaptic transmission	Andrade-Talavera et al 2013
Amygdala			
Basolateral amygdala	GluK1	- mediates synaptic transmission - required for HFF and LTP	Li & Rogawski 1998, Li et al 2005
Lateral amygdala	GluK1	- mediates synaptic transmission - required for LTP	Negrete-Diaz et al 2012, Shin et al 2010
Striatum			
Dorsal striatum	GluK2	- modulates inhibitory synaptic transmission	Chergui et al 2000
Nucleus accumbens	KAR	- mediates synaptic transmission	Crowder & Weiner 2002
Neocortex			
Layer II/III	GluK1	- modulates synaptic transmission	Campbell et al 2007
synaptosome	KAR	- mediates synaptic transmission	Rodriguez-Moreno & Sihra 2013
Olfactory bulb			
Mitral cell-Granule cell	AMPA/KAR	- modulates synchronization of synaptic activity	Schoppa 2006
	KAR	- modulates synaptic transmission	Davila et al 2007
	KAR/GluK1	- modulates excitatory and inhibitory synaptic transmission	Blakemore et al 2018
Cerebellum			
Purkinje cell	KAR	- mediates synaptic transmission - regulate HFF and LFF	Delaney & Jahr 2002, Falcon-Moya et al 2018
Golgi cell	GluK2	- mediates synaptic transmission	Bureau et al 2000
Stellate and basket cell	KAR	- regulates HFF and LFF	Delaney & Jahr 2002

Table 1-1. KARs are involved in synaptic functions of several brain regions other than the hippocampus

1.6. Aim of this study

Whether GluK1-containing KARs are important for MF function has been a matter of a longstanding debate. Pharmacological studies found that GluK1 plays a key role at the MF whereas genetic studies found that GluK2 is a key subunit. In this study, we aim to offer some clarification to the discrepancy over the role of GluK1 and GluK2 on MF function. Unique characteristics of MF were investigated using a combination of pharmacological and genetic approaches.

Since the observation that GluK1 antagonists block MF-LTP was made in DCG-IV insensitive slices (Sherwood et al 2012), we revisit the possibility that MF-LTP is differently regulated by GluK1 in DCG-IV sensitive or insensitive slices. In addition, MF characteristics depending on the sensitivity towards DCG-IV is investigated.

Validation and characterization of global GluK1 KO animals are carried out. This mouse model may serve as an ideal test bed for potential GluK2 antagonists, UBP2002 and UBP2038 since both drugs are not completely selective to GluK2 and they have antagonistic activity at GluK1 as well. To our knowledge, there is no study that has tested GluK2 antagonist in physiological conditions. Therefore, we aim to demonstrate the effect of GluK2 on MF functions such as HFF, LFF and MF-LTP.

Lastly, it is our aim to reveal the role of presynaptic GluK1-containing KARs at the MF. As one possibility is that there are mechanisms that compensate for the absent GluK1 in global GluK1 KO animals, inducible DG-GluK1 KO mice in which GluK1 is intact during critical developmental stages will be validated and MF function studied.

Chapter 2. Materials and Methods

2.1. Animals

2.1.1. General information

Wistar rats were used in chapter 3. Genetically modified mice with C57BL/6N background were used in chapter 4, 5 and 6. In the case of Wistar rats, adult male rats are used. For mouse studies, both genders and animals with varying age are used. The 2-week-old age group covers postnatal days 14 to 20 (P14 - P20), the 4-week-old age group covers P28-34 and adult means animals that are older than 8 weeks (usually 8 - 16weeks). All animals were housed and bred in the facility of The University of Bristol's Animal Services Unit (ASU). The room animals were housed in was kept under 12:12 h light-dark cycle. Up to 4 animals were housed per cage with food and water provided at all time. All animals used in this study are controlled by the Animals (Scientific procedures) Act, 1986, amended 2012. All experiments are carried out according to the policy and the regulation for the care and use of laboratory animal set out in the policy of the University of Bristol. For experiments with genetically modified mice, experimenter was blinded prior to the dissection.

2.1.2. Global GluK1 KO mice

Global GluK1 KO mice were generated using C57BL/6N as a background stain. A designed gene cassette (**Figure 2-1 a**) (UCDavis, KOMP) was inserted into the intron between exons 9 and 10 to disrupt the *Grik1* gene. There were no distinguishable changes in health status or difficulties in breeding.

2.1.3. DG-GluK1 KO mice

Global GluK1 KO mice that express flippase recognition target (FRT) and loxP sites in *Grik1* gene (**Figure 2-1 a**) were crossed with ubiquitous FLP expressing mice that express flippase to incise the cassette (gifted from Dr. Nina Balthasar). Offspring of these animals were, in turn, crossed with POMC-Cre mice that express Cre recombinase in DG specifically under the POMC promoter (Balthasar et al 2004, McHugh et al 2007). As Cre recombinase is expected to be expressed from postnatal weeks 2-3, this would allow knock out of presynaptic GluK1-containg KARs specifically after the early developmental stage producing DG specific GluK1 KO mice. All animals were genotyped and categorized into four groups; a) POMC-Cre$^{wt/wt}$; Grik1$^{wt/wt}$ (**Grik1$^{wt/wt}$**), b) POMC-Cre$^{wt/wt}$; Grik1$^{flx/flx}$ (**Grik1$^{flx/flx}$**), c) POMC-Cre$^{cre/cre}$; Grik1$^{wt/wt}$ (**POMC-Cre; Grik1$^{wt/wt}$**, also include POMC-Cre$^{cre/wt}$; Grik1$^{wt/wt}$) and d) POMC-Cre$^{cre/cre}$; Grik1$^{flx/flx}$ (**POMC-Cre; Grik1$^{flx/flx}$**, also include

POMC-Cre$^{cre/wt}$; Grik1$^{flx/flx}$). Animals were then bred within each group. The primer site for genotying is presented in **Figure 2-1 a** (Illustration taken from the information sheet, KOMP PCR design) and the primer sequences are provided in **Figure 2-1 b** (taken from the information sheet, KOMP PCR design). Genotyping is carried out by Dr. Robert Pope (University of Bristol, UK) and the result is checked for all animals used in this study.

a

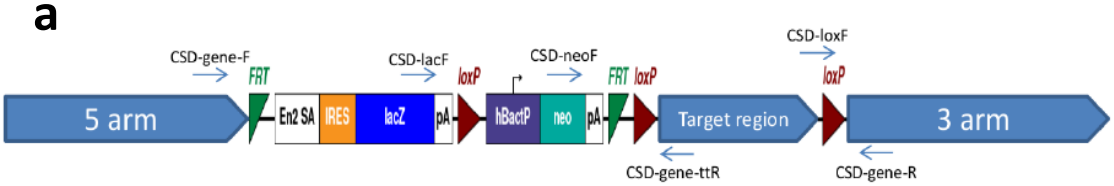

b

Cassette primers		Gene specific primers	
CSD-lacF	GCTACCATTACCAGTTGGTCTGGTGTC	CSD-Grik1-R	TAAGGGCCTCAGCATCTTCCTCTCC
CSD-neoF	GGGATCTCATGCTGGAGTTCTTCG	CSD-Grik1-ttR	AGGAGAGAGGATTAGTGAACGGTGC
CSD-loxF	GAGATGGCGCAACGCAATTAATG	CSD-Grik1-F	AAAAGACGAAACCCTGGAAATCGCC

Figure 2-1. Insertion sites for loxP and FRT
a. Illustration of insertion sites for loxP and FRT (Illustration taken from the information sheet provided by KOMP PCR design)
b. A table showing primer sequences for genotyping

2.2. Preparation for in vitro electrophysiology

2.2.1. Solutions

A stock of artificial cerebrospinal fluid (aCSF) solution is prepared at 10 times the final concentration. On the day of experiments, stock solution is diluted to 1-times concentration. Recording aCSF solution contains (in mM) NaCl (124), KCl (3), NaH_2PO_4 (1.4), $MgSO_4$ (1), $NaHCO_3$ (26), D-glucose (10), $CaCl_2$ (2). Sucrose solution is used as slicing solution. Sucrose solution contains (in mM) NaCl (87), D-Glucose (25), Sucrose (75), $NaHCO_3$ (25), KCl (2.5), NaH_2PO_4 (1.25),

$MgCl_2$ (7), $CaCl_2$ (0.5). aCSF and sucrose solutions are oxygenated with mixed gas (95% O_2 / 5% CO_2) at least 20 min prior to usage.

2.2.2. Anaesthesia

An induction chamber is connected to an oxygen concentrator and an isoflurane vaporizer (E-Z Anaesthesia, Euthanex Corp.). Perforated sheet metal flooring is provided for animals to avoid direct contact with isoflurane gas. When animals are placed in the induction chamber, a mixture of oxygen (1 L/min) and 5% isoflurane is introduced into the chamber. When animals are irresponsive to a toe pinch, it is removed from the chamber and cervical dislocation is carried out immediately. Decapitation is followed using a guillotine or scissors and the tip of the tail or an ear punch is taken for genotyping. Tail or ear tissue is put in an e-tube with the label of the experimental date and stored in a -20 °C freezer.

2.2.3. Slice preparation

The skin is cut with a knife (blade #22) exposing the skull. Interparietal bone and occipital bone are cut first and the midline of the skull is cut with fine scissors. Using forceps or rongeurs, the parietal bone is lifted up and the meninges are removed. After the olfactory lobe is cut, the brain is brought out and dropped to pre-chilled sucrose solution. The brain is dissected in a petri dish filled with pre-chilled sucrose solution. The cerebellum and olfactory bulbs are removed. The two hemispheres of the brain are split by cutting along the midline. The midbrain is taken out exposing the hippocampi on each side and the fibers to the fornix and the ventral part of hippocampus are cut. The hippocampus is gently pushed out and placed on a 2.5 % agar block. Excessive solution is soaked up around the hippocampi with filter paper. The agar block is attached to the slicing platform using super glue and placed into the slicer. Slicing chamber is surrounded by ice and filled with bubbled sucrose solution. All tools that are used in the dissection is pre-chilled in ice. 400 µm hippocampal slices are cut and transferred to room temperatured aCSF briefly to wash out the sucrose solution. Slices are incubated in aCSF warmed up to 32 °C for 20 min and transferred to room temperature aCSF and rested for 40 min.

2.2.4. *in vitro* electrophysiology

The electrophysiology rig consists of a recording chamber, a microscope, manipulators and stimulation boxes which sit on an air table in a faraday cage to avoid interference from mechanical disruption or electromagnetic noise. The microscope is installed above the recording chamber helping visual guidance of the manipulators to the slice. The recording chamber is surrounded by an oxygen tube and in-line heating coil generating a warm and humid environment. The temperature of the surrounding water is maintained at 32 °C providing a temperature of 29 ± 1 °C in the recording chamber. aCSF is warmed up at 35 °C in a water bath, circulated into the recording chamber and drained by a suction pump. Constant flow of aCSF at 2 ± 0.2 ml/min is checked and maintained throughout the experiments.

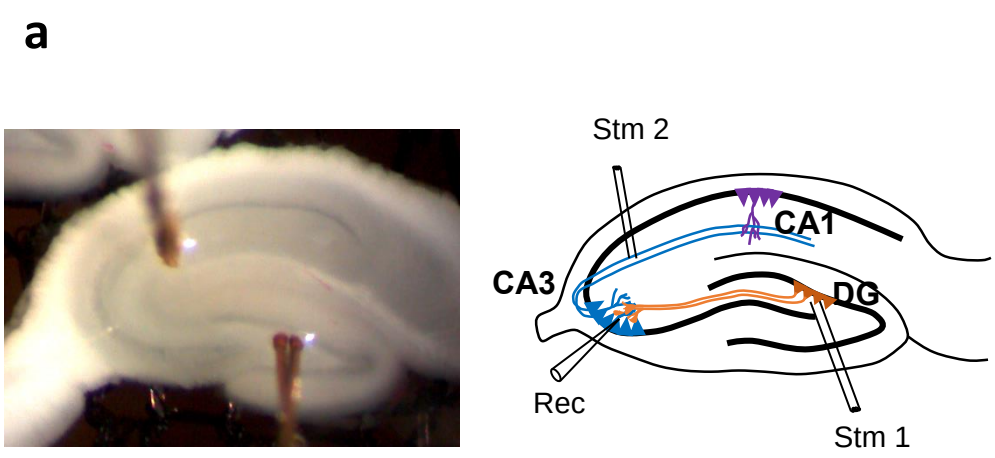

Figure 2-2. Location of two stimulating electrodes and the recording electrode **a.** Left panel: A snapshot of the slices. Right panel: A diagram showing location of recording and stimulating electrodes (Stm: stimulating electrode, Rec: recording electrode)

Glass pipettes for the recording electrodes are prepared using borosilicate glass and pulled using a micropipette puller (Sutter instruments) and it is filled with 4 M NaCl solution. Resistance of the electrodes is tested and only electrodes with a low resistance (3 - 7 mΩ) are used for

experiments. Twisted bipolar stimulating electrodes using 80% nickel 20% chromium wire (⌀ 0.05 mm) annealed with FORMBAR is used.

The recording electrode is placed in the stratum lucidum in CA3. There are two stimulating electrodes; one of them is placed just below granule cell layer (stratum granulosum) in the DG and the other in the Schaffer collateral in CA1 (**Figure 2-2 a**). Field excitatory postsynaptic field potentials (fEPSPs) are evoked every 30 s (0.033 Hz) in each pathway and placement of stimulating or recording electrodes is adjusted according to the size and shape of the synaptic responses. Prior to the beginning of experiments, 5 pulses of stimulation (50 Hz, 20 ms interval, high frequency stimulation, HFS) are delivered. From this point, HFS exclusively refers 5 pulses at 50 Hz and LFS refers 30 pulses at 1 Hz. Synaptic responses which express a clear and noticeable increase in fEPSP from 1st to 5th response are used for experiments. A tetanus at 100 Hz for 1 s is given to induce LTP and LFS at 1 Hz for 30 s is used to elicit LFF.

Two amplifiers, one an Axoclamp 2B amplifier (Axon Instrument, USA) and the other a FLA-01 Filter/Amplifier (Cygus Technology Inc.) are used to amplify the signal. Analogue signal is transformed to a digital signal using a Digiboard (National Instruments, BNC-2120) and 50/60 Hz noise is eliminated by using a Humbug (Quest scientific, Canada). Isolated stimulators DS2A (Digimeter Ltd.) are used to stimulate two inputs. fEPSPs are obtained and analysed using the WinLTP program (Anderson & Collingridge 2007). At the end of experiments, a snapshot of the placement of the recording and stimulating electrodes is taken by a frame fixed camera (Leica MS5).

2.3. Experimental scheme

2.3.1. General scheme

For those experiments that used genetic KO animals, the experimenter was blinded prior to the dissection and the genotype was also checked postnatally by genotyping.

Figure 3-1 contains experiments carried out in parasagittal and transverse slices. Parasagittal slices are used in Figure 3-7. All other experiments are carried out in transverse slices. Figure 3-1 a includes all the data from every condition as HFF was checked before a drug is applied. As the time point for PTP is after drug application, only the data obtained in the control condition is used in Figure 3-1 b and c. PTP and LTP data from all experiments are pooled in Figure 3-1 d regardless of drug application.

In ATPA experiments (Figure 4-1 to 4-6 and Figure 6-1 to 6-5), the peak depression points for each set of experiments varied slightly. Therefore, the time point for comparison is chosen for each set of experiments as follows: In Figure 4-1 to 4-3, the basal transmission at 36 min is selected for comparison in WT and KO animals and the point at 40 min is selected for Figure 4-4 to 4-6. The amplitude at 34 min were chosen for Figure 6-1 to 6-5.

The time line of drug application used in HFF and LFF experiments (Figure 4-9 to 4-13 and Figure 5-3 to 5-6) is plotted in **Figure 2-3 a**. 20 min of initial baseline is obtained in the presence of D-AP5 (50 μM) and then GYKI 53655 (30 μM) is added to the recording solution thereafter. HFF and LFF responses obtained in this condition are used as the control condition for each experiment. HFF and LFF responses are also obtained in the presence of drug (e.g. ACET,

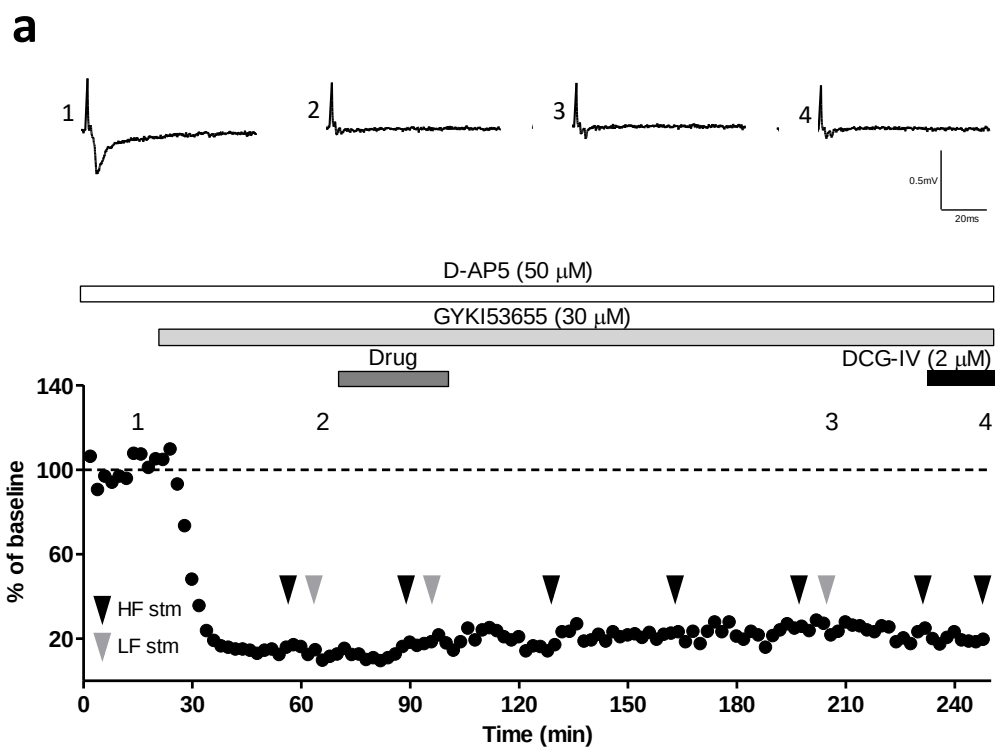

Figure 2-3. Drug application scheme for HFF and LFF experiments
a. An example figure demonstrating the drug application scheme. Upper panel: Sample traces of fEPSP are taken in each condition where numbers are indicated in the lower panel. Size of the fiber volley does not change throughout the experiment. Lower panel: 20 min of initial baseline is acquired in the presence of D-AP5 (50 μM) and GYKI 53655 (30 μM) is applied to the recording solution until the end of experiment. Arrows indicate when stimulations are given. Black arrow: HFS(5 pulses at 50 Hz), grey arrow: LFS (30 pulses at 1 Hz)

UBP2002 or UBP2038) and 2 h of wash out follows. During the washing out, HFF response is checked every 30 min for 2 h but only the response obtained at the 1 h 30 min time point is used to generate the data. LFF is checked only at 1 h 30 min of wash out. DCG-IV (2 μM) is added to the solution at the end of experiment and HFF is also checked in this condition. Within a set of experiments, 6 min of recording prior to LFF stimulation is used as baseline and another 6 min of recording follows.

Sample traces of fEPSPs shown in the upper panel of Figure 2-3 a are taken from each point where numbers are indicated in the lower panel. A measurable amplitude of fEPSPs is nearly absent in the control condition (**Figure 2-3 a, trace 2**) only leaving the fiber volley. The size of fiber volley stays the same until the end of the experiment indicating that stimulation intensity is constant throughout the experiments. Also, the fact that the amplitude of fEPSPs does not change after HFS and LFS demonstrates that HFS and LFS used in this study do not elicit long term plasticity.

Values used in the LFF summary bar chart are taken from the averaged last 5 points during LFS. 1 h after tetanus, the last 5 points were averaged and presented as the degree of MF-LTP.

HFS that consists of 5 pulses at 50 Hz (20 ms interval) is delivered to elicit HFF. Since HFF experiments are carried out in the presence of D-AP5 (50 μM) and GYKI 53655 (30 μM), there are no detectable fEPSPs in response to the first pulse. For this reason, facilitation presented as a percentage of the first response ($5^{th}/1^{st}$ amplitude, %) is not possible as the 5^{th} response compared to the 1^{st} response would be infinite. Therefore, 0.1 ms of baseline is taken at the time when the amplitude of the 4^{th} response is most decayed and the amplitude of the 5^{th} pulse is measured. The amplitude of the 5^{th} pulse in the control condition (D-AP5 and GYKI 53655) is set as 100%. As drug is applied and washed out, changes in the amplitude of the 5^{th} response are measured and compared to the control condition.

In all experiments, DCG-IV (2 μM) is applied for 15 min at the end of the experiments to ensure the response originates from the MF and only experiments that show > 70% of depression are included in the data except Figure 3-1 (Contractor et al 2001, Sherwood et al 2012).

For data obtained from Mr. Alen Eapan (**Figure 5-1 d**), experiments are carried out in 3-4 weeks old Wistar rats. 400 μm thick transverse slices are prepared and experiments are carried out in the condition that contains 2 mM of Ca^{2+} and 2 mM of Mg^{2+}.

2.3.2. Analysis

As GCs send long axonal projections to CA3 to form MF synapses, obtaining intact mossy fiber projections is difficult and often axons get cut when slices are prepared. Therefore, stronger intensity of stimulation (10 - 40 V for 0.2 ms) was given to evoke postsynaptic responses. Higher intensity stimulation generated bigger fiber volleys, sometimes contaminated by postsynaptic responses, making measuring the slope of fEPSPs rather unreliable. Therefore, we measured the amplitude of fEPSPs instead in this study as in previous studies (Breustedt & Schmitz 2004, Schmitz et al 2003, Sherwood et al 2012). Data are acquired and analysed using WinLTP (Anderson & Collingridge 2007). Amplitude of fEPSP is measured every 30 s and 4 consecutive responses are averaged over 2 min. Experiments are conducted after 20 - 30 min of stable baseline.

2.3.3. Calcium fluorescence assay

Data acquired from Dr. Robert Thatcher and Mr. Alen Eapen (University of Bristol, UK) is obtained from a calcium fluorescence assay using a FlexStation (Molecular Devices, LLC). HEK293 cells overexpressing human homomeric GluK1 (Q), GluK2 (Q) and GluK3 receptors are used in the calcium assay. The half maximal inhibitory concentration (IC_{50} value) is calculated based on the inhibitory constant (K_i value) obtained in the assay using the Cheng-Prusoff correction ($\mathrm{Ki} = \mathrm{IC50} / 1 + (\frac{[\mathrm{ligand}]}{\mathrm{Kd}})$). Glutamate is used as agonist in the experiment.

2.4. Statistics

Results are presented as mean ± standard error of the mean (SEM). For statistical comparisons, unpaired t-tests, spearman correlation, and one-way ANOVA (analysis of variance) are used as appropriate. If data is obtained from the same sample with consecutive treatments, one-way ANOVA repeated measures is used. Tukey test is used for post hoc multiple comparison test to compare all groups. Two-way ANOVA is used when there are more than two experimental factors and Bonferroni post hoc test is used for Two-way ANOVA. Statistical analysis is carried out using GraphPad Prism (GraphPad Software).

Summary graphs showing the level of LFF (Figure 3-3 d and 3-5 e), PTP (Figure 3-4 d and 3-6 e) and LTP (Figure 3-4 e and 3-6 f) are analysed by one-way ANOVA (Tukey post hoc test) only once including all groups together but presented into two graphs. Control conditions for each

experiment are presented twice (Figure 3-3 a and 3-5 a, Figure 3-4 a and 3-6 a) for comparison but not used twice for analysis.

For HFF experiments (Figure 4-10, 4-12, 5-3, 5-5 and 5-7), the DCG-IV group was excluded from the analysis (one-way ANOVA, repeated measures) since the DCG-IV group is presented only as a parameter to show that the synaptic responses are coming from the MF.

***p < 0.001, **p < 0.01, *p < 0.05.

2.5. Drugs

GluK1 and GluK2 antagonists (UBP3000, UBP2002 and UBP2038) are kindly provided by Prof. David Jane (University of Bristol, UK) and others are purchased from distributors. All drugs are prepared according to their provided datasheets and dissolved in suitable solvent. 100 - 1000 times concentrated stock is prepared and stored at -20°C until diluted in aCSF on the day of use.

ACET (Tocris)

ATPA (Tocris)

D-AP5 (HelloBio)

DCG-IV (Tocris)

GYKI 53655 (Tocris)

(*S*)-MCPG (Tocris)

UBP2002 (Prof. David Jane)

UBP2038 (Prof. David Jane)

UBP3000 (Prof. David Jane)

Chemical names

(*S*)-MCPG – (*S*)-α-Methyl-4-carboxyphenylglycine

ACET – (*S*)-1-(2-Amino-2-carboxyethyl)-3-(2-carboxy-5-phenylthiophene-3-yl-methyl)-5-methylpyrimidine-2,4-dione

ATPA – (*RS*)-2-Amino-3-(3-hydroxy-5-tert-butylisoxazol-4-yl)propanoic acid

CNQX – 6-Cyano-7-nitroquinoxaline-2,3-dione

D-AP5 – D-(-)-2-Amino-5-phosphonopentanoic acid

DCG-IV – (*2S,2'R,3'R*)-2-(2',3'-Dicarboxycyclopropyl) glycine

GYKI 53655 – 1-(4-Aminophenyl)-3-methylcarbamyl-4-methyl-3,4-dihydro-7,8-methylenedioxy-5H-2,3-benzodiazepine hydrochloride

NBQX – 2,3-Dioxo-6-nitro-1,2,3,4-tetrahydrobenzo[f]quinoxaline-7-sulfonamide disodium salt

UBP2002 – 6-iodo kynurenic acid

UBP2038 – 5,7-difluoro, 6-iodo kynurenic acid

UBP296 – (*RS*)-3-(2-carboxybenzyl) willardiine

UBP3000 – (*S*)-4-((3-(2-amino-2-carboxyethyl)-5-methyl-2,6-dioxo-3,6-dihydropyrimidin-1(2H)-yl)methyl)-2-phenylthiazole-5-carboxylic acid

UBP301 – (α*S*)-α-Amino-3-[(4-carboxyphenyl)methyl]-3,4-dihydro-5-iodo-2,4-dioxo-1(2*H*)-pyrimidinepropanoic acid

UBP302 – (*S*)-3-(2-carboxybenzyl) willardiine

UBP310 – (*S*)-1-(2-Amino-2-carboxyethyl)-3-(2-carboxy-thiophene-3-yl-methyl)-5-methylpyrimidine-2,4-dion

Chapter 3. Results: GluK1 antagonism does not change mossy fiber characteristics in Wistar rat

3.1. Introduction

Unlike Schaffer collateral-CA1 synapses, hippocampal MF synapses exhibit an NMDAR-independent form of LTP (Bortolotto et al 1999) and robust frequency facilitation. Frequency facilitation is a unique feature of the MF synapses as its neighbouring synapses do not exhibit such enhancement of synaptic response (Salin et al 1996). A broad range of frequency can be used, for example high frequency stimulation that consists of 5 pulses at 25 - 100 Hz (HFS) generates high frequency facilitation (HFF) in which the synaptic response shows a many fold increase. Low frequency stimulation (LFS) such as 30 pulses at 1 Hz also elicits facilitation of synaptic response with slow onset (low frequency facilitation, LFF) (Nicoll & Schmitz 2005, Salin et al 1996). To date, there is a general agreement that presynaptic KARs function as autoreceptors in this phenomenon, but the identity of the key KAR subunits has long been debated. For example, studies with specific GluK1 antagonists LY382884 (Bortolotto et al 1999, Lauri et al 2001a, Lauri et al 2001b), UBP310 (Dolman et al 2007) and ACET (Dargan et al 2009) demonstrated that specific GluK1 antagonism can block the induction of MF-LTP and HFF. However, genetic ablation of the GluK2 subunit impaired MF-LTP and HFF while genetic ablation of GluK1 did not (Breustedt & Schmitz 2004, Contractor et al 2001) suggesting a role for the GluK2 subunit.

A recent study suggested a possible explanation for this discrepancy could be that the slice orientation results in different lengths of axon and sizes of MF bouton, leading to differential involvement of KAR subunits (Sherwood et al 2012). The authors demonstrated that slices with different orientations possessed different sensitivity to the group II mGluR agonist, DCG-IV. As activation of group II mGluRs suppress MF transmission by a presynaptic action (Kamiya et al 1996), we were interested if there was a relationship between DCG-IV sensitivity and the involvement of KAR subunits in MF synapses. Therefore, we sought to find a link between DCG-IV sensitivity and specific features of MF synapses, for which the results are described in this chapter.

We carried out experiments separately with parasagittal or transverse slices and found variable degrees of DCG-IV sensitivity in both orientations. Therefore, we collected all experimental data from both orientations and plotted according to sensitivity to DCG-IV. Synapses that showed ≥ 70% of inhibition compared to baseline after 15 min of DCG-IV (2 μM) application were

categorized as 'DCG-IV sensitive synapses' and synapses that showed < 70% inhibition as 'DCG-IV insensitive synapse'.

It is worth noting that as the previous studies were carried out mainly in juvenile animals (P12-P35), it was best to experiment on juvenile animals. However, as the original aim was to conduct experiments *in vivo*, we chose to carry out experiments mainly on adult Wistar rats.

To explore the effect of GluK1 antagonism on MF function, we used a newly synthesised GluK1 antagonist, UBP3000, as well as ACET. UBP3000 is a willardiine derivative and an analogue of ACET. A calcium fluorescence assay confirmed that UBP3000 has antagonistic activity at GluK1 subunit but exhibits less potency toward GluK1 compared to ACET. Since group I mGluRs have been implicated to play a part in MF-LTP (Wallis et al 2015), antagonism of mGluRs by (*S*)-MCPG was also examined to define the role of mGluRs on MF.

3.2. Result

3.2.1. DCG-IV sensitive synapses express stronger characteristics of mossy fiber synapses

To look at the relationship between DCG-IV inhibition of MF transmission (Kamiya et al 1996, Yoshino et al 1996) and the MF features HFF and post tetanic potentiation (PTP), we plotted the sensitivity of these features to DCG-IV (15 min application, 2 µM). Those from transverse slices are represented by filled circles, those from parasagittal slices by open circles. HFF was measured by comparing the amplitude of the 5^{th} response to the 1^{st} response elicited by 5 pulses at 50 Hz stimulation (5^{th} / 1^{st} amplitude, %). Synapses which were strongly suppressed by DCG-IV had a clear tendency to show greater HFF demonstrating a positive correlation (n = 51, ***p = 0.0006, spearman correlation, one-tailed) (**Figure 3-1 a**). PTP, a form of short-term plasticity, is observed after a tetanic stimulation to an exceptional degree at MF synapses (Langdon et al 1995). In our experiments, the extent of DCG-IV sensitivity and PTP also showed a strong positive correlation. Thus, there was a clear tendency for DCG-IV sensitive synapses to show bigger PTP and for insensitive synapses to display smaller PTP (n = 15, ***p < 0.001, spearman correlation, one-tailed) (**Figure 3-1 b**). The HFS that induces HFF consisted of 5 pulses at 50 Hz and is below the threshold to induce LTP. The single tetanus that elicits PTP and MF-LTP consisted of 100 pulses at 100 Hz. There was a positive correlation between the degree of PTP and HFF such that synapses with higher HFF expressed bigger PTP (n = 14, ***p < 0.001, spearman correlation,

two-tailed) (**Figure 3-1 c**) and synapses with bigger PTP developed more robust MF-LTP (n = 55, ***p < 0.001, spearman correlation, two-tailed) (**Figure 3-1 d**).

Interestingly, in Figure 3-1 a and b, we observed that synaptic responses from parasagittal slices (open circle) and transverse slices (filled circle) are very different in terms of DCG-IV sensitivity. The majority of parasagittal responses were DCG-IV insensitive (DCG-IV insensitive: 81.8%, 9 out of 11 experiments; DCG-IV sensitive: 18.2%, 2 out of 11 experiments). On the other hand, synaptic responses from transverse slices were mainly DCG-IV sensitive (DCG-IV sensitive: 83.7%, 36 out of 43 experiments; DCG-IV insensitive: 16.3%, 7 out of 43 experiments) **(Figure 3-1 e**). Taken together, we confirmed that DCG-IV sensitive responses express a high level of HFF and PTP that are unique features of MF synapses. Also, these features are very prominent in transverse slices. This indicates that DCG-IV sensitive response is most likely to represent 'pure MF'. Since transverse slices contain a high proportion of DCG-IV sensitive responses, we decided to use transverse slices based on this finding.

3.2.2. GluK1 antagonism does not affect LFF

Based on the observation that DCG-IV sensitive synapses are more likely to show features that are unique to MF synapses, we decided to focus on DCG-IV sensitive synapses and tested GluK1 antagonists on LFF and MF-LTP to see whether GluK1 antagonism affects normal MF synaptic function. For GluK1 antagonism, we chose a highly potent GluK1 antagonist ACET (Dargan et al 2009). Along with ACET, we also tested a newly synthesised compound that is an analogue to ACET, UBP3000 (synthesised by the laboratory of Prof. David Jane, University of Bristol, UK) (**Figure 3-2 a and b**). A calcium fluorescence assay in which HEK293 cells expressing homomeric GluK1 (Q) was employed to check the affinity of UBP3000 to the GluK1 subunit. The affinity of UBP3000 to the GluK1 subunit (K_i = 54.8 ± 11.5 nM, n = 3) was weaker compared to ACET (K_i = 5.93 ± 0.74 nM, n = 3) (**Figure 3-2 c**, data provided by Dr. Robert Thatcher, University of Bristol, UK, n = 3). UBP3000 showed a selective antagonistic effect against the GluK1 subunit (data not shown, unpublished result, Prof. David Jane). As a novel GluK1 antagonist, we used UBP3000 along with ACET for GluK1 antagonism.

It has been shown that a specific protocol (e.g. 1 Hz for 30 s) of LFS applied to MF synapses induces a slow onset of synaptic facilitation (Salin et al 1996, Scanziani et al 1997). To elicit LFF, the frequency was increased from 0.033 Hz (the baseline frequency) to 1 Hz for 30 s. In the control condition, this LFS induced a gradual increase of MF response (to 239.1 ± 18.1% of

baseline, n = 7) (**Figure 3-3 a, left panel**). Example traces in the control condition are taken from the points indicated in the graph and presented in the right panel of **Figure 3-3 a**.

A relatively high concentration of UBP3000 (3 µM) was chosen for the test as its affinity is 10 times weaker than ACET for GluK1. LFS facilitated the MF response to 299.1 ± 23.2% of baseline in the presence of UBP3000, not statistically different to the control condition (n = 5, $p > 0.05$, one-way ANOVA) (**Figure 3-3 b,** the grey trace within the graph shows LFF in the control condition). In interleaved experiments, ACET (50 nM) was tested. In the presence of ACET, the response reached 234.2 ± 33.9% of baseline (n = 5, **Figure 3-3 c**) showing comparable LFF to the control condition. Summary chart shows that GluK1 antagonism does not change the degree of LFF ($p > 0.05$, one-way ANOVA) (**Figure 3-3 d**).

NMDAR-independent MF-LTP in DCG-IV sensitive synapses was investigated using the same compounds as above. In control conditions, a classic tetanus stimulation (100 Hz, 1 s) induced a clear enhancement of the MF response which lasted 1 h after the induction (149.8 ± 23.8% of baseline, n = 8) (**Figure 3-4 a, left panel**). Sample traces during LTP experiments are taken from the Figure 3-4 a and presented in the right panel (**Figure 3-4 a, right panel**). 20 min of UBP3000 (3 µM) application did not affect the basal transmission and was unable to block MF-LTP (162.6 ± 33.5% of baseline, n = 7, $p > 0.05$, one-way ANOVA) (**Figure 3-4 b and e**). Also, ACET did not affect MF transmission and failed to block MF-LTP (141.8 ± 13.7% of baseline, n = 5, $p > 0.05$, one-way ANOVA) (**Figure 3-4 c and e**).

The degree of PTP varied over a great range in general and the level of PTP between groups was not significantly different (464.2 ± 58.3% for control, 276.4 ± 40.0% for UBP3000, 389.1 ± 56.0% for ACET, $p > 0.05$, one-way ANOVA) (**Figure 3-4 d**).

3.2.3. Co-application of the mGluR antagonist (*S*)-MCPG with GluK1 antagonism does not affect LFF and MF-LTP

Previously, it was shown that inhibition of both GluK1 subunit and mGluRs by ACET and MCPG together could block MF-LTP *in vivo* (Wallis et al 2015). We wanted to test whether this combination could block LFF and MF-LTP. The control experiments in Figure 3-5 a are taken from Figure 3-3 a for comparison. A broad mGluR antagonist (*S*)-MCPG (Bashir et al 1993) at a relatively high concentration (500 µM) was chosen for near-complete inhibition of mGluRs. Firstly, the effect of application of (*S*)-MCPG alone was tested on LFF. The synaptic response was facilitated to 278.7 ± 18.5% of baseline which is a comparable degree to the control condition (n

= 6) (**Figure 3-5 b**). A combination of UBP3000 and (*S*)-MCPG was examined next. A similar degree of LFF was elicited (286.3 ± 35.9% of baseline, n = 7) (**Figure 3-5 c**). In interleaved experiments, co-application of ACET (50 nM) with (*S*)-MCPG did not change the magnitude of facilitation induced by LFS (243.4 ± 31.6% of baseline, n = 5) (**Figure 3-5 d**). The summary chart shows that GluK1 antagonism even with mGluR inhibition does not change the degree of LFF ($p > 0.05$, one-way ANOVA) (**Figure 3-5 e**).

A combination of GluK1 and mGluR antagonism was tested on MF-LTP as well. As previously shown (Figure 3-6 a is taken from Figure 3-4 a for comparison), MF-LTP is readily induced in the control condition (**Figure 3-6 a**). (*S*)-MCPG application alone did not affect the basal transmission (**Figure 3-6 b**) and the degree of PTP and LTP was comparable to the control condition (LTP: 169.1 ± 21.3% of baseline, n = 6, **Figure 3-6 e and f**). UBP3000 and (*S*)-MCPG together also did not affect synaptic transmission and MF-LTP was readily induced (1 out of 6 experiments had 200 µM of (*S*)-MCPG; including this experiment did not change analysed result) (162.7 ± 21.0% of baseline, n = 6) (**Figure 3-6 c**). Lastly, MF-LTP was tested in the presence of ACET with (*S*)-MCPG together. This combination also had no effect on transmission and MF-LTP induction (165.1 ± 13.5% of baseline, n = 5) (**Figure 3-6 d**). Addition of (*S*)-MCPG with GluK1 antagonists did not alter the degree of PTP (464.2 ± 58.3% for control, 452.6 ± 104.6% for (*S*)-MCPG, 317.8 ± 62.7% for UBP3000 + (*S*)-MCPG, 421.6 ± 59.5% for ACET + (*S*)-MCPG, $p > 0.05$, one-way ANOVA) (**Figure 3-6 e**). In summary, these combinations of antagonist did not affect PTP or LTP (**Figure 3-6 e and f**; $p > 0.05$, one-way ANOVA).

3.2.4. ACET does not block NMDAR-independent LTP in parasagittal slices

In transverse slices that are sensitive to DCG-IV application, we were not able to block MF-LTP with GluK1 antagonists. Additional blockade of mGluRs by (*S*)-MCPG was also ineffective. Since the previously GluK1 antagonism successfully blocked MF-LTP were in parasagittal slices (Sherwood et al 2012), we decided to test ACET in DCG-IV insensitive parasagittal slices. To be consistent with previous observation, we chose juvenile animals (P14). In control condition, the application of D-AP5 (100 µM) for 20 min did not change the basal transmission and a tetanus in the presence of D-AP5 readily induced NMDAR-independent LTP (162.5 ± 17.5% of baseline, n = 7) (**Figure 3-7 a**). The application of ACET (50 nM) with D-AP5 (100 µM) did not change the basal transmission and LTP was expressed at a comparable level to the control conditions (164.5 ± 22.3%, n = 6) (**Figure 3-7 b**). In both experiments, DCG-IV did not reduce the synaptic transmission. The level of PTP expressed in both conditions were similar (144.5 ± 14.6% for

control, 159.9 ± 22.8% for ACET, $p > 0.05$, unpaired T-test) (**Figure 3-7 c**) and the degree of LTP was also comparable ($p > 0.05$, unpaired T-test) (**Figure 3-7 d**).

3.3. Discussion

3.3.1. The unique feature of MF synapses

MF synapses show low release probability in normal conditions (Moore et al 2003). However, giant MF boutons innervate CA3 pyramidal neurons with multiple active zones (Acsady et al 1998), this means that MF synapses can release vast amounts of glutamate at once into the synaptic cleft when stimulated repetitively. On the other hand, small *en passant* terminals or filopodial extension innervate interneurons in stratum lucidum. Because of these structural differences, only MF synapses show frequency dependent facilitation while A/C synapses do not (Salin et al 1996). Previous research showed that MF-CA3 pyramidal neuron connections show greater HFF compared to MF-interneurons connections when 5 pulses at 20 Hz were delivered (Toth et al 2000). Also, a tetanus induced LTP in pyramidal cells while no change or LTD was elicited in interneurons (Maccaferri et al 1998, Toth et al 2000). This indicates synapses that exhibit a higher degree of HFF and LTP are more likely to be pure MF-CA3 pyramidal neuron connections. This fits our observation that the DCG-IV sensitive pathway expresses stronger HFF and PTP while DCG-IV insensitive synapses show HFF and PTP to a lesser degree.

3.3.2. The discrepancy over GluK1 antagonism in different slice orientation

Based on the assumption that DCG-IV sensitive slices are 'pure MF', we carried out experiments in transverse slices and found no effect of GluK1 antagonists on LFF, PTP and MF-LTP. This is consistent with the genetic studies with GluK1 KO animals (Breustedt & Schmitz 2004, Contractor et al 2001). However, the ineffectiveness of GluK1 antagonism could be due to the slice preparation used in genetic studies (transverse slice). Therefore, we tried to repeat the same experiments in parasagittal slices that are DCG-IV insensitive. Interestingly, we indeed observed LTP was induced in the presence of D-AP5 in DCG-IV insensitive slices, however, ACET was ineffective to block it. Our results are therefore not consistent with the theory put forward by Sherwood et al (2012) that slice orientation influences the involvement of GluK1 in MF function.

3.3.3. UBP3000 as a novel GluK1 antagonist

As a pharmacological approach using subunit specific antagonists is an effective way to investigate the role of KAR subunits, we obtained a newly synthesised compound through

collaboration with Prof. Jane's group. UBP3000, a willardiine-derivative that is an analogue of ACET was used. We checked its antagonistic effect and affinity against the GluK1 subunit in HEK293 cells using a calcium fluorescence assay and applied it to our electrophysiology experiments. UBP3000 is structurally very similar to ACET and selective to GluK1, however, it expresses 10 times weaker antagonistic activity at the GluK1 subunit. Our study on the function of GluK1 at MF synapses using ACET and UBP3000 revealed that GluK1 antagonism does not affect LFF, PTP and MF-LTP.

3.3.4. Role of mGluRs and GluK1 containing-KARs in synaptic plasticity at MF

There remains controversy regarding the role of mGluRs in MF function. Genetically modified mice lacking mGluR1 (Hsia et al 1995) and mGluR2 (Yokoi et al 1996) showed intact MF-LTP. The broad mGluR antagonist MCPG did not inhibit LTP in CA3 in some *in vitro* conditions (Mellor & Nicoll 2001). On the other hand, in other conditions, MCPG (Bashir et al 1993) and a group I mGluR antagonists efficiently blocked MF-LTP *in vitro* (Suzuki & Okada 2010, Yeckel et al 1999) and *in vivo* (Hagena & Manahan-Vaughan 2015). Our observation that a high dose of (*S*)-MCPG did not block MF-LTP in adult rat is consistent with the former study. Taken together, although the direct function of mGluRs in MF-LTP is still in question, they appear to have a role in modulating synaptic plasticity at MF synapses in some conditions (Mukherjee & Manahan-Vaughan 2013).

There was a study with *in vivo* recordings in adult Wistar rats that showed a combination of GluK1 and mGluR antagonism blocks MF-LTP (Wallis et al 2015). Therefore, we initially expected to see a further reduction of LFF with this combined treatment, if there is any inhibition by GluK1 antagonism. However, we did not see any alteration with or without (*S*)-MCPG on LFF, suggesting mGluRs does not have a role in this type of plasticity. Further highlighting the controversial role of mGluRs on LFF, there are studies that suggest that it is enhanced by mGluR inhibition. It was suggested that low frequency stimulation (1 - 4 Hz) can increase glutamate concentration at the synaptic cleft leading to activation of presynaptic mGluRs (Kwon & Castillo 2008b, Toth et al 2000). These activated presynaptic mGluRs, in turn, suppress glutamate release, creating negative feedback of MF synapses (Kwon & Castillo 2008b, Scanziani et al 1997). As in our experimental conditions, we could not demonstrate either a reduction or facilitation of LFF by (*S*)-MCPG application alone, the role of mGluRs still remains to be elucidated.

GluK1 antagonism with either ACET or UBP3000 on MF-LTP and LFF revealed that blocking GluK1-containing subunits does not impede potentiation caused by either low frequency (1 Hz

for 30 s) or high frequency (100 Hz for 1 s) stimulation. This augments the idea from KO studies that GluK1 is not the critical subunit that regulates MF functions (Breustedt & Schmitz 2004, Contractor et al 2001) and argues against the previous pharmacological studies (Bortolotto et al 1999, Lauri et al 2001a). Why is there a difference between previously published results and the ones presented here? In our study, we mainly used slices from adult rats while previous studies that show GluK1 antagonist blocked MF-LTP were carried out in juvenile rats. As GluK1 mRNA expression in CA3 is nearly absent in adult (Bahn et al 1994), it is possible that by the time animals reach full maturation, the role of the GluK1 subunit is diminished. The fact that a depressant effect of the GluK1 specific agonist ATPA is robust in young and juvenile animals and is lost in adult also supports this idea (Clarke & Collingridge 2002). Here, we tested the effect of ACET on MF-LTP in juvenile parasagittal slices, in an attempt to as closely match the conditions in which a role of GluK1 has been found as possible. However, we again found that ACET had no effect, therefore our results are not consistent with a role for GluK1 at early stages of development. Previous pharmacological studies reported that administration of various GluK1 antagonists blocked MF-LTP were carried out in female animals (Dr. Zuner Bortolotto, personal communication), therefore it remains a possibility that GluK1 plays a role specifically in female juvenile rats. Further studies on the role of GluK1 throughout development as well as possible sex difference will need to be performed to determine whether this is the case.

3.4. Conclusion

We investigated the relationship between DCG-IV sensitivity and unique MF features. When plotted according to DCG-IV sensitivity, we confirmed that DCG-IV sensitive synapses are more likely to have higher degree of PTP and HFF. This strong correlation indicates that synapses that shows high DCG-IV sensitivity reflect pure MF synapses.

In these DCG-IV sensitive synapses, we tested whether antagonism of GluK1 and mGluRs block LFF, PTP and NMDAR-independent LTP. With any combination of drug, we were unable to block LFF, PTP or LTP. The ineffectiveness of GluK1 antagonism did not differ according to DCG-IV sensitivity. This implies that GluK1-containing KARs may not play a critical role in regulating synaptic plasticity at CA3 MF synapses.

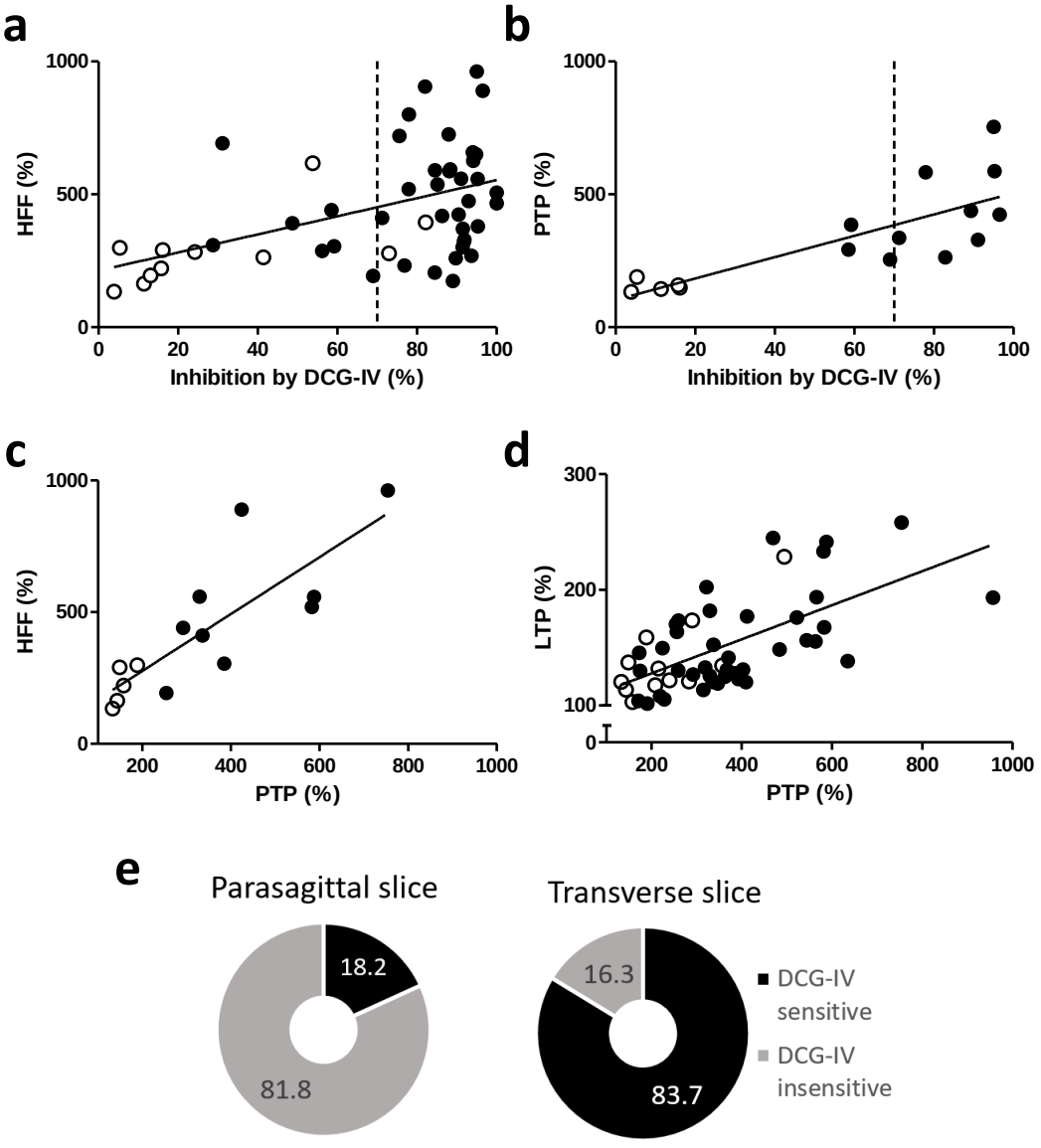

Figure 3-1. Characteristics of mossy fibre synapses and DCG-IV sensitivity in adult Wistar rat shows strong correlation
a. Correlation between DCG-IV sensitivity and HFF (n = 51, ***p = 0.0006).
b. Correlation between DCG-IV and PTP (n = 16, ***p < 0.001).
c. Correlation between PTP and FF (n = 14, ***p < 0.001).
d. Correlation between PTP and LTP (n = 55, ***p < 0.001).
e. Pie charts showing the percentage of DCG-IV sensitive response in the different slice preparations.
Dotted line in a and b: threshold line at 70% of inhibition, filled circle: transverse slices, open circle: parasagittal slices

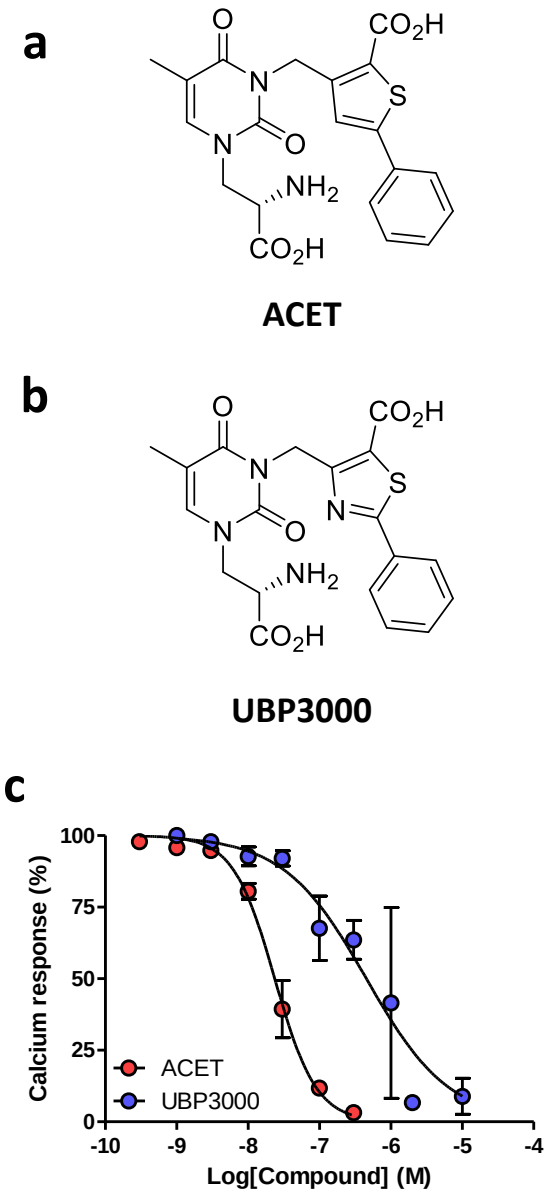

Figure 3-2. A newly synthesised GluK1 antagonist UBP3000
a. Structure of ACET, a potent GluK1 antagonist.
b. Structure of UBP3000, an analogue of ACET.
c. Concentration-response curve for ACET and UBP3000 on GluK1 obtained in calcium fluorescence assay (data provided by Dr. Robert Thatcher, University of Bristol, UK, n = 3).

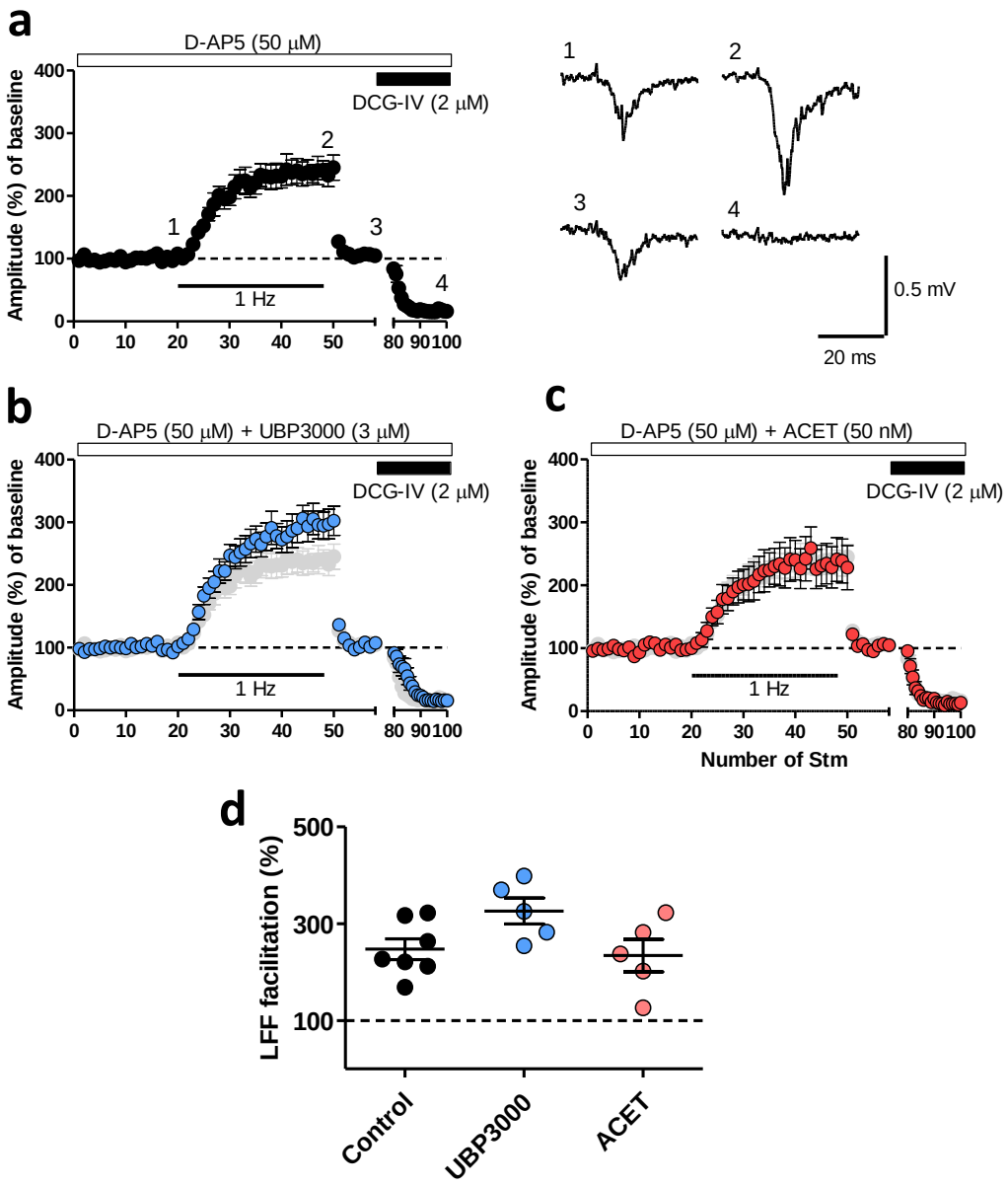

Figure 3-3. LFF is not affected by GluK1 antagonism.
a. Left panel: LFF is evoked by 30 s of 1 Hz stimulation. Right panel: Example traces are taken from where numbers are indicated in the graph.
b. 3000 does not block LFF.
c. ACET does not block LFF.
d. Summary graph for GluK1 antagonism on LFF ($p > 0.05$, one-way ANOVA)
Light grey trace in **b** and **c:** LFF in the control condition.

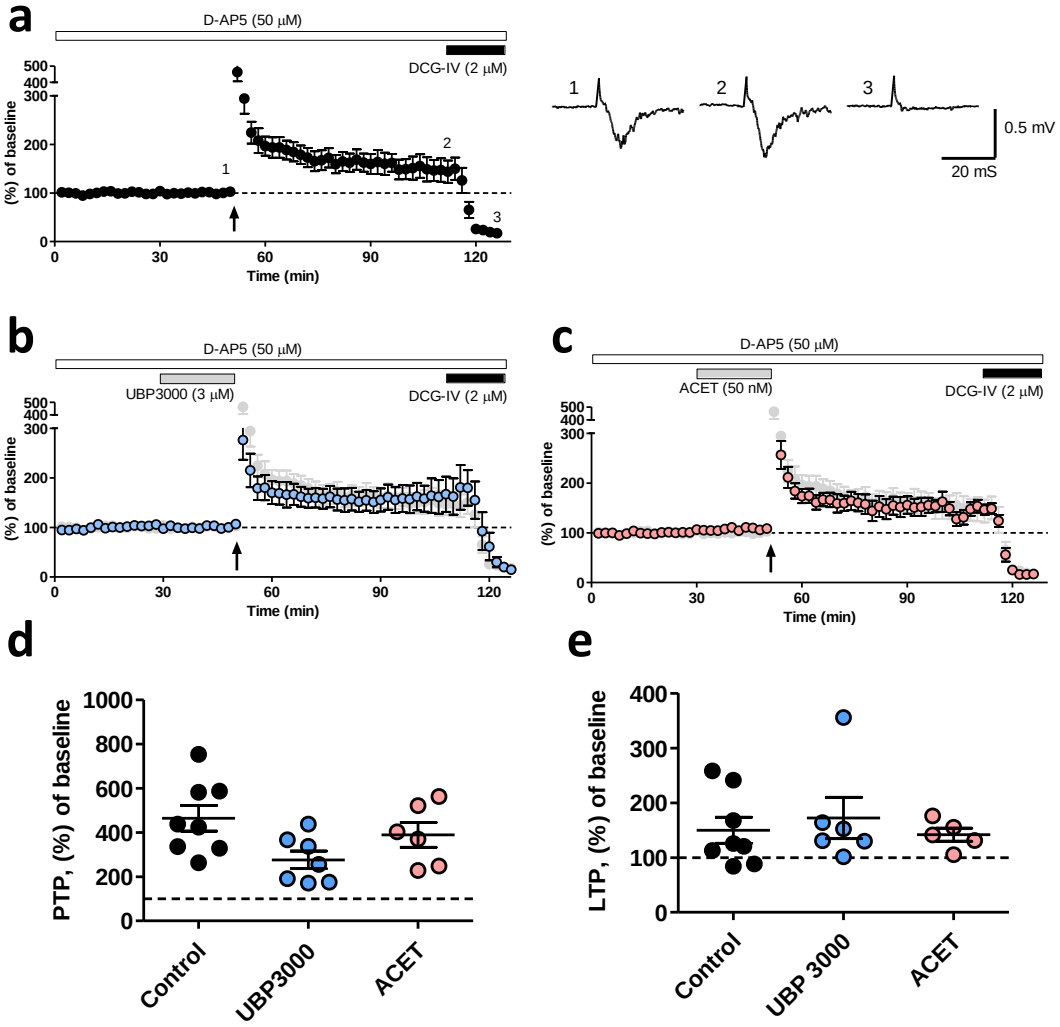

Figure 3-4. GluK1 antagonism does not affect MF-LTP. Various antagonist and combinations of antagonist used to investigate effect of GluK1 antagonism.
a. Adult Wistar rats express NMDAR-independent LTP in MF pathway in the hippocampus (n = 8). Right panel shows the sample traces are taken from the graph where the number are inserted.
b. Effect of UBP3000 (3 μM) on MF-LTP (n = 7).
c. ACET (50 nM) has no effect on MF-LTP (n = 6).
d. The degree of PTP in the presence of GluK1 antagonists ($p > 0.05$, one-way ANOVA)
e. Summary chart showing the degree of MF-LTP ($p > 0.05$, one-way ANOVA).
Light grey trace in **b** and **c**: MF-LTP in the control condition. Black arrow: a tetanus (100 Hz for 1s)

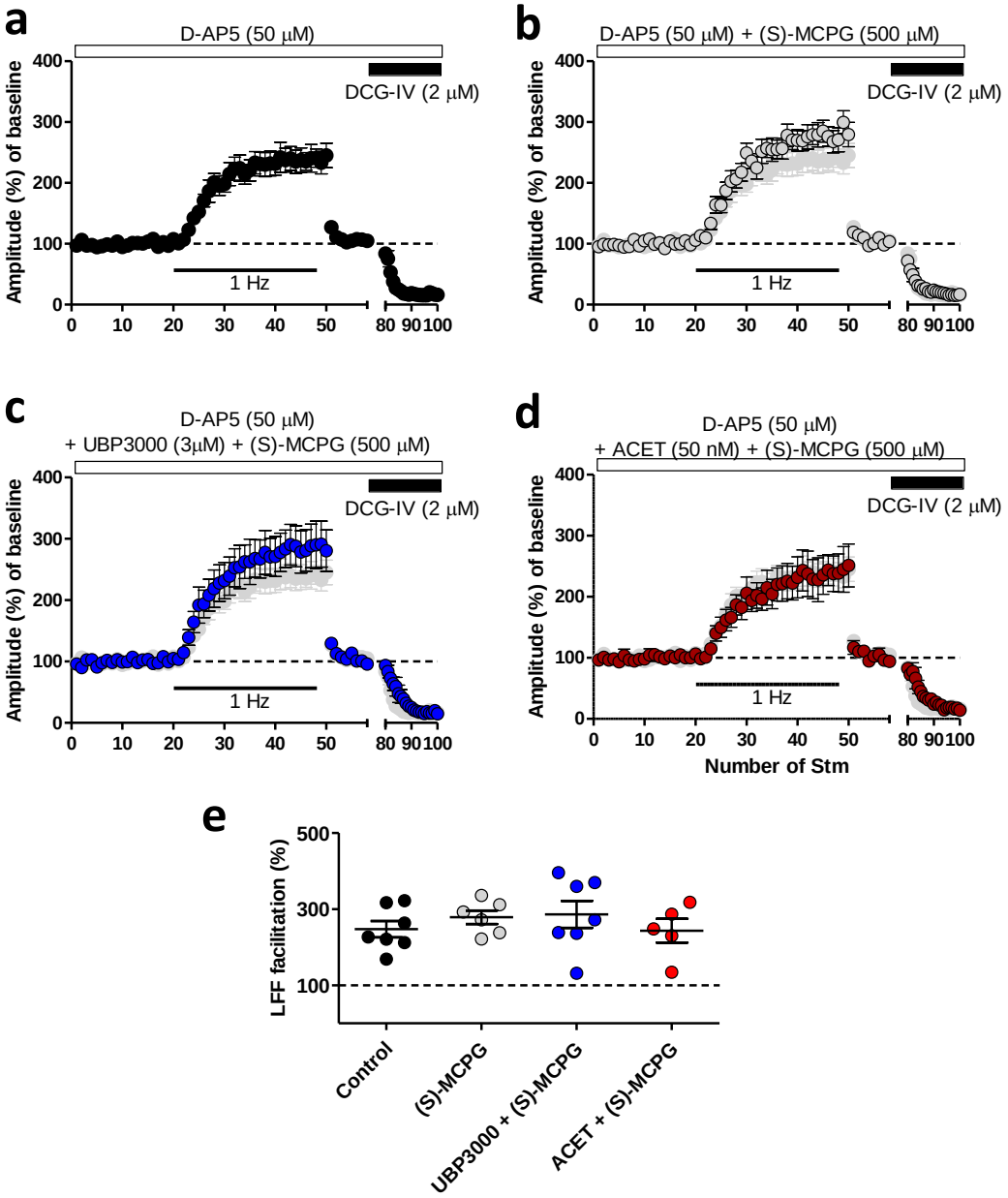

Figure 3-5. Additional antagonism of mGluRs does not affect LFF.
a. LFF in the control condition.
b. (*S*)-MCPG does not alter LFF.
c. Combination of UBP3000 and (*S*)-MCPG does not block LFF.
d. ACET with (*S*)-MCPG does not block LFF.
e. Summary graph for GluK1 antagonism on LFF ($p > 0.05$, one-way ANOVA).
Light grey trace in **b, c** and **d**: LFF in the control condition

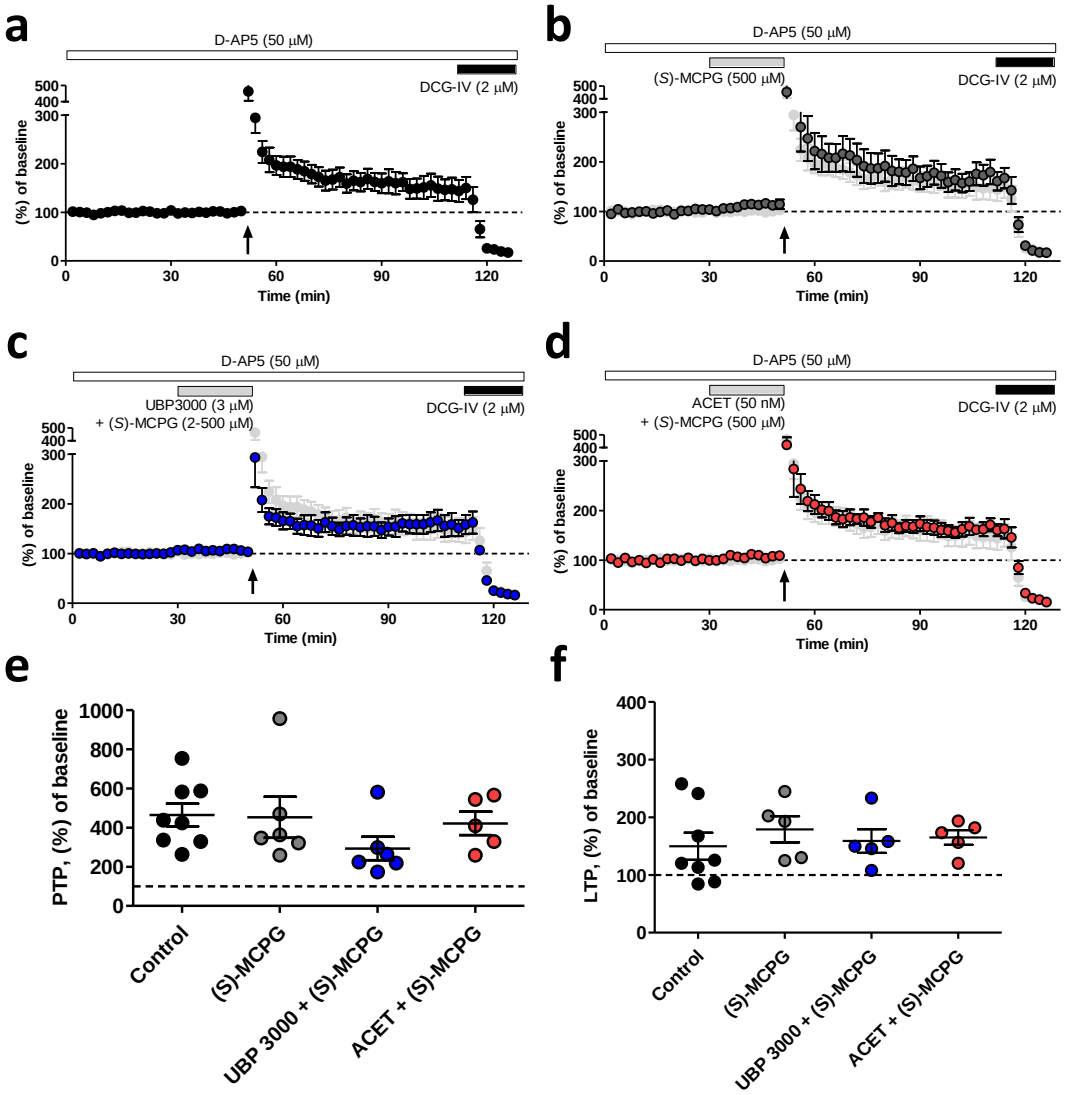

Figure 3-6. Additional mGluR antagonism does not affect MF-LTP.
a. NMDAR-independent LTP in the control condition (n = 8).
b. (*S*)-MCPG (500 µM) does not affect degree of MF-LTP (n = 5).
c. Combination of UBP3000 (3 µM) with (*S*)-MCPG (2-500 µM) does not affect MF-LTP (n = 6).
d. ACET (50 nM) with (*S*)-MCPG (500 µM) has no effect on MF-LTP (n = 6).
e. The degree of PTP in various combinations of antagonists ($p > 0.05$, one-way ANOVA).
f. Summary chart showing the degree of MF-LTP ($p > 0.05$, one-way ANOVA).
Light grey trace in **b, c** and **d**: MF-LTP in the control condition. Black arrow: a tetanus (100 Hz for 1s)

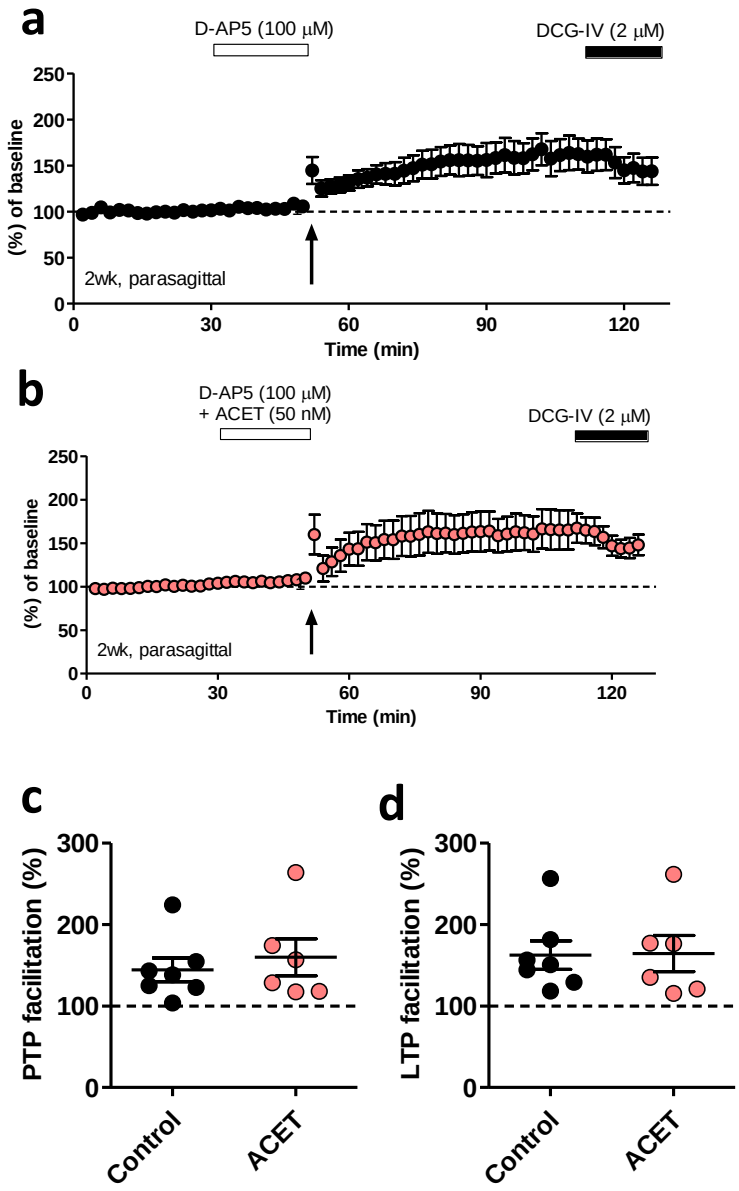

Figure 3-7. NMDAR-independent LTP in parasagittal slices
a. Expression of NMDAR-independent LTP in parasagittal slices (n = 7).
b. ACET does not block LTP (n = 6).
c. The degree of PTP is comparable ($p > 0.05$).
d. The degree of LTP is similar between two groups ($p > 0.05$).
Black arrow: a tetanus (100 Hz for 1s)

Chapter 4. Results: Investigating the role of GluK1 subunit in global GluK1 KO mice

4.1 Introduction

There is general agreement that presynaptic KARs are essential for synaptic transmission and an NMDAR-independent form of LTP at the MF. However, which KAR subunit plays the pivotal role has remained highly controversial. Pharmacological studies show that MF-LTP is blocked by specific GluK1 antagonists and HFF is reduced (Bortolotto et al 1999, Lauri et al 2001a). In contrast, genetic deletion of GluK2, but not GluK1, led to profound impairment of MF-LTP and HFF (Breustedt & Schmitz 2004). To address this discrepancy, we generated a DG-specific GluK1 KO which limit deletion of the protein only in the GC layer. In the process of generating these DG-GluK1 KO, we made a global GluK1 KO (also called Grik1 KO). In this chapter, we validate and characterize this global GluK1 KO mice by examining basic features of MF function, in particular including NMDAR-independent LTP, PTP, LFF and HFF.

To validate that global GluK1 KO mice do not express functional GluK1 subunit, we used the GluK1 specific agonist ATPA. ATPA was synthesised as an analogue of AMPA (Krogsgaard-Larsen et al 1982). In later studies, ATPA was found to be specific to GluK1 over other subunits (Clarke et al 1997) and to presynaptically reduce excitatory transmission in CA1 (Vignes et al 1998) as well as in CA3 region (Lauri et al 2001b). This depressant effect of ATPA on basal transmission was age-dependent (Clarke & Collingridge 2002), therefore, we divided age groups into three (2, 4, and more than 8 weeks old) then observed ATPA's effect on MF and A/C synapses throughout development. We speculated that ATPA would reduce basal transmission in all age groups in WT mice but to a different degree depending on developmental stage and that no reduction would be seen in global GluK1 KO mice.

After validation of functional GluK1 KO with ATPA, we investigated whether GluK1 KO animals preserve unique characteristics of MF such as NMDAR-independent LTP and frequency facilitation. To examine a broad range of frequency, we chose to deliver 30 pulses at 1 Hz for LFF and 5 pulses at 50 Hz for HFF. While investigating HFF and LFF, we applied D-AP5 (50 μM) as well as GYKI 53655 (30 μM) in the recording solution to block NMDARs and AMPARs throughout the experiments. GYKI 53655 is a non-competitive AMPA antagonist that acts on the allosteric modulatory site of AMPARs (Donevan & Rogawski 1998). As KARs do not have this site (Lerma et al 1993), we were able to isolate only KAR-mediated response with GYKI 53655 at the concentration of 30 μM (Wilding & Huettner 1995).

It is worth noting that during HFF, the response after each pulse did not fully recover to the baseline before the next pulse was delivered. In addition, the presence of D-AP5 and GYKI 53655 made it impossible to measure the amplitude of the 1st response during HFF. Therefore, we measured the amplitude of the 5th response during HFF and used it to show the degree of HFF. For statistical comparison, the amplitude of the 5th response during drug application and wash out were compared to the control condition.

4.1 Result

4.1.1. Validation of global GluK1 KO mice using ATPA

In a previous study, Lauri et al (Lauri et al 2001b) showed that 1 µM of ATPA, applied for 20 min, reduced MF synaptic transmission > 50% in rat hippocampal slices. We chose 10 min application of the same dose of ATPA to use in our experiments. ATPA's effect appeared after a short time lag. After 14-16 min of initiation of ATPA application, basal transmission reached the peak depression in MF and A/C and recovered to the baseline by 30 min of wash out. 15 min of DCG-IV (2 µM) application at the end of the experiments was used to dissect MF responses from A/C as only pure MF is depressed by group II mGluR activation.

In 2-week-old WT mice, ATPA depressed the synaptic transmission to 50 ± 8.5% of baseline in MF (n = 4) and 72.1 ± 0.0% of baseline in A/C synapses at 36 min (n = 3, **Figure 4-1 a**). In 4-week-old WT mice, ATPA reduced MF responses to 80.9 ± 9.9% of baseline (n = 6) while A/C responses reached 85.3 ± 4.7% of baseline (n = 6, **Figure 4-1 b**). In adult mice (8-16 weeks old), the effects of ATPA was nearly absent. At the peak of the depression of MF response, ATPA showed a very small effect (92.7 ± 9.0% of baseline, n = 5), and at the A/C pathway ATPA had no effect (99.0 ± 4.9% of baseline, n = 5, **Figure 4-1 c**).

The same type of experiments was interleaved in global GluK1 KO mice. After 20 min of stable baseline, ATPA was applied for 10 min and washed out for 30 min followed by DCG-IV application. As 36 min was the peak depression point in WT, we chose the same time point to measure the amplitude of MF and A/C to compare it to the response in WT mice.

ATPA application in 2-week-old GluK1 KO mice slice showed that basal transmission was not depressed in MF (99.8 ± 5.7% of baseline, n = 4) as well as in A/C (92.4 ± 8.4% of baseline, n = 4, **Figure 4-2 a**). In 4-week-old mice, MF showed 106.8 ± 5.6% of baseline (n = 7) and A/C showed

105.3 ± 4.5% of baseline (n = 7, **Figure 4-2 b**). In adult slices, MF showed 100.2 ± 5.6% of baseline (n = 6) and A/C showed 103.9 ± 2.4% of baseline (n = 6, **Figure 4-2 c**).

To summarise, the degree of peak depression was compared directly between WT and global GluK1 KO mice according to their developmental stage. When depression in MF was compared in WT and KO mice there was a clear difference between the two genotypes (**p < 0.01, two-way ANOVA, Bonferroni post hoc test) demonstrating only WT was affected by ATPA. The difference was also clear in 4-week-old mice (*p < 0.05, two-way ANOVA, Bonferroni post hoc test) but faded in adult animals as there was no significant difference between WT and KO (**Figure 4-3 a**).

ATPA induced depression on A/C synapses was also compared. At 2 weeks, ATPA reduced A/C responses in WT but no significant difference was detected between WT and KO. At 4 weeks, there was a depressant effect of ATPA on A/C while no changes were seen in KO (*p < 0.05, Two-way ANOVA, Bonferroni post hoc test). Both WT and KO adult mice were not affected by ATPA. This demonstrates that ATPA acts in an age-dependent manner in A/C as well as MF (**Figure 4-3 b**).

We demonstrate that ATPA as a GluK1 agonist can be used in mice even though there is the age-dependent limitation. Also, based on the result that KO mice showed no inhibition by ATPA in MF or A/C throughout development, we confirm that global GluK1 KO mice have no functional GluK1.

Unlike our results in mice, in adult rat hippocampal slices responses have shown more profound inhibition in response to ATPA (Clarke & Collingridge 2002) although it was on CA1. To achieve a greater distinction between WT and KO mice at a later developmental stage, we increased the dose of ATPA from 1 µM to 2 µM and application time from 10 min to 20 min. 2 µM of ATPA led to a more prompt and prolonged depression, therefore, the peak depression point was set at 40 min when ATPA application finished. In 2-week-old WT mice, depression reached 47.1 ± 3.9% of baseline (n = 4) while A/C reached 73.5 ± 11.7% of baseline (n = 4, **Figure 4-4 a**). In adult WT animals, the same application of ATPA reduced MF responses down to 82.8 ± 3.2% of baseline (n = 3) and 78.2 ± 9.6% of baseline in A/C (n = 3, **Figure 4-4 b**).

The same experiments were carried out in GluK1 KO animals. In 2-week-old mice, ATPA decreased MF responses to 82.9 ± 3.8% of baseline (n = 5) and A/C to 91.1 ± 10.0% of baseline (n = 5, **Figure 4-5 a**). In adult animals, a similar minor depression was observed both in MF (89.4 ± 3.4% of baseline, n = 4) and A/C (89.5 ± 9.0% of baseline, n = 4, **Figure 4-5 b**).

2 μM of ATPA resulted in a quicker and more prolonged depression of MF response in 2-week-old WT slices which was significantly greater than in KO (***$p < 0.001$ for 2wk, Two-way ANOVA, Bonferroni post hoc test). There was also a noticeable decrease of MF synapses in WT adult animals however this was no greater than in KO's (**Figure 4-6 a**). It affected A/C synapses to a somewhat similar degree regardless of age in WT and KO animals (**Figure 4-6 b**). The inhibition of A/C was greater in WT animals, however, not significantly greater than in KO animals. Based on the result that KO animals showed minor depression all throughout experiment regardless of developmental stage, it is reasonable to conclude that, at this concentration, ATPA is having off-target effects affecting not only GluK1 but possibly other receptors or subunits.

4.1.2. Investigation on the role of GluK1 in global GluK1 KO

After the validation of global GluK1 KO with ATPA, we wanted to examine a key characteristic of the MF, NMDAR-independent LTP. A study demonstrated that thorny excrescence-MF complex develops gradually during first 3 postnatal weeks (Amaral & Dent 1981) and immunohistochemistry shows that GluK1 protein in the hippocampus reaches its peak around 4 weeks and decrease gradually with time (data not shown, personal communication with Ms. Enaam Al Momany, University of Bristol, UK). Therefore, we chose two groups of age, 4-week old and 8 to 16-week old (adult) mice, to test. The inducibility of NMDAR-independent LTP, the degree of LTP, and PTP were examined.

The classic tetanus stimulation (100 Hz for 1 s) was delivered after 30 min of baseline to induce MF-LTP in the presence of D-AP5. In 4-week old WT mice, robust and clear enhancement of synaptic responses were observed over a 1 h period (n = 5, **Figure 4-7 a**). The time course of MF-LTP in KO mice was indistinguishable to that in KO (n = 7, **Figure 4-7 b**). PTP was expressed to a comparable degree in WT (303.3 ± 12.0% of baseline, n = 5) and in KO mice (291.7 ± 16.8% of baseline, n = 7, **Figure 4-7 c**). When the degree of LTP 1 h after the induction was directly compared, there was no significant difference observed between WT (121.9 ± 3.3% of baseline, n = 5) and KO (120.1 ± 11.4% of baseline, n = 7, **Figure 4-7 d**, $p > 0.05$, unpaired t-test).

MF-LTP and PTP were also observed and compared in fully developed mice. A single tetanus induced MF-LTP which lasted for 1 h after the induction in adult WT mice (**Figure 4-8 a**) as well as in KO (**Figure 4-8 b**). A variable degree of PTP was observed within the group but the degree of PTP was comparable between adult WT (372.0 ± 30.4% of baseline, n = 5) and KO mice (398.2 ± 29.4% of baseline, n = 4, **Figure 4-8 c**, $p > 0.05$, unpaired t-test). Synaptic facilitation recorded 1 h after the induction was 112.5 ± 8.4% of baseline for WT (n = 5) and 124.4 ± 11.9% of baseline

in KO mice (n = 4, **Figure 4-8 d**, p > 0.05, unpaired t-test). This indicates lack of GluK1 subunit does not affect short term or long term plasticity.

The next feature examined was HFF. As described earlier, 4-week-old mice were chosen for HFF and LFF experiments due to the relatively high expression of GluK1. 5 pulses at 50 Hz were delivered to MF synapses to elicit HFF in the presence of D-AP5. In both WT (n = 5, **Figure 4-9 a**) and KO mice (n = 20, **Figure 4-9 b**), robust facilitation was induced. Superimposition of traces from WT and KO indicates there was no difference in kinetics during HFF between two genotypes (**Figure 4-9 a + b**). The amplitudes after each pulse were measured and compared to the 1st response. HFS led the 5th response to reach 617.9 ± 42.5% of the 1st response in WT mice, while it reached 795.4 ± 60.2% of the 1st response in KO mice (p > 0.05, two-way ANOVA repeated measures) (**Figure 4-9 c**).

Next, we added GYKI 53655 (30 µM) on top of the D-AP5 (50 µM) in the bathing solution to investigate specifically KAR-mediated response. In WT animals, this combination of drugs completely abolished any detectable postsynaptic response only leaving the fiber volley (experimental scheme demonstrated in **Figure 2-3 a**). When HFS was delivered, the clear and robust enhancement from the 1st response to the 5th response was observed (control condition, **Figure 4-10 a**). It is worth noting that no direct comparison between the amplitude of 1st and 5th pulses was taken to avoid misinterpretation of data. This is because the 1st response is nearly absent with combination of D-AP5 and GYKI 53655 during HFF, therefore, direct measurement of the 1st amplitude could lead misleadingly high value of the 5th amplitude. Instead, we measured the amplitude of the 5th response of during HFF.

As Dargan 2009 showed that GluK1 specific antagonist ACET reduces the level of synaptic facilitation induced by HFS (20 - 25 Hz) (Dargan et al 2009), we speculated that we should be able to mimic the reduction of HFF with ACET in WT but not in KO.

As speculated, 20 min of ACET (50 nM) reduced the amplitude of the 5th response produced by HFS (68.8 ± 5.5% of control, **Figure 4-10 b**). 1 h 30 min of washing out restored this reduction close to the control condition although this was statistically insignificant (88.4 ± 12.3% of control, **Figure 4-10 c**). The response was later eliminated with mGluR 2/3 agonist, DCG-IV (18.1 ± 3.3% of control, **Figure 4-10 d**). The summary chart demonstrates that ACET indeed decreases the amplitude of the 5th response during HFF in WT (**Figure 4-10 e**; n = 8, **p = 0.0088, one-way ANOVA repeated measures, **p < 0.01 for ACET and wash out, Tukey post hoc test) establishing a role of GluK1 in HFF.

Not only HFF but also LFF was examined with ACET in WT mice. In control conditions, a change in frequency from 0.033 Hz to 1 Hz for 30 s induced a gradual enhancement of MF responses reaching 272.1 ± 21.5% of baseline (**Figure 4-11 a**). When ACET was present, the degree of facilitation reached 217.4 ± 12.3% of baseline (**Figure 4-11 b**) and washing out did not have a significant impact on LFF (250.1 ± 31.3% of baseline, **Figure 4-11 c**). Even though ACET caused a compelling reduction in HFF, LFF was not significantly affected by GluK1 antagonism with ACET in WT (**Figure 4-11 d**, n = 5, p = 0.1336, one-way ANOVA repeated measures).

As described earlier, validation with ATPA of the global GluK1 KO has confirmed that these animals carry no functional GluK1 subunit, therefore, we postulated that ACET application should not affect HFF nor LFF in KO animals. The same HFS delivered to KO slices elicited a robust enhancement from the 1st to the 5th response in control conditions (**Figure 4-12 a**). 50 nM of ACET did not significantly alter the amplitude of the 5th response of HFF (79.0 ± 9.9% of control, **Figure 4-12 b**). There was no statistical difference after washing out (102.1 ± 9.8% of control, **Figure 4-12 c**). The response was greatly reduced after DCG-IV (28.5 ± 10.6% of control, **Figure 4-13 d**). The summary graph indicates ACET has no effect on the amplitude of the 5th response during HFF in GluK1 KO animals (n = 4, **Figure 4-12 e**, p = 0.0625, one-way ANOVA repeated measures).

In LFF experiments, LFS readily induced robust facilitation (343.2 ± 33.0% of baseline, **Figure 4-13 a**) in KO. ACET had no effect on LFF (308.0 ± 50.4% of baseline, **Figure 4-13 b**) while LFF reached 406.8 ± 39.3% of baseline after washing out (**Figure 4-13 c**). The summary chart shows there is no significant alteration caused by ACET in KO (n = 4, **Figure 4-13 d**, p = 0.1498, one-way ANOVA repeated measures).

4.3. Discussion

4.3.1. Validation of global GluK1 KO

We used the GluK1 specific agonist ATPA to validate the global GluK1 KO. In a previous study, Clarke and Collingridge (2002) showed that 1 μM of ATPA was enough to depress synaptic transmission in juvenile to adult rat (6 - 10 weeks old, note that it was recorded in CA1). Similarly, our results confirmed that ATPA loses its depressant effect on MF transmission as animal ages. In fact, the effect was nearly absent in adult mice which worked as a limiting factor. Increased dose and the application time of ATPA was tested in an attempt to detect an effect of ATPA in adult mice, however, it led unforeseen off-target effects, as revealed in the KO. Previous studies showed that ATPA is most potent at GluK1-containing receptors, but it also possesses the agonistic activity at AMPARs (Lauridsen et al 1985, Stensbol et al 1999). Therefore, it is most likely that the off-target effect of ATPA seen in KO animals is due to ATPA acting on AMPARs.

4.3.2. The role of GluK1 at mossy fiber synapses

MF synapses are known as detonator or teacher synapses due to their characteristics, including that they amplify the signal, change excitability and conveying information within the DG-CA3-CA1 circuit (Lisman 1999, McNaughton & Morris 1987). KARs as autoreceptor are recognized as the most prominent contributor to these MF functions. KARs are widely expressed in the CNS (Petralia et al 1994) and are especially abundant in the hippocampus (Bahn et al 1994, Darstein et al 2003). Particularly, presynaptic KARs are found to play the critical role in regulating synaptic transmission and synaptic plasticity in CA3 (Bortolotto et al 1999, Lauri et al 2001a, Schmitz et al 2000, Schmitz et al 2001a).

To elucidate which subunit of KAR is responsible for MF function, various approaches have been taken including pharmacological studies using subunit specific antagonists and genetic manipulation of KAR generating subunit specific KO mouse models. In the previous studies, GluK2 KO mice showed an impairment of KAR-mediated synaptic transmission and HFF while GluK1 KO mice had intact HFF (Breustedt & Schmitz 2004, Contractor et al 2001, Mulle et al 1998). GluK3 KO also showed impaired MF-LTP and synaptic facilitation (Pinheiro et al 2007) and GluK5 KO showed heterosynaptic MF-LTP is impaired while other features of MF are intact (Contractor et al 2003).

In pharmacological studies, various antagonists specific for GluK1 were generated and tested on MF transmission and MF-LTP. UBP296 (More et al 2004) and LY382884 blocked MF-LTP and

reduced HFF (Bortolotto et al 1999, Lauri et al 2001a). Dargan et al. (2009) showed MF-LTP was blocked by ACET and presynaptic Ca^{2+} transients during HFF were also reduced by ACET demonstrating the importance of the GluK1 subunit in MF function.

Discrepancies in observations made in GluK1 KO mouse models and GluK1 antagonist studies led us to generate DG specific GluK1 KO mice which lack presynaptic GluK1 subunit. As a first step towards DG-GluK1 KO mice, we disrupted GluK1 expression in the whole body by inserting a gene cassette in the GluK1 gene resulting in global GluK1 KO.

Using this mouse model, our results revealed that ablation of GluK1 subunit does not affect MF-LTP and HFF which are consistent with previous studies on GluK1 KO. On the other hand, the result from KAR-mediated HFF with ACET in WT demonstrated there is a clear reduction due to antagonism of GluK1 while KO mice did not show the same reduction. As this result not only confirms that GluK1 KO does not contain functional GluK1 but also suggests GluK1 may contribute to HFF in WT mice. As both results partially agree with the previous studies with GluK1 KO and GluK1 antagonists, we postulate generic deletion of GluK1 gene can be compensated by other subunits leaving MF function undisrupted. However, when a pharmacological measure is taken, there may still be an effect, small but evident, of GluK1 subunit.

4.3.3. Involvement of other KAR subunits

Even though the reduction of the amplitude of the 5^{th} response caused by ACET during HFF was apparent, effect of ACET was negligible during LFF in WT mice. This was surprising since we expected to see a similar reduction in LFF as we observed in HFF if GluK1 is involved in LFF. This inconsistency may be due to the presence of GYKI 53655. Perrais et al. (2009) reported that high dose GYKI 536550 (50 µM) partially blocks HFF and LFF. In this study, a lower dose of GYKI 53655 (30 µM) was used yet this could attenuate any effect from ACET during HFF and LFF. In addition, GYKI 53655 has been reported to affect GluK3-containing KARs (IC_{50} = 63 ± 10 µM for GluK3 homomer, IC_{50} = 32 ± 5 µM for GluK2b(R)/3 tetramer) (Perrais et al 2009). However, as GYKI 53655 was used at all times throughout experiments in both genotypes, the effect of GluK3 antagonism by GYKI 53655 should be equal.

In the same context, ACET is reported to be specific to GluK1 over GluK2 (Dargan et al 2009, Dolman et al 2007, Perrais et al 2009), but it also was reported to affect the GluK3 subunit (Perrais et al 2009). ACET does not affect GluK2/3 heteromers and the IC_{50} for GluK3 homomer

is 92 ± 9 nM. As the dose used in this study is 50 nM, which is sub-IC_{50} value, therefore, it is expected to have a very minor effect. In reality, these discrepancies could be resolved when specificity for GluK1 over GluK3 is improved.

4.3.4. Future direction of the study

In addition to the need to establish the compensatory effects in GluK1 KO animals contributing to our results, there are several further avenues of future research.

It has been reported that mRNA of GluK1 expression is nearly absent (Wisden & Seeburg 1993) or at very low intensity in granule cell (Bahn et al 1994). Expression of GluK2/3 heteromers does not change in GluK1 KO animals also suggests that GluK1 act barely as an assembly partner for GluK2 or GluK3 (Ball et al 2010). Interestingly, GluK1 is expressed in GAD-expressing interneuron in the hippocampus (Paternain et al 2000). There is still a debate about whether GluK1 agonist depresses excitatory synaptic transmission via GABA release (Clarke & Collingridge 2002, Lauri et al 2001b, Schmitz et al 2000); it is well agreed that activation of KARs regulate synaptic transmission of interneurons (for GluK1 in CA3, see Clarke et al 1997, Clarke & Collingridge 2004, Cossart et al 1998, but also see Mulle et al 2000). If GluK1 expresses on interneurons in CA3, not in presynaptic MF boutons, mediating excitability of the network in CA3 (either via GABA or not), it is well expected to detect no changes in MF function. This hypothesis fits in with our current observation that GluK1 KO animals did not show any impairment on MF-LTP, HFF or kinetics changes.

Heterosynaptic MF-LTP can also be induced by giving stimulation in A/C (Schmitz et al 2003) which suggests the role of KARs is not necessary for synaptic plasticity at CA3 but may reduce the threshold for plasticity. That increased excitability of the network by application of K^+ (5 mM) can restore impaired MF-LTP (Pinheiro et al 2007) also support this idea.

A study by Kwon and Castillo (Kwon & Castillo 2008b) also questioned the role of presynaptic KARs as autoreceptor facilitating neurotransmitter release at MF-CA3 synapses and raised the possibility that activation of postsynaptic KARs is more involved in enhancing CA3 network excitability rather than directly regulating distinctive feature of MF. The authors demonstrated that inhibition of hyperexcitability of CA3 network by TTX reduced the degree of PPF, HFF and LFF which are originally attributed to the role of presynaptic KARs.

Therefore, it will be interesting to revisit the possibility that interneurons expressing GluK1 have a role on the CA3 network excitability modulating MF features as well as the role of postsynaptically expressed GluK1 using global GluK1 KO animals.

4.4. Conclusion

The data in this chapter demonstrates a clear depressant effect of ATPA on the MF and the A/C in WT animals which is absent in GluK1 KO, confirming that global GluK1 KO does not carry functional GluK1-containing KARs. Also, we identified an age-dependent effect of ATPA in MF and A/C synapses in mice hippocampal slices as seen in rat slices in the past. Since ATPA's depressant effect diminishes with animals' age and the effective time window of ATPA is small, its ability to validate GluK1 subunit in adult animals is greatly restricted. Therefore, measures other than an application of ATPA should be taken in the future to validate the existence of GluK1 subunit in adult animals.

In global GluK1 KO mice, we did not observe impairment of MF-LTP or HFF suggesting that there could be mechanisms that compensate for the genetic ablation of GluK1 subunits from early developmental stages. These allow normal function of the MF to develop. However, based on the pharmacological study showing the reduction of amplitude during HFF caused by ACET, our results also confirm that GluK1-containing KARs contribute to HFF to some degree.

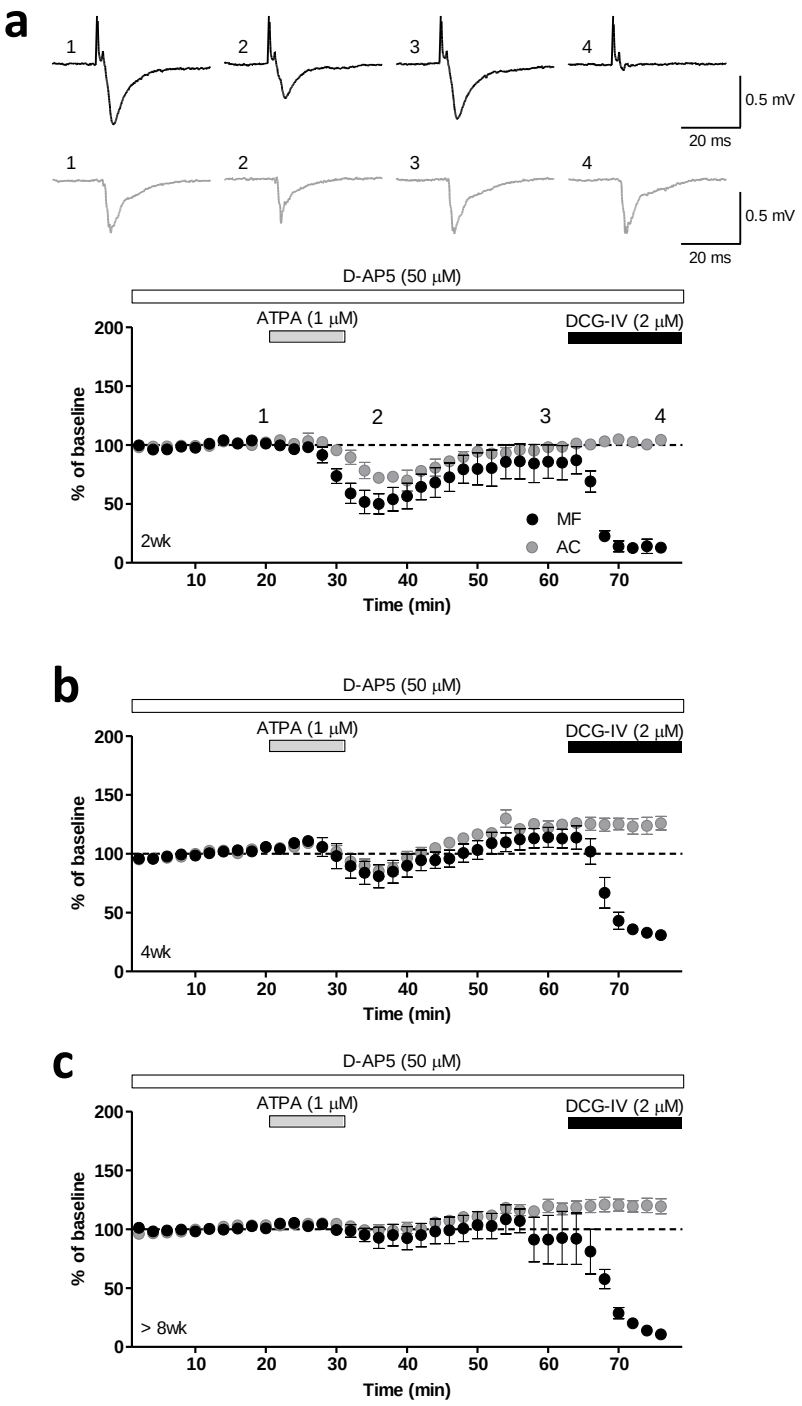

Figure 4-1. Effects of ATPA on basal synaptic transmission at CA3 synapses in WT animals. In WT animals, prominent depressing effect of ATPA on basal transmission is observed in 2-week-old mice and it is nearly absent in adult mice.
a. ATPA significantly depresses basal transmission to nearly 50 % of baseline in 2-weeks-old WT mice (n = 4). Upper panel shows the sample traces taken from the point where the numbers are inserted in the graph. Black traces: MF, grey traces: A/C.
b. Minor depressing effect is observed in 4-week-old mice (n = 6).
c. Depressing effect of ATPA is nearly absent in adult animals (n = 5). Filled circle: MF, grey circle: A/C

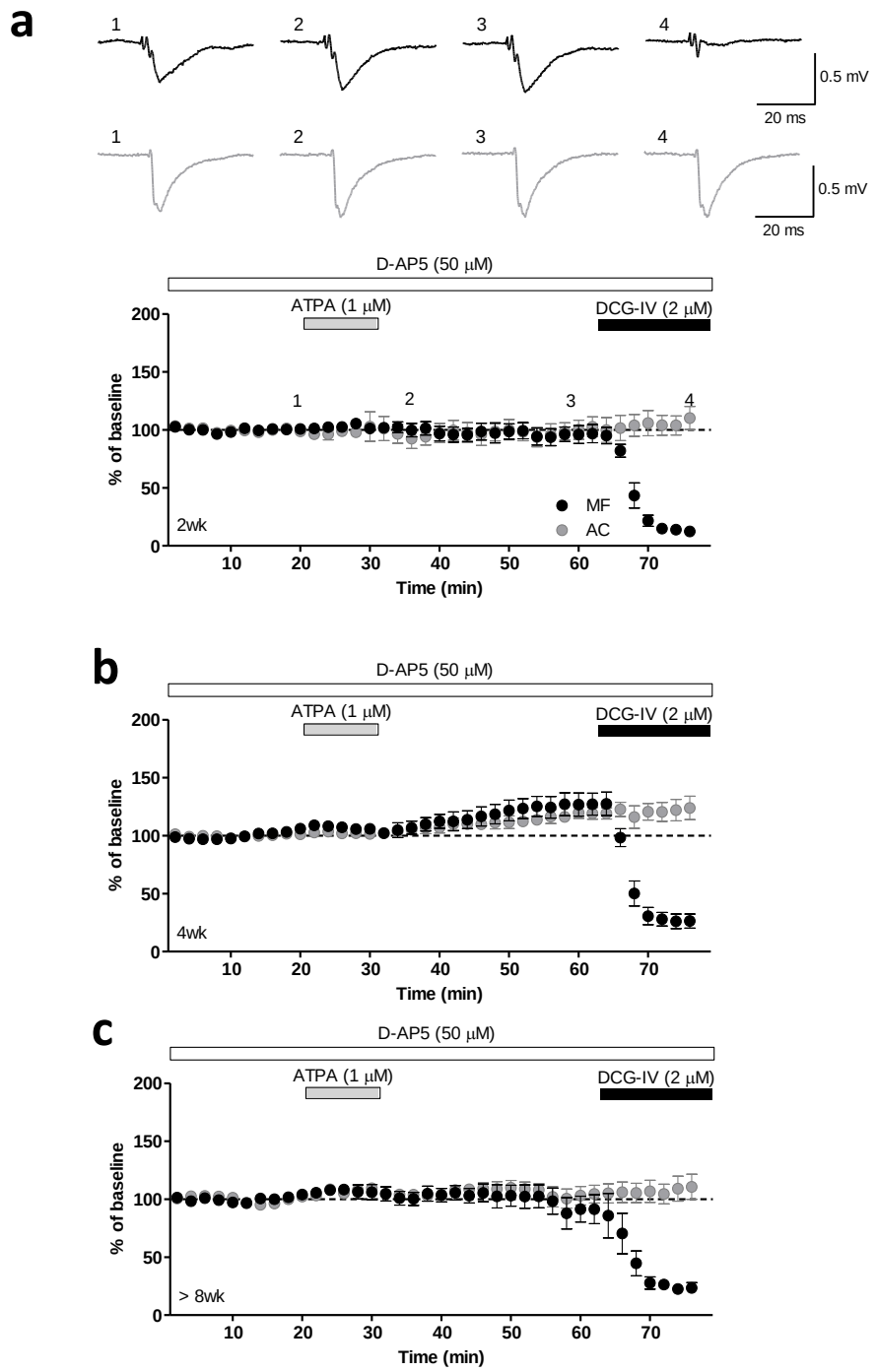

Figure 4-2. Effects of ATPA on basal synaptic transmission at CA3 synapses in global GluK1 KO animals. ATPA does not affect synaptic transmission in global GluK1 KO animals.

a. ATPA's depressant effect on synaptic transmission is absent in 2-3 week old KO animals (n = 4). Upper panel shows the sample traces taken from the point where the numbers are inserted in the graph. Black trace; MF, grey trace; AC.

b. Synaptic transmission is not affected by ATPA in 4-5 week old KO animals (n = 7).

c. ATPA does not alter synaptic transmission in adult KO animals (n = 6). Filled circle: MF, grey circle: A/C

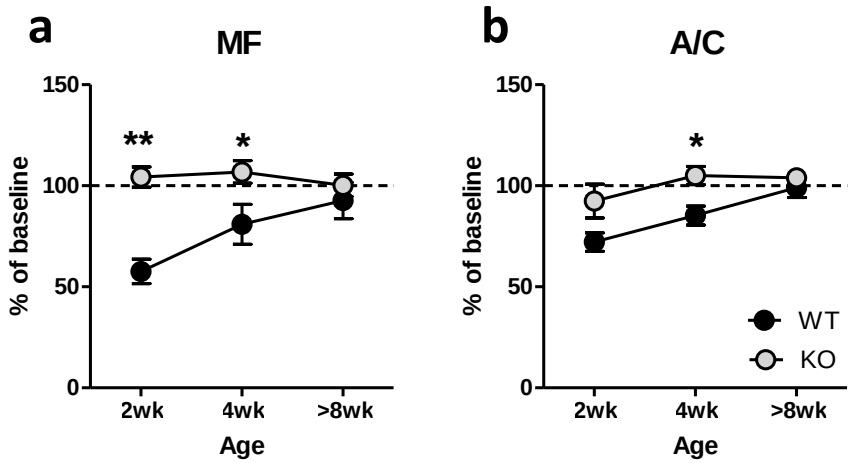

Figure 4-3. Summary chart of ATPA's depressant effect on MF and A/C.
ATPA reduces synaptic transmission in MF and A/C in WT animals in age-dependent manner while KO shows no changes in MF and A/C in any developmental stage.
a. In MF synapses, depression of ATPA is most evident at 2 weeks and the effect fade away when animal is fully developed. KO shows no changes over development and not affected by ATPA
b. A/C synapses show smaller depression compared to MF but still evident in WT which lack in KO. Filled circle: WT, grey circle: global GluK1 KO. *p < 0.05, **p < 0.01

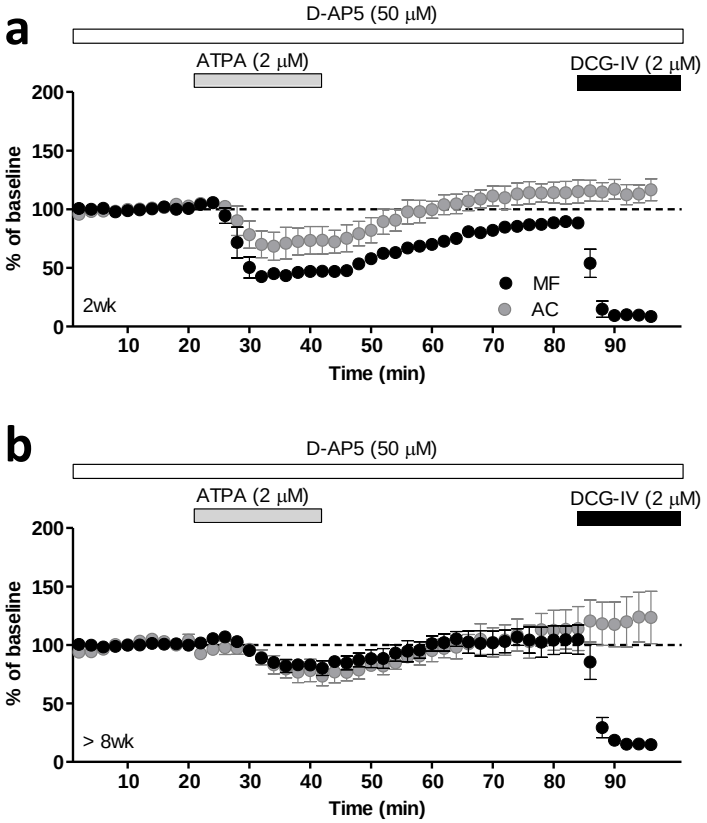

Figure 4-4. Effects of higher concentration and longer perfusion time of ATPA on basal synaptic transmission at CA3 synapses in WT mice.
a. In 2-week-old WT animals, increased dose of ATPA application has prolonged and substantial depressing effect on MF as well as A/C (n = 5).
b. Depressant effect of ATPA is evident when dose and time is prolonged in adult WT animals (n = 4). Filled circle: MF, grey circle: A/C

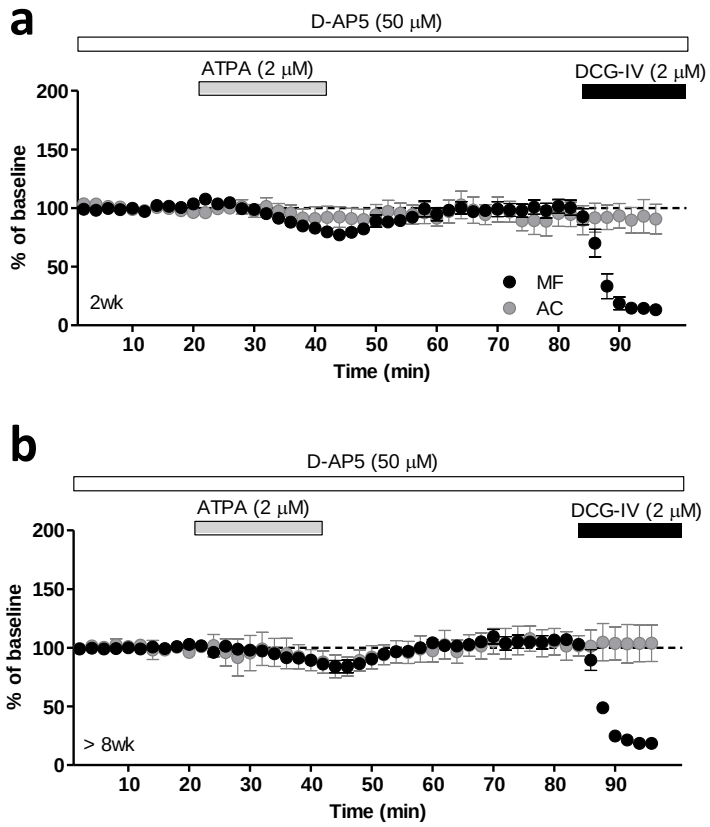

Figure 4-5. Effects of higher concentration and longer perfusion time of ATPA on basal synaptic transmission at CA3 synapses in KO mice.
a. ATPA holds slight depressing effect on synaptic transmission of MF in KO animals
b. Minor depressant effect of ATPA on synaptic transmission of MF and A/C is observed in adult KO animals. Filled circle: MF, grey circle: A/C

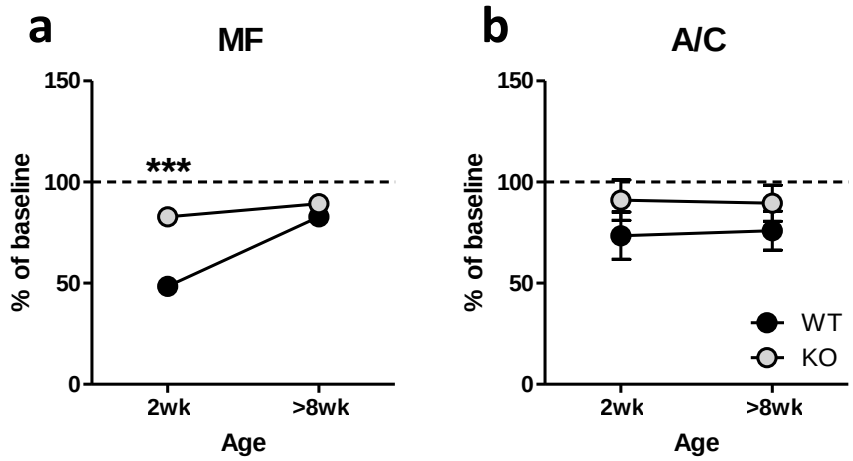

Figure 4-6. Increased dose and application time of ATPA off-target effects.
a. APTA decreases synaptic transmission of MF in not only 2wk but also adult, however, KO is also affected.
b. Depression of A/C is evident in WT regardless of age, but no difference from KO is observed. Filled circle: WT, grey circle: global GluK1 KO. ***p < 0.001.

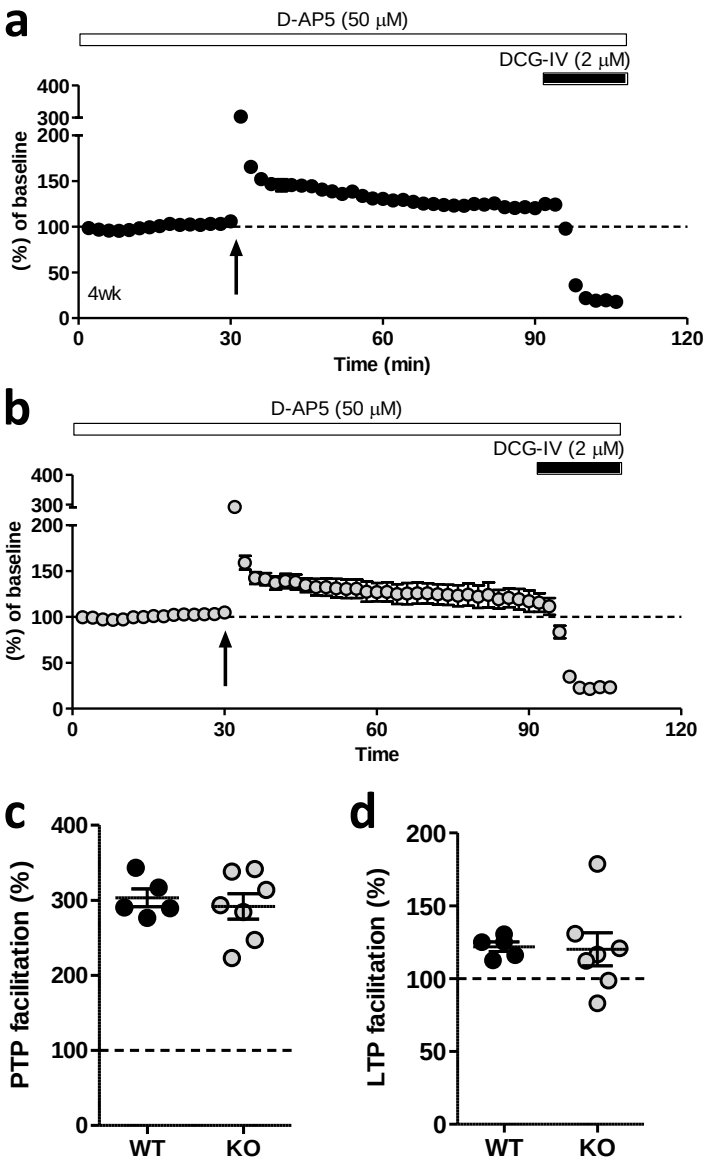

Figure 4-7. NMDA-independent LTP at MF in 4-weeks-old GluK1 WT and KO animals. A single tetanus (100 Hz for 1 s) was given to evoke LTP at mossy fiber pathway
a. A stable MF-LTP is induced in WT (n = 5).
b. Comparable degree of MF-LTP is induced in global GluK1 KO animals (n = 7). Sample traces of KO animals displayed above the graph. **c**. Degree of PTP in KO animals is similar to WT animals.
d. Summary of LTP facilitation 1 h after the tetanus. Black arrow: tetanus stimulation (100 Hz, 1 s), filled circle: WT, grey circle: global GluK1 KO

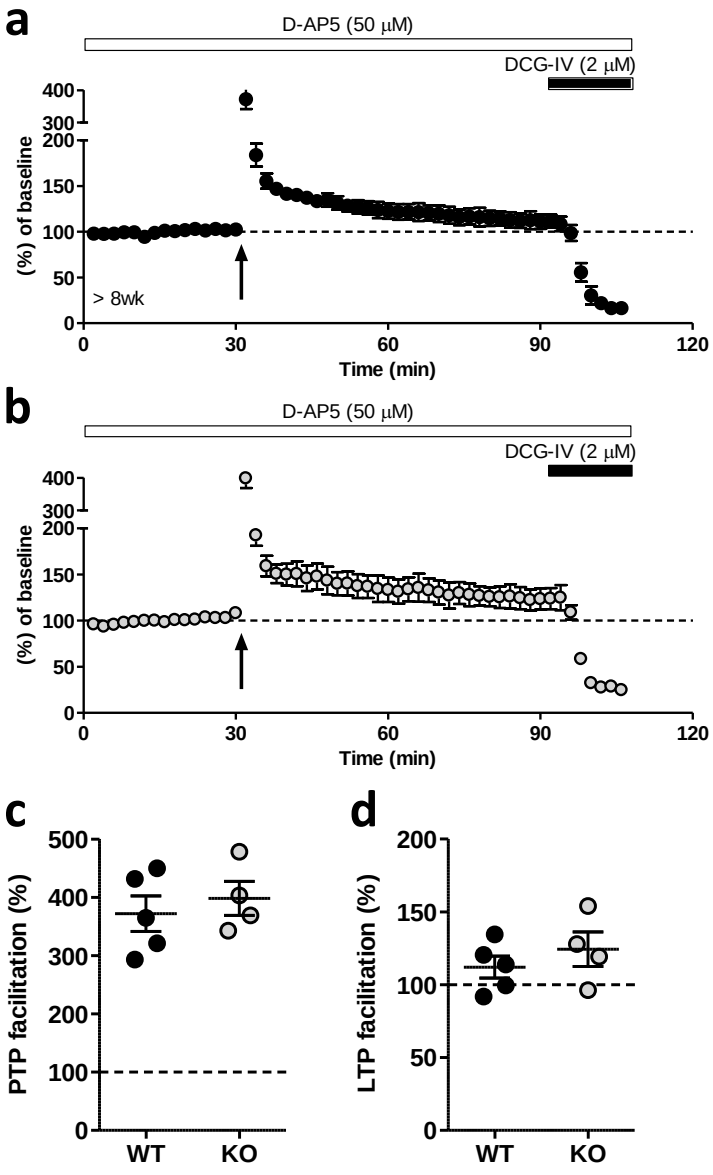

Figure 4-8. NMDA-independent LTP at MF in adult GluK1 WT and KO animals.
a. A stable MF-LTP is present in adult WT animals (n = 5).
b. Global GluK1 KO animals also express comparable degree of LTP (n = 4).
c. Degree of PTP in KO animals is similar to WT animals.
d. Summary charts showing degree of MF-LTP is similar between WT and KO. Black arrow: tetanus stimulation (100 Hz, 1 s), filled circle: WT, grey circle: global GluK1 KO

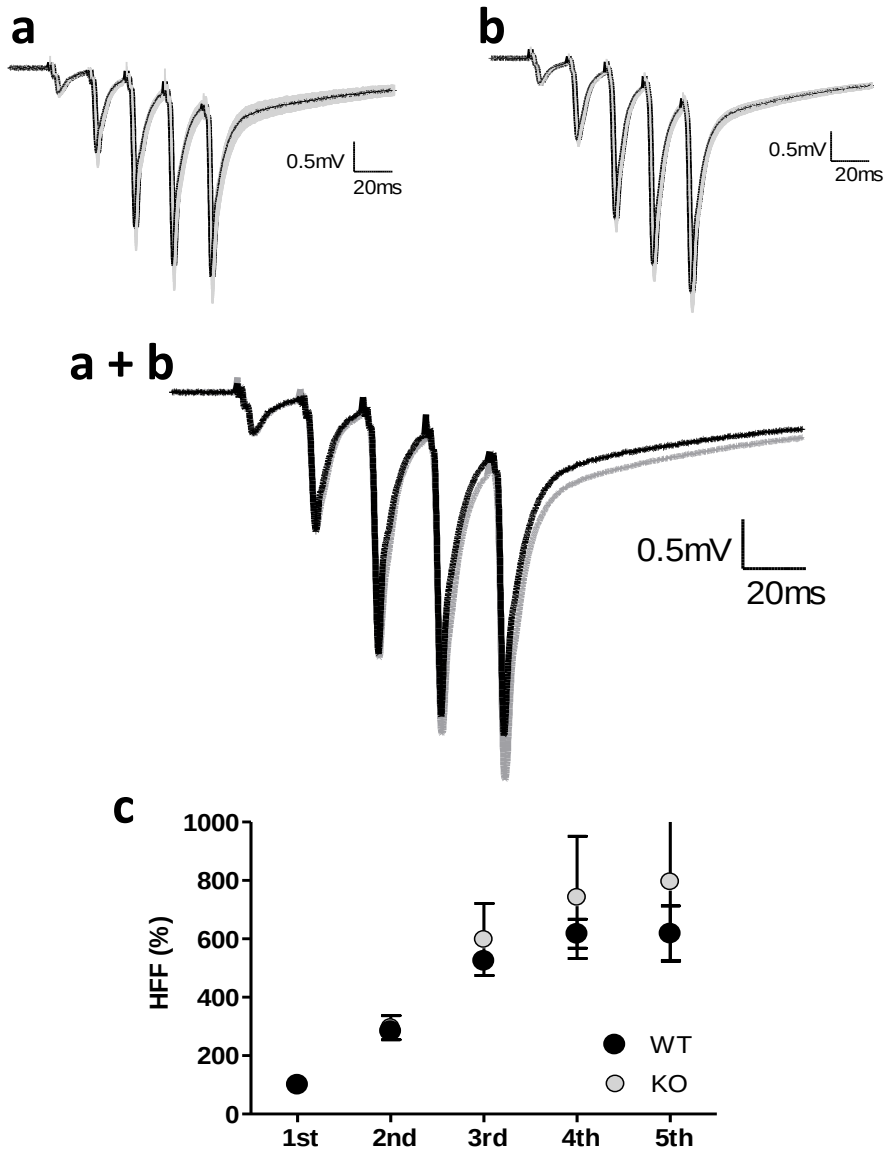

Figure 4-9. HFS (5 pulses at 50 Hz) induces HFF in WT and KO mice.
a. A robust increased is observed in WT animals (n = 5)
b. KO also express HFF (n = 20)
a + b. Overlapped trace of WT and KO shows that GluK1 WT and KO animals express comparable degree of HFF and share similar kinetics of HFF
c. Direct comparison of amplitude after each pulse shows no significant difference between genotype. Filled circle: WT, grey circle: global GluK1 KO

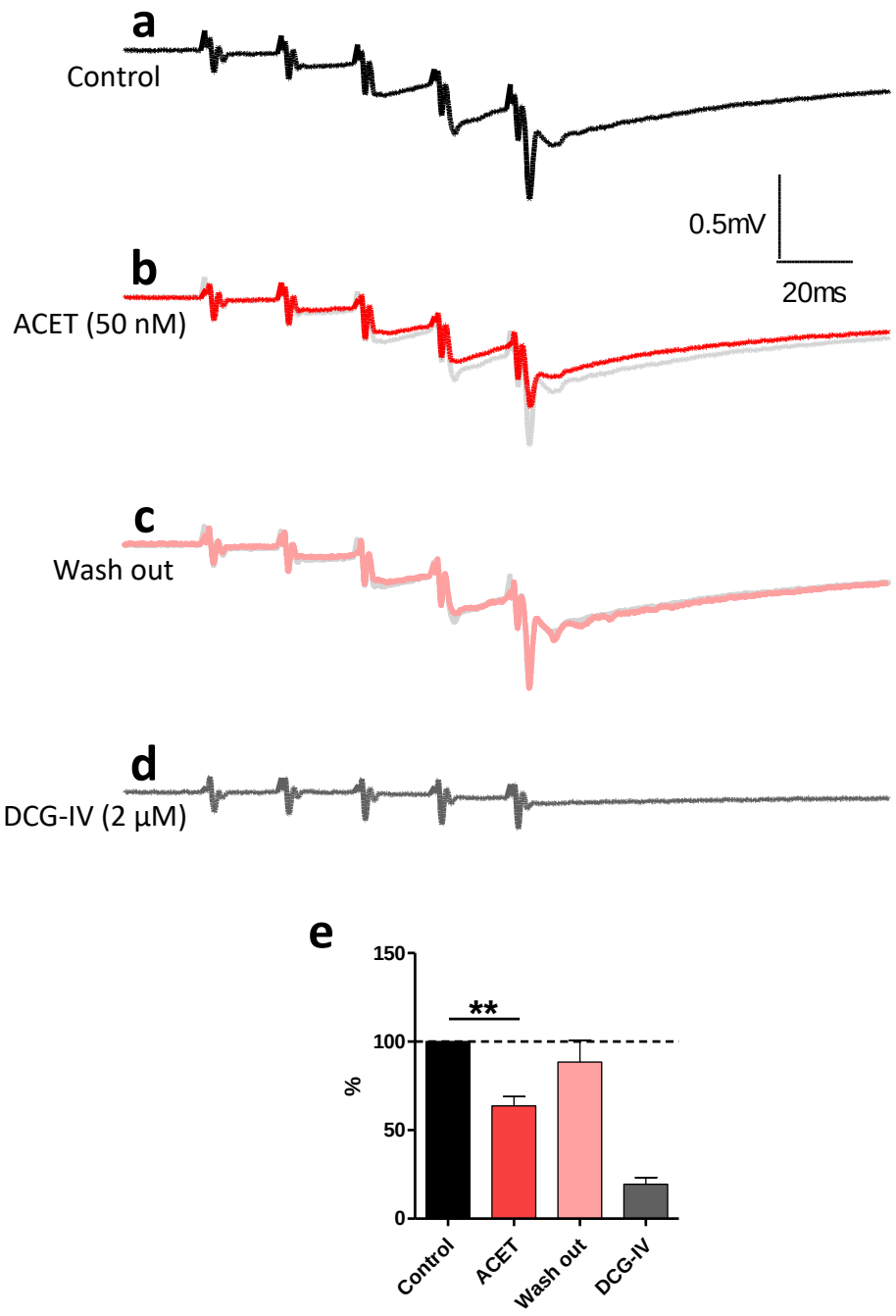

Figure 4-10. ACET reduces amplitude of 5th response in WT animals.
a. Expression of KAR-mediated HFF.
b. ACET decreases the amplitude of 5th pulse in HFF.
c. 1 h 30 min of washing out insignificantly restore depression.
d. DCG-IV blocks HFF.
e. Summary graph showing ACET reduces HFF. Light grey line: HFF in control condition (n = 8). **p < 0.01.

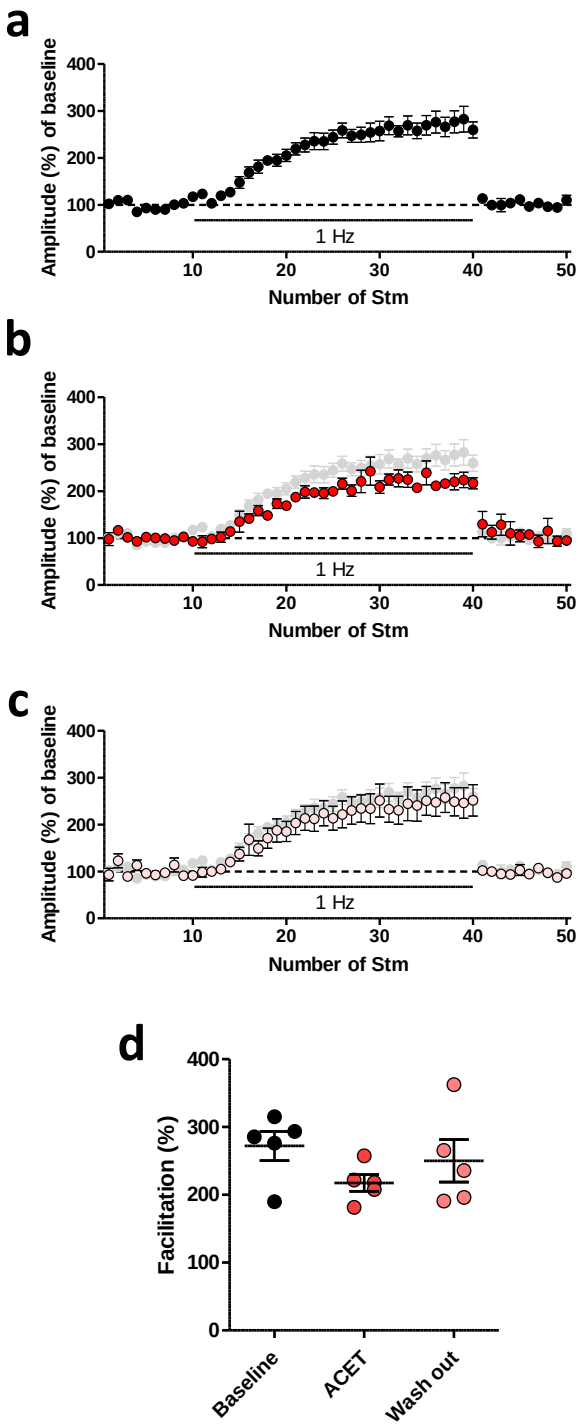

Figure 4-11. ACET does not affect LFF evoked by 1 Hz in WT.
a. Expression of LFF in control condition.
b. Amplitude of LFF is not altered with ACET.
c. Amplitude of LFF after 1 h 30 min washing out.
d. Bar chart demonstrates there is no significant differences between groups. Light grey line: LFF in control condition (n = 5).

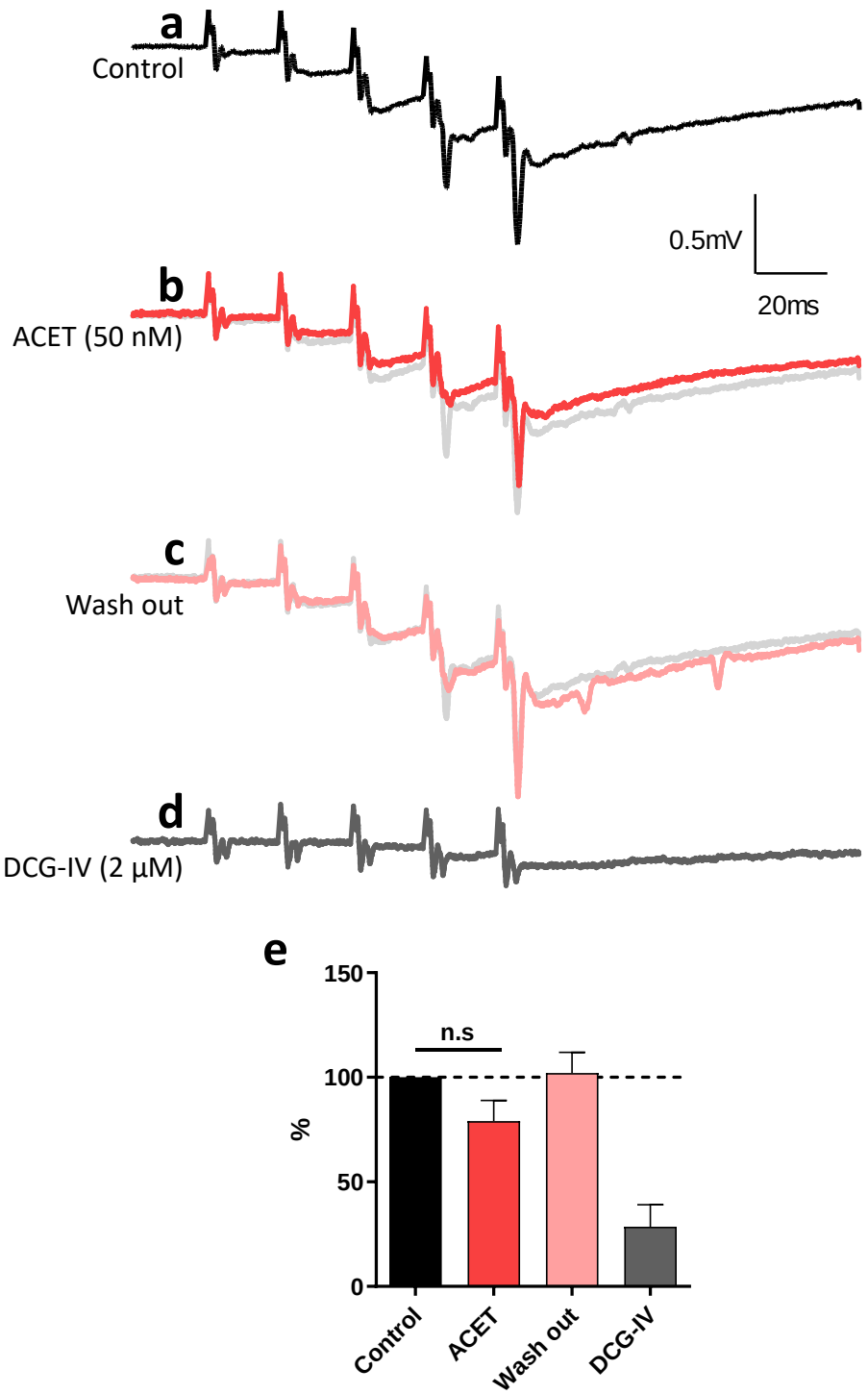

Figure 4-12. Global GluK1 KO animals do not significantly respond to ACET during HFF.

a. Expression of HFF in control condition.

b. Application of ACET does not significantly decrease the amplitude of the 5th pulse.

c. HFF after 1 h 30 min of washing out.

d. Expression of HFF in the presence of DCG-IV.

e. Summary graph showing ACET does not change the amplitude of 5th response in global GluK1 KO. Light grey line: HFF in control condition (n = 4).

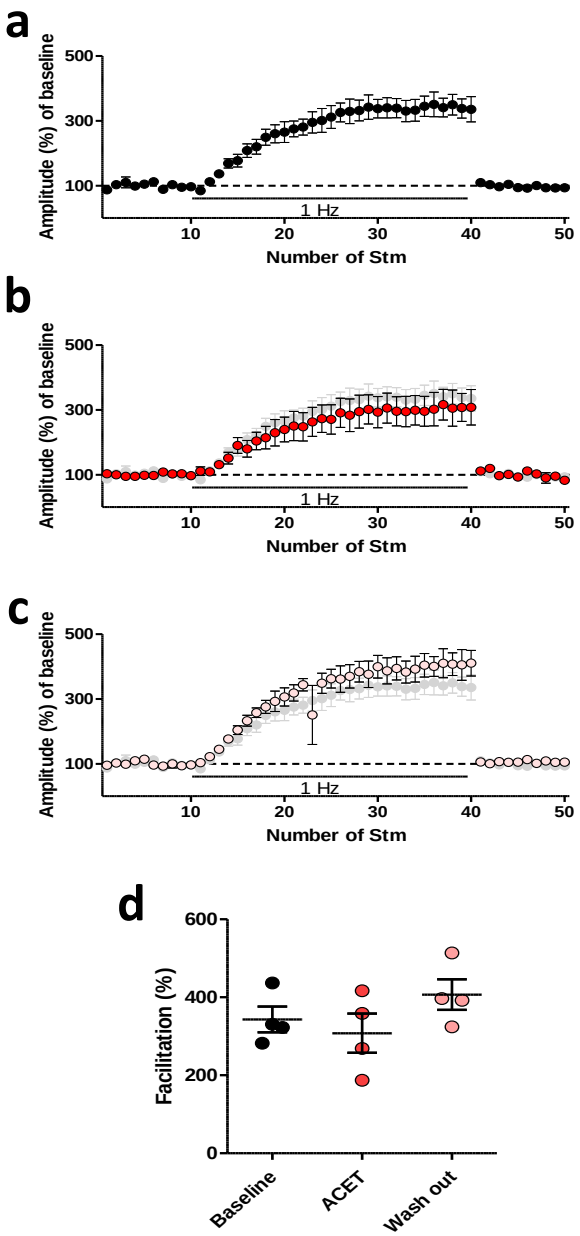

Figure 4-13. In GluK1 KO mice, LFF is not affected by ACET.
a. Expression of LFF in control conditions.
b. ACET does not disturb LFF.
c. No significant changes is observed in LFF after washing out.
d. Summary chart shows there is no difference between groups. Light grey line: LFF in control condition (n = 4).

Chapter 5. Results: Pharmacological study of the GluK2 subunit in Mossy fiber synapses

5.1. Introduction

In the previous chapter, we characterised the global GluK1 KO mice and confirmed that generic deletion of GluK1 subunit from early development does not affect unique MF properties directly. In this chapter, we exploit this mouse model to test the effects of two potential GluK2 antagonists, UBP2002 (6-iodo kynurenic acid) and UBP2038 (5,7-difluoro, 6-iodo kynurenic acid) on those MF functions.

Kynurenic acid is an endogenous glutamate receptor ligand and is biosynthetically produced from L-tryptophan. It was found to be a broad-spectrum antagonist for glutamate receptors (Ganong et al 1983, Perkins & Stone 1982). As kynurenic acid attenuates neurotoxicity caused by overexcitation of glutamate receptors, it has been used in studies of epilepsy, as well as other neurobiological disorders, for its anticonvulsant and neuroprotective effects. Many agonists and antagonists based on kynurenic acid have been synthesised for their therapeutic potential (Kessler et al 1989, Leeson et al 1991, Stone 2000). Serial studies on kynurenic acid revealed that kynurenic acid works as a weak antagonist of NMDARs by binding at the glycine site (Birch et al 1988) and it distinguishes KARs from AMPAR (Coleman et al 1986). More recent study also confirmed that it antagonizes subunit specific KARs, for example GluK2 homomers (Alt et al 2004). As an attempt to examine the role of specific KAR subunits other than GluK1, we synthesised several kynurenic acid-derived compounds which could potentially show selective antagonism for GluK2-containing KARs.

Compounds with 5, 6 and 7-substitution of the phenyl ring in kynurenic acid were synthesised by Prof. David Jane's group (University of Bristol, UK) (**Figure 5-1 a, b and c**). In UBP2002, introduction of an iodine atom at the 6-position of kynurenic acid removed activity at NMDARs of kynurenic acid and created an antagonistic effect on the GluK2 subunit. UBP2038 is a fluorinated derivative of UBP2002 with fluorine atoms introduced at 5 and 7-positions. UBP2038 (5, 7-difluorine, 6-iodo-kynurenic acid), exhibits better potency and selectivity on human GluK2 homomers compared to UBP2002. We used these two compounds to investigate the role of GluK2 on the unique features of MF - CA3 synapses including MF-LTP, HFF and LFF. Since all experiments were carried out in hippocampal slices taken from global GluK1 KO mice, involvement of GluK1 subunit was eliminated creating the optimal condition for us to test these compounds.

It is worth noting that since UBP2002 and UBP2038 also show antagonistic effect on AMPARs, GYKI 53655 was added to the aCSF solution at all time (excluding Figure 5-1 and 5-2) as well as D-AP5. Also 4-week-old animals were used in this chapter for the consistency of the experiments.

5.2. Result

5.2.1. Effect of UBP2002 on NMDAR-independent LTP and HFF

We used a calcium fluorescence assay to measure efficacy of UBP2002 and UBP2038 toward GluK1 and GluK2, using HEK293 cells expressing human GluK1 (Q) and GluK2 (Q) respectively. The assay revealed that kynurenic acid derivative UBP2002 (**Figure 5-1 b**) has a K_i value of 19.3 ± 1.6 µM on human GluK2 (n = 8) and 30.5 ± 4.9 µM on GluK1 (n = 9) displaying slight selectivity toward to GluK2 (**Figure 5-1 d,** data provided by Dr. Robert Thatcher and Mr. Alen Eapan, University of Bristol, UK). UBP2038 (**Figure 5-1 c**) shows higher activity than UBP2002 to human GluK2 receptor (K_i for GluK2 is 5.0 ± 0.4 µM, n = 30; K_i for GluK1 is 11.6 ± 0.9 µM, n = 40) (**Figure 5-1 d**, data provided by Dr. Robert Thatcher and Mr. Alen Eapan, University of Bristol, UK). Both drugs also showed an antagonistic effect toward GluA1-containing homomers. The K_i value of UBP2002 on GluA1 was 324.8 ± 70.9 µM (n = 5) and the K_i value of UBP2038 toward GluA1 was 24.1 ± 2.3 µM (n = 25, **Figure 5-1 d**, data provided by Dr. Robert Thatcher and Mr. Alen Eapan, University of Bristol, UK).

UBP2002 and UBP2038 were further examined in CA1 synapses of rat hippocampal slices for their antagonistic properties on native receptors (**Figure 5-1 e**). The application of UBP2002 led to significant depression of basal transmission with an IC_{50} value of 45.21 ± 1.86 µM on native AMPARs (n = 4 for 10 µM, n = 4 for 30 µM, n = 5 for 100 µM). UBP2038 also depressed synaptic transmission with IC_{50} value of 3.58 ± 0.09 µM on AMPARs (n = 5 for 1 µM, 10 µM and 100 µM) (**Figure 5-1 e**, data provided by Mr. Alen Eapan, University of Bristol, UK).

Previous studies using GluK2 KO mice demonstrated that HFF, LFF and MF-LTP were impaired in this mouse model, suggesting GluK2 subunit plays an important role in MF function (Breustedt & Schmitz 2004, Contractor et al 2001). Therefore, we examined MF-LTP, HFF and LFF at MF-CA3 synapses while blocking GluK2 with UBP2002 and UBP2038.

Inducibility of MF-LTP was checked with UBP2002. Previously it has shown in Figure 5-1 e, UBP2002 can depress basal transmission at CA1 synapses because it also antagonises AMPARs.

Consequently, synaptic transmission was also reduced at MF synapses. 30 min of UBP2002 (100 μM) application led to robust depression to 35.1 ± 2.1% of baseline (**Figure 5-2 a**).

A tetanus is given at the end of UBP2002 application to elicit MF-LTP and the expression is monitored for 1 h (n = 6, **Figure 5-2 a**). Because synaptic transmission was depressed by UBP2002, interleaved experiments without the tetanus were carried out to determine whether MF-LTP is induced or not by comparing the amplitude 1 h after the tetanus (n = 4, **Figure 5-2 b**). In the experiments with the tetanus, the amplitude of MF synapse reached 73.2 ± 3.7% of baseline after 1 h of LTP induction and MF response without the tetanus showed 86.9 ± 10.9% of baseline. There was no significant difference of amplitude between two groups in the presence of UBP2002 (**Figure 5-2 c**, $p < 0.05$, unpaired T-test).

To check whether impairment of MF-LTP by UBP2002 can be restored, we recorded extra 30 min after LTP was compared (2^{nd} baseline; from 120 to 150 min in the graph) and delivered the 2^{nd} tetanus (**Figure 5-2 a**). The amplitude 1 h after the 2^{nd} tetanus was 74.0 ± 8.5% of baseline (n = 6, **Figure 5-2 d**, $p > 0.05$, unpaired T-test) which was comparable to interleaved control experiments without a tetanus (77.4 ± 9.6% of baseline, n = 4, **Figure 5-2 d**, $p > 0.05$, unpaired T-test).

Next, we investigated the effects of UBP2002 on HFF and LFF at MF synapses. The same condition used for HFF and LFF in the chapter 4 (recording in the presence of 50 μM of D-AP5 and 30 μM of GYKI 53655) was applied in these experiments. HFS (5 pulses at 50 Hz) was delivered in control conditions leading to a propound enhancement of KAR-mediated response from 1^{st} to 5^{th} response (**Figure 5-3 a**). 20 min of UBP2002 application was carried out and HFS was given. A clear and noticeable decrease of the trace during HFF was observed with UBP2002 (**Figure 5-3 b**) which was reversed with 1 h 30 min of washing out (**Figure 5-3 c**). DCG-IV application was followed for 15 min and abolished enhancement completely (**Figure 5-3 d**) confirming HFF is generated by MF synapses. For statistical comparison, the amplitude of 5^{th} responses with or without drugs were compared. On average, UBP2002 reduced the 5^{th} amplitude to 57.1 ± 6.7% of control which was reversed to 107.6 ± 14.3% of control with wash out of UBP2002. DCG-IV blocked synaptic response (n = 5, 5^{th} response; 34.2 ± 8.8% of control, $^{**}p = 0.0082$, one-way ANOVA repeated measures, $^{*}p < 0.05$ for control and UBP2002, $^{**}p < 0.01$ for UBP2002 and wash out, Tukey post hoc test) (**Figure 5-3 e**).

LFS (1 Hz for 30 s) was given to examine the effect of UBP2002 (100 μM) during LFF. 1 Hz for 30 s of stimulation elicited a gradual increase in synaptic response in MF (345.9 ± 63.8%, **Figure 5-**

4 a). This enhancement was mitigated by 20 min of UBP2002 (100 µM) application (to 240.0 ± 37.1%), although this was statistically insignificant (**Figure 5-4 b**). 1 h 30 min of washing out restored the effect of UBP2002 (436.0 ± 67.4%, **Figure 5-4 c**). Between three groups, difference was evident, especially between UBP2002 and wash out (n = 4, **Figure 5-4 d**) (**p = 0.0059, one-way ANOVA repeated measures, **p < 0.01 for UBP2002 and wash out, Tukey post hoc test). This data clearly shows that the presence of UBP2002 interferes with LFF at MF synapses.

5.2.2. Effect of GluK2 antagonism by UBP2038 on HFF and LFF

In a preliminary study using HEK293 cells, we observed that UBP2038 has higher activity than UBP2002 to human GluK2 receptors (**Figure 5-1 d**). As UBP2038 has higher activity and better selectivity for GluK2 than UBP2002, we used half the concentration (50 µM) of UBP2002 to test its activity first on HFF and secondly on LFF. In control conditions, HFS induced a robust facilitation from the 1st to 5th response (**Figure 5-5 a**). When applied at a concentration of 50 µM, UBP2038 led a significant decrease of the amplitude of 5th response during HFF (45.2 ± 3.5%, **Figure 5-5 b**) and its effect was readily reversible as after 1 h 30 min of washing out the amplitude of the 5th response was restored nearly back to that in control conditions (83.8 ± 10.9%, **Figure 5-5 c**). Elimination of HFF was observed with 15 min of DCG-IV application as expected (21.8 ± 2.2%, **Figure 5-5 d**). Direct comparison of the amplitude of 5th response revealed that UBP2038 at a concentration of 50 µM substantially blocks HFF in reversible manner (n = 8, *** p < 0.001, one-way ANOVA repeated measures, ***p < 0.001 for control and UBP2002, **p < 0.0.1 for UBP2002 and wash out, Tukey post hoc test) (**Figure 5-5 e**).

In control conditions, LFS induced a progressive facilitation of the MF response reaching 284.9 ± 36.3% of baseline (**Figure 5-6 a**). This degree was partially reduced to 148.4 ± 17.4% of control with UBP2038 administration (**Figure 5-6 b**). When the drug was washed out for 1 h 30 min, the facilitation returned to 295.0 ± 89.6% of control on average. Although it seemed there is evident trend that UBP2038 reduce the degree of LFF in reversible manner, the difference was not statistically significant (**Figure 5-6 c**) (n = 5, *p = 0.0303, one-way ANOVA repeated measures, *p < 0.05 for UBP2038 and wash out, Tukey post hoc test) (**Figure 5-6 d**).

5.3. Discussion

5.3.1. Development of GluK2 antagonist

Since dysregulation of KARs in the CNS has been implicated in temporal lobe epilepsy (Das et al 2012, Li et al 2010), schizophrenia (Ibrahim et al 2000, Pickard et al 2006) and mood disorder (Milanesi et al 2015, Paddock et al 2007, Lerma & Marques 2013), there is therapeutic potential for compounds that are active at KARs. To date, several GluK1 specific antagonists exist and are active under physiological conditions. For example, LY382884 (Bortolotto et al 1999), UBP310 (Dolman et al 2007, Mayer et al 2006) and ACET (Dargan et al 2009, Dolman et al 2007) were found to be highly specific to GluK1 subunit providing a pharmacological tool to examine the role of GluK1-containing KARs on synaptic function. However, the development of GluK2 antagonist has been difficult as many of compounds exhibit poor selectivity toward GluK2. Few antagonists were designed but none have been proven to be specific for GluK2 or tested under physiological conditions (Kaczor et al 2015, Schiavini et al 2015)

Here in Bristol, more recently we synthesised kynurenic acid derivatives which could be potentially GluK2 antagonists. Replacement of the hydrogen at the 6-position in the phenyl ring was substituted with iodine (Leeson et al 1991) making UBP2002. Following additional substitution at the 5 and 7-positions with fluorine, we produced UBP2038.

Using a calcium fluorescence assay, we found UBP2002 to be slightly selective for GluK2 over GluK1 (1.6 times more selective to GluK2) and show robust selectivity (16.8 times) for GluK2 over GluA1. In contrast, UBP2038 had better potency for GluK1, GluK2 and GluA1. Encouragingly, the selectivity of UBP2038 for GluK2 over GluK1 was 2.4 times better than UBP2002, but it had higher activity for AMPARs compared to UBP2002 as well (4.9 times selective to GluK2 over GluA1).

In order to investigate the effect of the two compounds on the GluK2 subunit alone, we used global GluK1 KO mice to rule out any possibility of GluK1 subunit involvement. Also, during HFF and LFF experiments, we applied GYKI 53655 to block AMPARs circumventing the potential issue with antagonistic activity of UBP2002 and UBP2038 on AMPAs. This combination of genetic pruning and pharmacological intervention provided ideal conditions to test UBP2002 and UBP2038 as potential GluK2 antagonists. UBP2002 and UBP2038 may not be used under physiological conditions as a GluK2 antagonist due to its activity on AMPAR and GluK1 subunit,

however, this approach is a valuable starting point for GluK2 antagonist design and will aid future development of subunit specific KARs.

5.3.2. Role of GluK2 in MF

A lack of pharmacological tools for specific GluK2 antagonist led KAR studies to focus on genetic approaches generating GluK2 KO animals. Breustedts and Schmitz (2004) demonstrated that KAR-induced synaptic transmission by application of KA was absent in GluK2 KO mice. Synaptic facilitation at 100 Hz and 0.33 Hz were also impaired in this mouse model, sensitivity to KA was greatly reduced and CA3 postsynaptic KA currents were not present in GluK2 KO animals (Mulle et al 1998). Seizures induced by KA injection into the hippocampus were also reduced in the animals (Mulle et al 1998). Using the genetic mouse model lacking GluK2 indicates an important physiological role of GluK2 subunit in synaptic function at MF synapses.

From a behavioural perspective, GluK2-lacking animals displayed impaired performance in hippocampus related learning and memory tasks (Ko et al 2005). These authors have shown that GluK2 KO mice failed to sustain a contextual fear memory while WT animals showed freezing behaviour up to 2 weeks after the fear conditioning. Another study demonstrated that GluK2 KO mice acquired spatial memory without deficit while spatial reversal learning is impaired indicating behavioural flexibility is affected by lack of GluK2 (Micheau et al 2014). Taken together with physiological observation from GluK2 KO study (Mulle et al 1998), it is clear that GluK2 subunit is critical for MF synaptic function and may affect learning and memory processes.

Our observation that MF-LTP is blocked and that HFF and LFF are attenuated by UBP2002 and UBP2038 support the idea that GluK2 is a key subunit for MF function. As this is the first study demonstrating the properties of GluK2 subunit using a pharmacological tool, further study using UBP compounds in behavioural context may be possible to reveal other roles of GluK2.

5.3.3. Effect of UBP2002 on MF-LTP and HFF

Figure 5-2 demonstrated that MF-LTP was not induced in the presence of UBP2002. After 1 h 30 min of washing out LTP was still not induced (Figure 5-2). On the other hand, the reduced amplitude of the 5th response in HFF caused by UBP2002 application was readily reversed with 1 h 30 min of washing out (Figure 5-3). One possibility for this discrepancy could be that we did not have MF-LTP in those slices in the first place. Another possibility is that 1 h 30 min was not sufficient for UBP2002 to wash out for MF-LTP. In this sense, MF-LTP is more sensitive to GluK2 antagonism than HFF, this means a longer wash out may be needed. Since the interleaved

experiment without a tetanus did not restore back to the baseline level, it is most likely that UBP2002 was not completely washed out in given time.

5.3.4. Limitation and future direction of the study

GluK2 subunit KARs is highly expressed in CA1 and CA3 region of the hippocampus. Not only presynaptic granule cell expresses mRNA of GluK2 but also it is expressed in postsynaptic CA3 pyramidal neurons (Bureau et al 1999, Wisden & Seeburg 1993). This subunit of KARs can form functional homomeric KARs itself or heteromeric KARs with GluK1 and GluK3-5 (Egebjerg et al 1991). The first evidence that GluK2 assembles in high affinity KAR subunits and in particular with GluK5 subunits to make heteromeric GluK2/5 receptors, was Wenthold et al. (1994). In the study, they demonstrated that a GluK2 antibody co-immunoprecipitated with a GluK5 antibody in rat brain tissue. Another group showed that GluK5 immunoreactivity was reduced in CA3 region in the GluK2 KO mice (Ruiz et al 2005) suggesting GluK2/5 may be the main configuration of KARs in the CA3 region.

The efficacy of UBP2002 and UBP2038 were determined in the preliminary study using recombinant human homomeric GluA1, GluK1 and GluK2 receptors overexpressed in HEK293 cells. Even though GluK1-3 can form functional homomeric KARs, heteromeric KARs are thought to be the main combination existing in physiological conditions. Since no experiment was carried out on GluK2-containing heteromeric KARs or GluK3 subunits, the efficacy of UBP2002 and UBP2038 on these KARs is not known. For this reason, it is possible that the dose used in our study may antagonise GluK2-containig heteromers and GluK3 subunit at some degree which could contribute to impairment of MF-LTP, HFF or LFF. Therefore, the efficacy of UBP2002 and UBP2038 on GluK2 or GluK3 containing KARs should be assessed separately and tested on MF functions.

Another problem we encountered was linked to the fact that we could not distinguish the pre and postsynaptic effects of GluK2 antagonist in our field potential recordings configuration. Application of antagonist in slices affects GluK2 at both sites, making it difficult to dissect the impact of presynaptic GluK2 antagonism from postsynaptic GluK2 antagonism. Although MF function is mostly attributed to presynaptic KARs functioning as an autoreceptor, patch recording from presynaptic or postsynaptic cell directly should be exercised to examine the role of GluK2 in detail.

5.4. Conclusion

In this chapter, we used two kynurenic derivatives UBP2002 and UBP2038. UBP2038 is a newly synthesised compound while UBP2002 has been reported previously (Leeson et al 1991). In our study we tested two compounds in native tissue, investigating the physiological role of GluK2 subunit. By combining genetic and pharmacological tools, we demonstrated UBP2002 and UBP2038 could be potential GluK2 antagonists.

Our set of results suggest that GluK2 plays a role in the induction of MF-LTP, on MF properties such as HFF and LFF. Therefore, our data is consistent with previous findings and strongly indicates that GluK2 plays important role in MF function.

This study is the first pharmacological study to address the GluK2 antagonism and demonstrates that this KARs subunit play a pivotal physiological function at MF synapses.

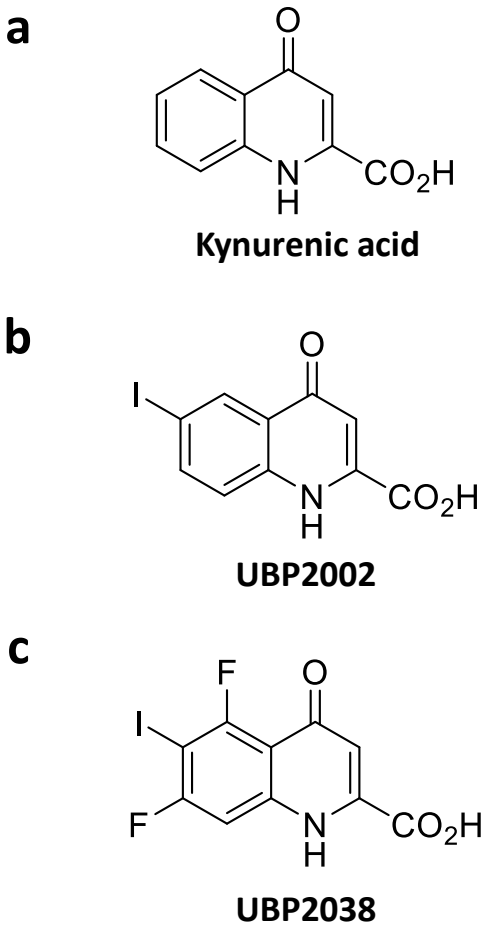

d

K_i value (in µM)	UBP2002	UBP2038
GluK1	30.5 ± 4.9	11.6 ± 0.9
GluK2	19.3 ± 1.6	5.0 ± 0.4
GluA1	324.8 ± 70.9	24.1 ± 2.3

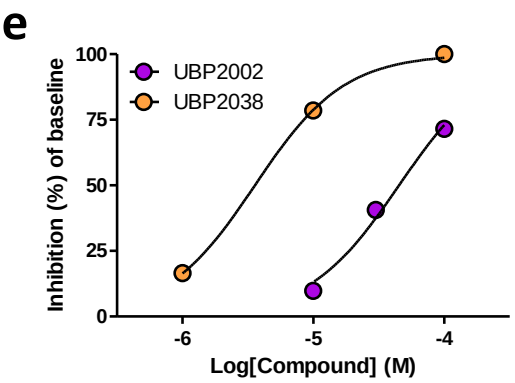

Figure 5-1. Chemical structure of UBP2002 and UBP2038 based on the Kynurenic acid.

a. Structure of kynurenic acid.

b. Structure of UBP2002 showing hydrogen is substituted with iodine at 6-position.

c. 5 and 7-positions of UBP2002 are substituted with fluorine making UBP2038.

d. Table for K_i value of UBP2002 and UBP2038 on GluK1, GluK2 and GluA1 receptors.

e. The dose response curve of UBP2002 and UBP2038 on native AMPARs in the CA1 of rat hippocampus (d and e, data provided by Mr. Alen Eapan, University of Bristol, UK).

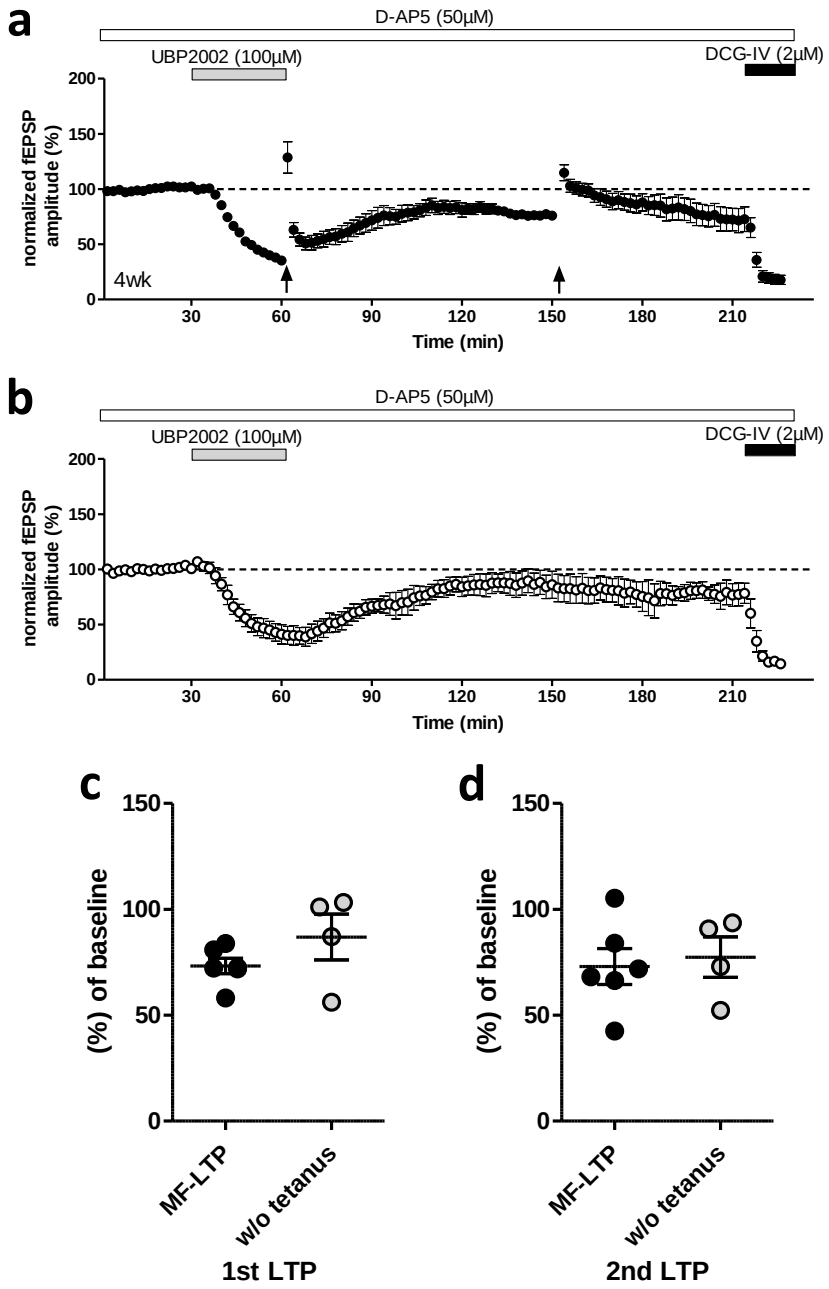

Figure 5-2. MF-LTP in the presence of UBP2002.

a. A tetanus is given to elicit MF-LTP in the presence of UBP2002

b. Interleaved experiments without a tetanus in the presence of UBP2002.

c. Bar chart showing degree of facilitation after 1st MF-LTP is evoked.

d. Chart showing degree of MF-LTP after 2nd MF-LTP is evoked. Black arrow: a tetanus (100 Hz for 1 s).

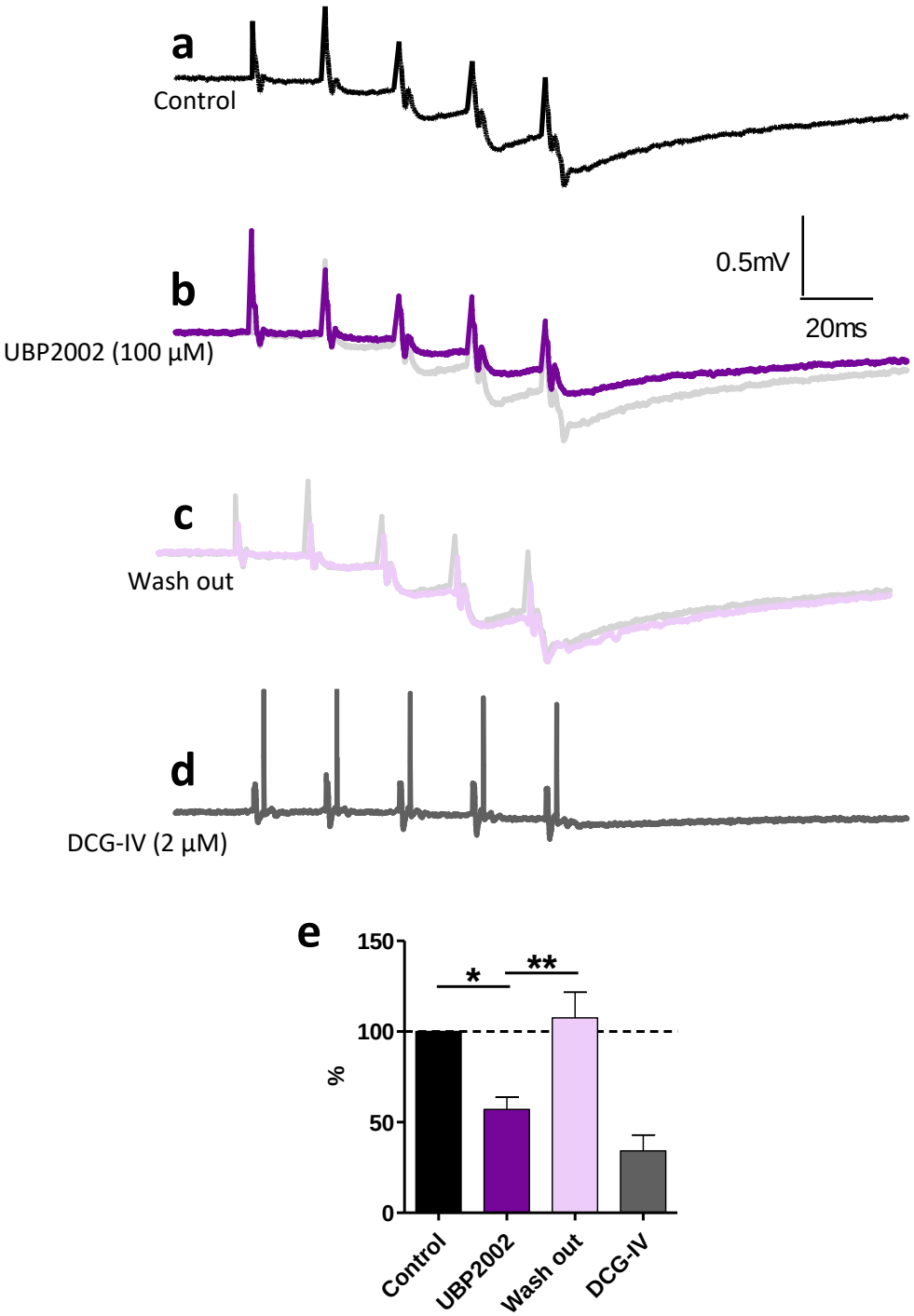

Figure 5-3. Impact of GluK2 antagonism on mossy fiber HFF in GluK1 KO
a. HFF expression in the presence of D-AP5 and GYKI 53655.
b. Trace in the presence of UBP2002 during HFF.
c. Washing out readily reverses effect of UBP2002 to control level.
d. Synaptic responses is abolished with DCG-IV.
e. Summary graph showing UBP2002 partially decreases the amplitude of 5th response in a reversible manner. Light grey line: HFF in control condition (n = 5). *p < 0.05, **p < 0.01.

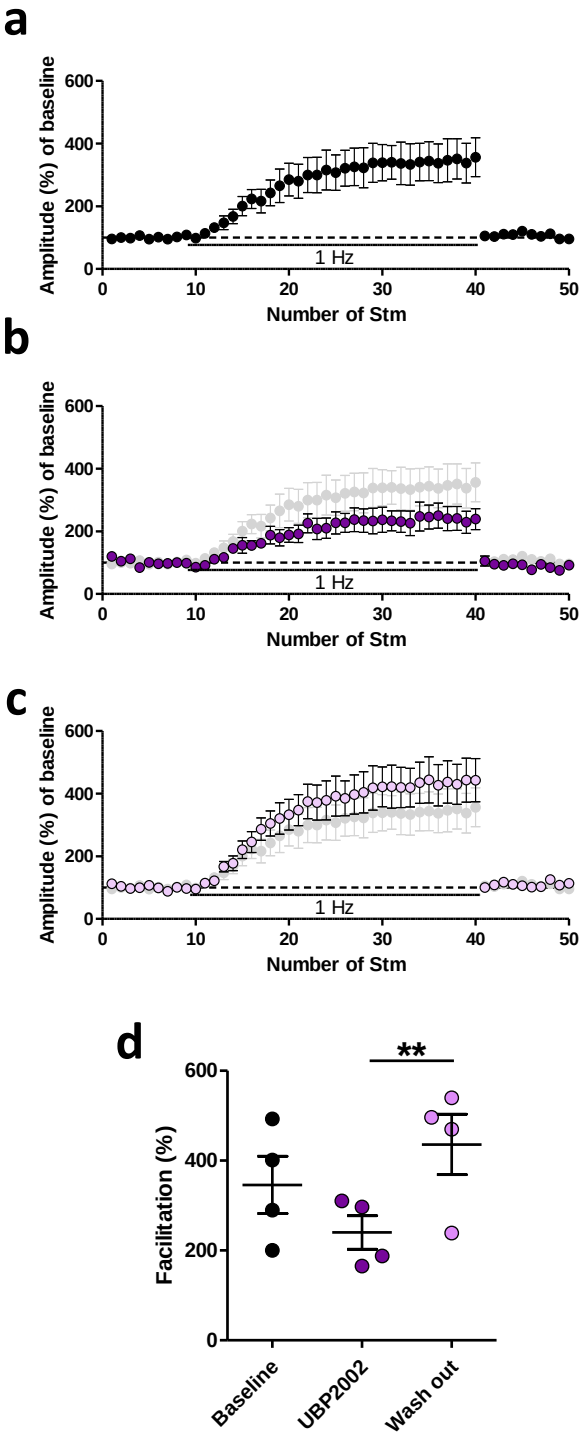

Figure 5-4. The effects of UBP2002 on MF LFF.
a. Expression of LFF in control conditions.
b. Expression of LFF during UBP2002 application.
c. Amplitude of LFF after washing out.
d. Summary chart showing the effect of UBP 2002 and washing out. Light grey: LFF in control condition (n = 4). **p < 0.01.

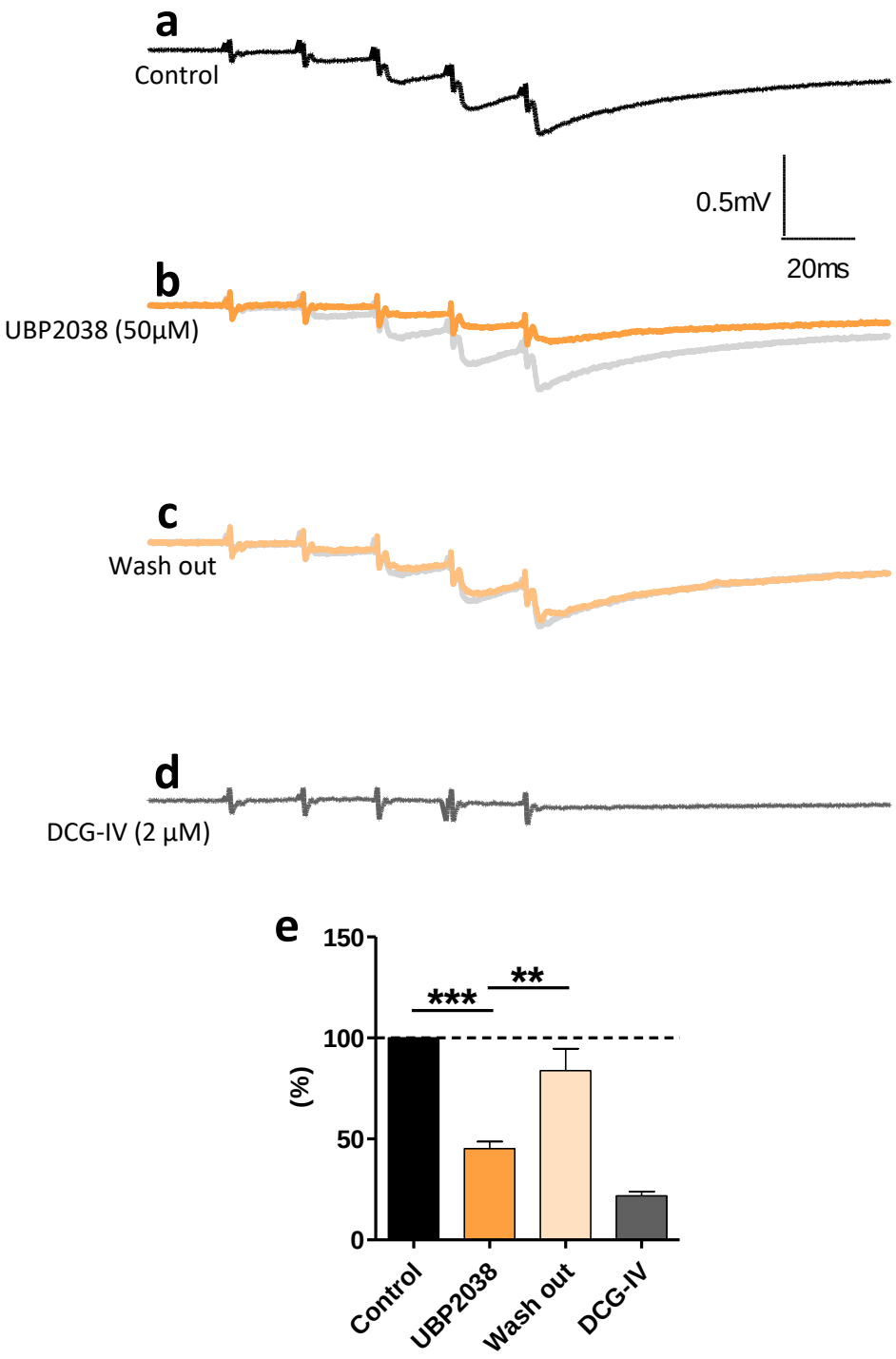

Figure 5-5. Impact of UBP2038 on mossy fiber HFF.
a. HFF is developed in D-AP5 and GYKI 53655.
b. Trace in the presence of UBP2038.
c. Washing out partially recovers degree of HFF.
d. HFF with DCG-IV.
e. Bar chart demonstrating UBP2038 significantly decreases the amplitude of 5th response in a reversible manner. Light grey line: HFF in control condition (n = 8). **p < 0.01, ***p < 0.001.

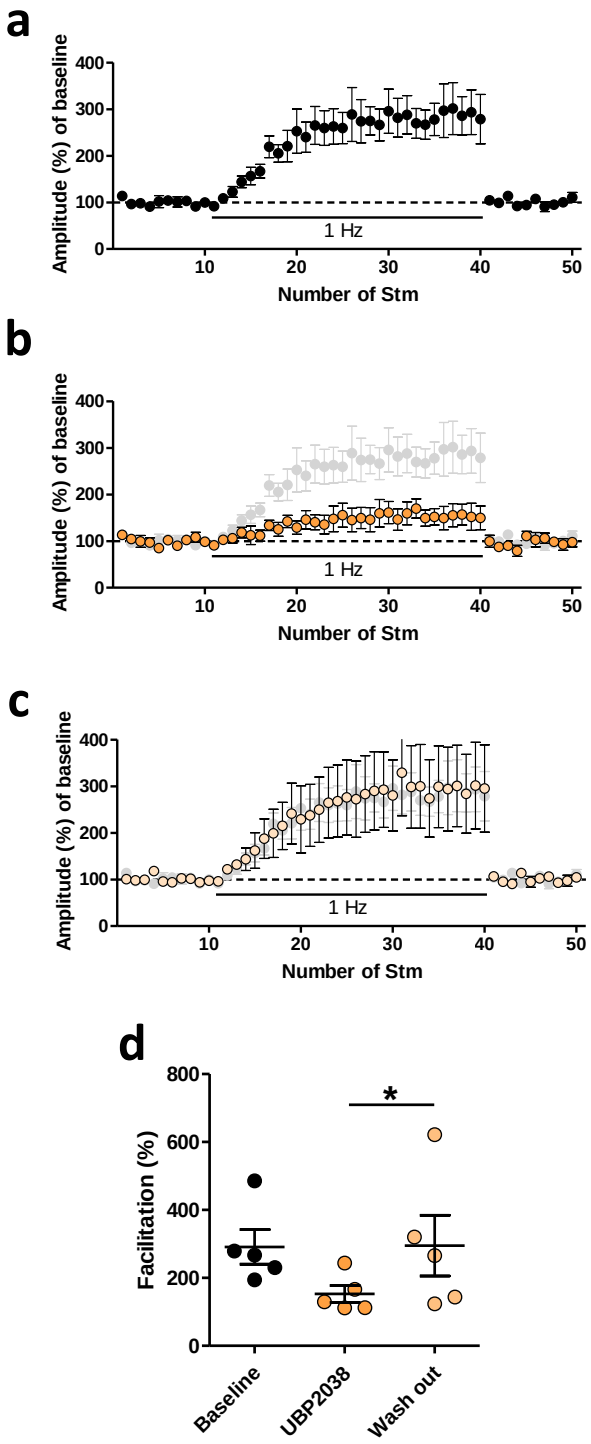

Figure 5-6. The effect of UBP2038 on MF LFF.
a. LFF expression in control conditions.
b. Amplitude of LFF in the presence of UBP 2038.
c. Expression of LFF after washing out.
d. Bar chart showing degree of LFF during UBP 2038 application and washing out. Light grey: LFF in control condition (n = 5). *p < 0.05.

Chapter 6. Results: Investigation of GluK1-containing KARs in DG-GluK1 KO

6.1. Introduction

In previous studies, it was shown that MF-LTP requires presynaptic Ca^{2+} enhancement (Tong et al 1996). It was also suggested that GluK1-containing KARs are expressed presynaptically (Bortolotto et al 2005, Lauri et al 2005) and upon their activation there is increased probability of neurotransmitter release at MF-CA3 synapses (Maeda et al 1997, Salin et al 1996). While it is generally agreed that presynaptic KARs have a role in normal synaptic transmission and plasticity at MF-CA3 synapses, a controversy remained about which subunit of KARs are crucial for MF functions. Several pharmacological studies suggested the GluK1 subunit is important for MF-LTP and HFF (Bortolotto et al 1999, Dargan et al 2009, Lauri et al 2001a, Lauri et al 2001b). In contrast, others suggested that the GluK2 subunit had a more prominent role than GluK1. The later hypothesis was based on genetic ablation of the GluK2 subunit (Breustedt & Schmitz 2004, Contractor et al 2001, Mulle et al 1998). Therefore, our aim was to resolve the controversy and find out which subunit plays a critical role on MF by investigating DG-GluK1 KO animals. DG-GluK1 KO animals would have the GluK1 subunit deleted selectively in the presynaptic side, hence, it would be an ideal model to investigate the role of presynaptic GluK1-containing KARs.

Hippocampal expression of GluK1 regulates network development in neonates (Clarke et al 2014, Sallert et al 2007, Vesikansa et al 2012). It also regulates network excitability of CA3 via changing probability of release of GABA (Caiati et al 2010) or by being expressed on interneurons in CA3 (Paternain et al 2000). We adopted Cre-loxP system to generate conditional KO mice in which GluK1 would be knocked-out after the critical developmental stage and its expression would be confined only in GC in DG. In this way, we keep early development intact and do not disrupt the expression of GluK1 on interneurons which could affect network excitability.

Homozygous Grik1 floxed mice which express loxP sites in the target Grik1 gene were crossed with POMC-Cre mice generating DG-GluK1 KO mice. POMC-Cre mice (Balthasar et al 2004) express Cre recombinase primarily in hippocampus especially granule cell in DG. Cre protein starts to emerge from 2-3 postnatal week and expression is sustained for up to 6 months (McHugh et al 2007). Therefore, DG-GluK1 KO mice develop normally with undisturbed GluK1 expression until this developmental point. Also, the ablation of GluK1 will be limited to granule cells which leads to knock out of primarily presynaptic GluK1-containing KARs in area CA3.

We applied the same approach used in chapter 4 to validate the animals. The presence of the GluK1 subunit was tested by applying the GluK1 specific agonist ATPA to cause synaptic

depression in MF and A/C synapses. In the previous study using POMC-Cre mice, the authors confirmed that the target protein was nearly absent at 16 postnatal weeks (McHugh et al 2007). Therefore, we divided the animals into 3 groups (2, 4, 8-16 weeks) to track the point at which GluK1 was ablated.

It is worth noting that littermates from POMC-Cre; Grik1$^{flx/wt}$ x POMC-Cre; Grik1$^{flx/flx}$ would be ideal for the experiment, however, due to limitations of time and resources we bred animals into four groups, a) POMC-Cre$^{wt/wt}$; Grik1$^{wt/wt}$ (**Grik1$^{wt/wt}$**), b) POMC-Cre$^{wt/wt}$; Grik1$^{flx/flx}$ (**Grik1$^{flx/flx}$**), c) POMC-Cre$^{cre/cre}$; Grik1$^{wt/wt}$ (**POMC-Cre; Grik1$^{wt/wt}$**, also include POMC-Cre$^{cre/wt}$; Grik1$^{wt/wt}$) and d) POMC-Cre$^{cre/cre}$; Grik1$^{flx/flx}$ (**POMC-Cre; Grik1$^{flx/flx}$**, also include POMC-Cre$^{cre/wt}$; Grik1$^{flx/flx}$). The first three groups are used as the corresponding control genotypes for the fourth group. Age matched litters from four groups were selected for experiments and the experimenter was blinded on the day of experiment.

6.2. Result

6.2.1. Validation of DG-GluK1 KO mice

We expected that three control genotypes would show normal depression of MF and A/C synapses in young animals and degree of depression would get smaller as animals get older due to age-dependency of ATPA effect seen in chapter 4 (**Figure 4-1 to 4-3**) and according to the literature (Clarke & Collingridge 2002). We hypothesised that the experimental group would show a similar degree of depression at 2 weeks, but, be resistant to the synaptic depression at later developmental stages, possibly from 4 weeks. Also, the resistance to ATPA's depressant effect was expected to be observed selectively in MF synapses as GluK1 subunit would be knocked out only in MF not in A/C synapses.

The first group, which does not express loxP site and Cre protein (Grik1$^{wt/wt}$) was tested with ATPA. 1 μM of ATPA for 10 min depressed basal synaptic transmission of MF and A/C synapses and reached the peak at 34 min in 2 weeks-old mice (88.9 ± 10.6% of the baseline for MF, 80.6 ± 13.4% of the baseline for A/C, n = 3) (**Figure 6-1 a**). MF and A/C synapses showed a slight depression in 4 weeks-old mice (88.7 ± 6.3% of the baseline for MF, 83.3 ± 5.9% of the baseline for A/C, n = 3) (**Figure 6-1 b**). ATPA's effect was nearly absent both in MF and A/C synapses in 8-16 weeks-old animals (105.3 ± 3.9% of baseline for MF, 108.4 ± 4.9% of baseline for A/C, n = 5) (**Figure 6-1 c**). Thus, in Grik1$^{wt/wt}$ mice, we confirmed that ATPA depresses MF and A/C synapses and depressant effect is not observed in adult animals.

Grik1$^{flx/flx}$ mice has loxP sites in Grik1 gene but do not express Cre protein. Because there is no Cre recombinase, loxP sites are preserved and no disruption of the Grik1 gene is expected. In 2 weeks-old mice, the application of ATPA reduced synaptic transmission of MF and A/C synapses at 34 min (76.0 ± 0.6% of the baseline for MF, 71.1 ± 15.7% of the baseline for A/C, n = 3) (**Figure 6-2 a**). The depressant effect of ATPA was reduced in 4 weeks-old animals, reaching down to 81.1 ± 8.5% of baseline for MF and 94.7 ± 7.4% of the baseline for A/C, n = 3) (**Figure 6-2 b**). In adult animals, synaptic transmission was not affected by ATPA, at peak depression time (34 min), basal transmission of MF recorded 102.7 ± 3.3% of baseline and 113.1 ± 8.8% of baseline for A/C (n = 7) (**Figure 6-2 c**).

In POMC-Cre; Grik1$^{wt/wt}$ mice, it was expected to have Cre recombinase expressed in DG but no loxP site in Grik1 gene to cleave, thus, this line is also corresponding control for DG-GluK1 KO animal. In 2 weeks-old mice, at 34 min, clear depression (65.0 ± 14.0% of the baseline, n = 4) was observed in MF synapses. A/C showed similar depression (83.3 ± 8.8% of the baseline, n = 3) (**Figure 6-3 a**). In 4 weeks-old mice, this effect was greatly reduced in MF and A/C synapses. The MF response reached 94.9 ± 3.3% of the baseline and A/C reached 96.3 ± 3.9% of the baseline (n = 3) (**Figure 6-3 b**). Similar to 4 weeks-old mice, adult showed no changes in basal transmission by application of ATPA in MF and A/C synapses (109.2 ± 3.9% of the baseline for MF, 108.4 ± 4.9% of the baseline for A/C, n = 4) (**Figure 6-3 c**).

In interleaved experiments, ATPA's depressant effect was tested in POMC-Cre; Grik1$^{flx/flx}$ mice. As Cre expression starts at 2-3 postnatal week, we expected to see similar degree of depressant effect of ATPA compared to control lines in 2 weeks-old mice but depression at lesser degree in 4 and 8-16 weeks-old animals. 1 μM of ATPA reduced basal transmission at MF and A/C synapses in 2 weeks-old mice (58.6 ± 10.3% of baseline for MF, 77.9 ± 13.3% of baseline for A/C, n = 3) (**Figure 6-4 a**). In 4 weeks-old mice, synaptic transmission was reduced 88.8 ± 5.7% of baseline for MF synapses (n = 6) and 82.1 ± 10.3% of baseline for A/C synapses (n = 5) (**Figure 6-4 b**). In adult mice, the application of ATPA did not change basal transmission in MF (110.5 ± 6.3% of the baseline) and A/C synapses (102.0 ± 6.5% of baseline, n = 5) (**Figure 6-4 c**).

The degree of depressant effect of ATPA was compared within the same age group. In 2 weeks-old mice, all three control groups and the experimental group showed reduced synaptic transmission of MF below the baseline level ($p > 0.05$, one-way ANOVA) (**Figure 6-5 a**). A/C synapses showed similar degree of depression after ATPA in 2 weeks-old mice and no difference was found ($p > 0.05$, one-way ANOVA) (**Figure 6-5 b**).

The effect of ATPA in 4 weeks-old animals were compared. The amplitude of MF response was reduced after ATPA application in all four groups and had no significant difference between them ($p > 0.05$, one-way ANOVA) (**Figure 6-5 c**). The reduction on A/C synapses of the experimental group was comparable to three control groups ($p > 0.05$, one-way ANOVA) (**Figure 6-5 d**). This suggests that sufficient GluK1 subunit is still present at 4 weeks-old animals leading depression of synaptic transmission caused by ATPA.

Lastly, ATPA was tested in adult animals. The depression of basal transmission of MF and A/C synapses seen in young animals were clearly absent in adult mice in all four groups. The amplitude of MF synapses from four groups were comparable to each other ($p > 0.05$, one-way ANOVA) (**Figure 6-5 e**). A/C synapses from four groups also showed similar degree of changes after ATPA application ($p > 0.05$, one-way ANOVA) (**Figure 6-5 f**).

Taken together, we confirmed that the effect of ATPA was clearly seen in all four groups at 2 weeks-old mice in which Cre protein has not been expressed yet. We did not observe any statistical difference in the degree of depression caused by ATPA between the control groups and the experimental group in later developmental stage (> 4 weeks). This indicates that at 4 weeks, Cre recombinase is not expressed to the degree required to effectively ablate GluK1, so GluK1 subunit is still present in granule cells of DG. In adult mice, ATPA no longer had an effect in the control conditions, therefore we cannot confirm knock out of GluK1 in adult mice by ATPA application.

6.2.2. Role of presynaptic GluK1 on MF-LTP in fully developed mice

In theory, Cre recombinase should start to express around postnatal week 2-3 and be robustly present when they reach full maturity (> 8weeks), therefore, GluK1 protein should be substantially decreased in granule cell in DG. We wondered whether lack of presynaptic GluK1 subunit would alter expression of MF-LTP at this age.

8-16 weeks-old mice from Grik1$^{flx/flx}$ and POMC-Cre; Grik1$^{flx/flx}$ were tested with a classical tetanus stimulation (100 Hz, 1 sec) to elicit MF-LTP in the presence of D-AP5 (50 µM). In Grik1$^{flx/flx}$ mice, this stimulation induced MF-LTP and facilitated response that stayed 1 h after the induction (n = 3) (**Figure 6-6 a**). Similar and stable MF-LTP expression was observed in POMC-Cre; Grik1$^{flx/flx}$ mice (n = 4) (**Figure 6-6 b**). The magnitude of PTP (**Figure 6-6 c**, $p > 0.05$, unpaired t-test) and LTP was comparable (**Figure 6-6 d**, $p > 0.05$, unpaired t-test) between two groups. This result indicates that ablation of presynaptic GluK1 does not affect PTP or impede MF-LTP.

6.3. Discussion

6.3.1. Validation of DG-GRIK1 KO

With this set of experiments, we aimed to validate DG-GluK1 KO animals which lack GluK1 subunit in DG by investigating the modulatory effect of the GluK1 subunit on synaptic transmission at MF synapses. In an attempt to validate the animals as a model, we used the GluK1 specific agonist ATPA as described in chapter 4. However, we were unable to confirm presynaptic GluK1 is knocked-out sufficiently in DG-GluK1 KO mice due to the age-dependent effect of ATPA. ATPA's effect was evident in all four lines in early developmental stage (2 weeks-old), similar to the previous results presented in chapter 4. By the time the animals reach full maturation (8-16 weeks) when presynaptic GluK1 subunit is thought to be knocked-out by robust Cre expression, MF synapses do not show sensitivity toward to ATPA anymore. We did not observe any effect of genotype at the intermediate time point (4 weeks), possibly because Cre expression was not yet sufficient to have an effect.

Another way to validate the DG-GluK1 KO is to observe depression of A/C synapses caused by ATPA. It is known that ATPA can depress A/C synapses as well as MF (Lauri et al 2001b). If GluK1 is sufficiently knocked-out in GC, MF response should be resistant to ATPA and only A/C responses should be reduced. Reduction of A/C should be seen regardless of Cre expression as only DG would express Cre. However, we did not observe significant difference of depression between A/C and MF synapses at 4 weeks of age as well as by the time animals reach the time point when GluK1 is thought to be knocked-out, sensitivity of A/C to ATPA is also lost.

In both ways, we were unable to prove that GluK1 had been knocked out in DG-GluK1 KO mice. Although the observation made on DG-GluK1 KO in this chapter is consistent with the earlier results with GluK1 KO animals that ATPA's depressant effect on MF and A/C disappear quickly after 4 weeks. Failure to observe an effect of ATPA within the effective time window led to the validation being unsuccessful. This indicates that Cre is not expressed to the required extent by 4 weeks of age and as the effect of ATPA is no longer a valid measure of GluK1 subunit activity after 4 weeks of age, an alternative approach must be taken in future studies to verify its presence.

6.3.2. Mechanism of ATPA's depressant effect

It has been suggested that ATPA's depressant effect is an indirect action via presynaptic $GABA_B$ receptors. Evidence for this idea was given by Schmitz (Schmitz et al 2000). In a series of

experiments the authors showed that selective antagonism of $GABA_B$ by SCH50911 reverses ATPA's depressant effect. Based on this result, they assumed that GluK1-containing KARs are expressed on interneurons and activation of GluK1 by ATPA releases GABA to act on presynaptic $GABA_B$ receptors leading to depression of synaptic activity. However, another group in subsequent study showed the same drug (SCH50911) failed to block ATPA's effect (Lauri et al 2001b) suggesting it is not working via $GABA_B$ receptors. GluK1 has been detected in glutamic acid decarboxylase (GAD)-expressing cells (Paternain et al 2000). If this is the primary expression site of GluK1, the expression of Cre recombinase in DG would not affect the expression of GluK1 in GAD-expressing cells. Consequently, ATPA would depress synaptic transmission regardless of Cre expression. We do not know whether the lack of ATPA effect in our approach can be attributed to this possibility, therefore, the answer to this question remains open. An alternative approach could be taken, for example, crossing animals expressing GAD-CRE with floxed Grik1 mice to generate GAD-specific GluK1 KO mice.

6.3.3. Presynaptic GluK1 subunit on MF function

We carried out experiments investigating MF-LTP and PTP based on an assumption that presynaptic GluK1 would be sufficiently knocked-out in DG-GluK1 KO animals that are older than 8 weeks. If it was true, the observation that the magnitude of PTP and MF-LTP in DG-GluK1 were comparable to corresponding WT indicates that presynaptic GluK1 may not play important role on synaptic plasticity. Indeed, low expression level of GluK1 in adult animal supports this notion (Bahn et al 1994). Also, previous pharmacological studies that have found a role for GluK1 in MF function were carried out in juvenile animals (P12 - P35) (Bortolotto et al 1999, Lauri et al 2003). Thus, knocking out of GluK1 protein after full maturation may have very minor effect and not have any impact on synaptic function. Although we do not know whether this is the case as validation of the animals was unsuccessful, the result is consistent with our previous findings in adult rat that GluK1-specific antagonist did not alter synaptic plasticity in chapter 3.

6.3.4. Future direction of the study

In this study, it is important to confirm that only presynaptic GluK1 is knocked-out. Without valid evidence that shows DG-GluK1 lacks GluK1 subunit specifically in presynaptic membrane, further investigation on role of presynaptic GluK1 cannot be made. It will be necessary to confirm that the level of GluK1 protein drops with Cre expression over time. Looking at RNA level using *in situ* hybridization would be one way to find the right time window for experiment.

Imaging of MF synapses would be another way. Expression of presynaptic marker and co-localization of GluK1 could be checked in WT and DG-GluK1 KO animals. Alternatively, western blotting with an antibody against Cre recombinase, yet indirect, could be another way to validate animals.

6.4. Conclusion

As an attempt to understand the role of presynaptic GluK1 subunit at MF synapses, we have generated DG-GluK1 KO that would not carry GluK1-containing KARs in presynaptic terminal of MF. However, validation of the animals with ATPA was not successful. Further investigation with alternative measures should be taken to verify GluK1 subunit is sufficiently knocked-out in DG-GluK1 KO.

From MF-LTP and PTP experiment, we did not observe difference in the degree of MF-LTP and PTP suggesting presynaptic GluK1 subunit may not be a key subunit that regulate synaptic plasticity, at least in adult animals.

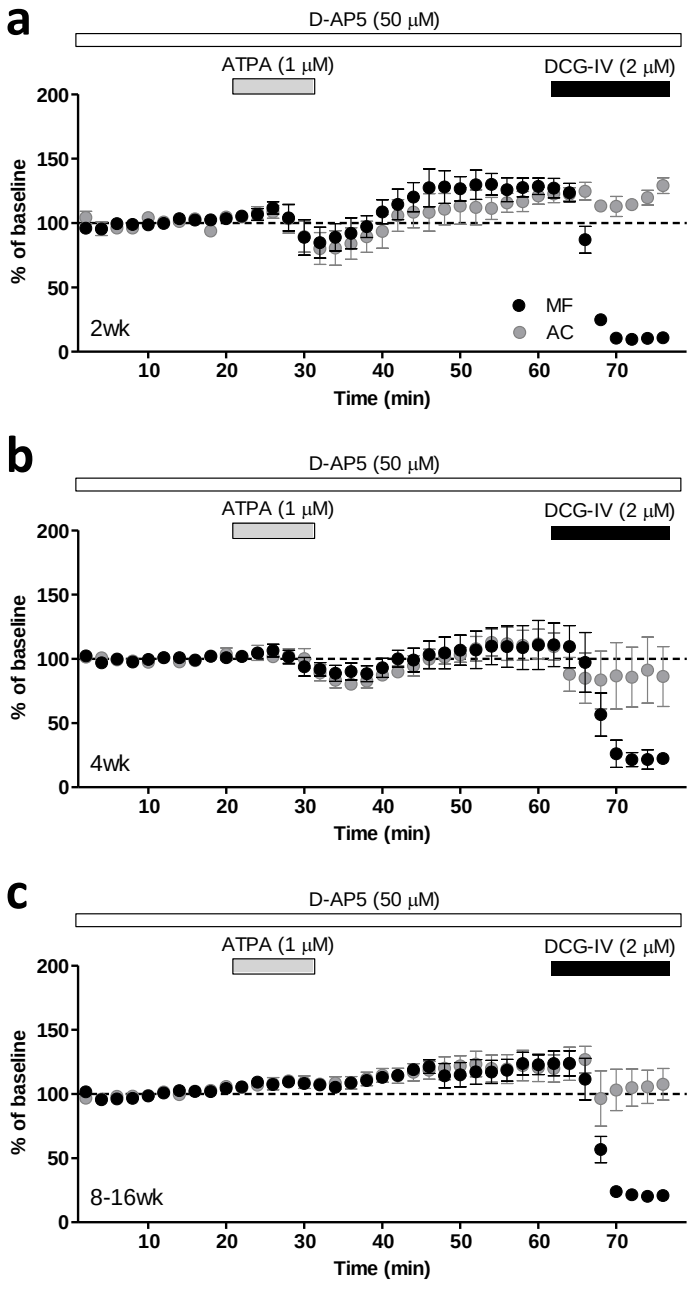

Figure 6-1. Validation of DG-specific GluK1 KO mice using ATPA in Grik1$^{wt/wt}$ mice

a. Depressant effect of ATPA in 2 week old mice (n = 3).

b. Depressant effect of ATPA in 4 week old mice (n = 3).

c. Depressant effect of ATPA in 8-16 week old mice (n = 5).

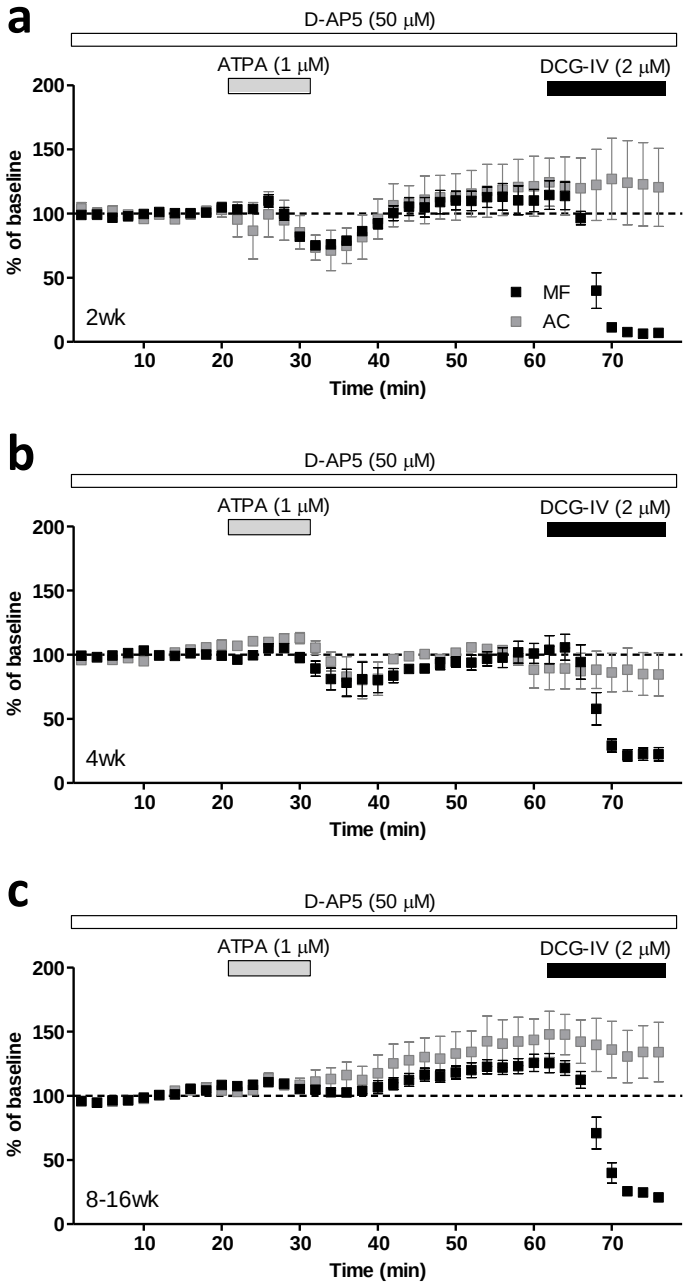

Figure 6-2. Validation of DG-specific GluK1 KO mice using ATPA in Grik1$^{flx/flx}$ mice

a. Depressant effect of ATPA in 2 week old mice (n = 3).

b. Depressant effect of ATPA in 4 week old mice (n = 4).

c. Depressant effect of ATPA in 8-16 week old mice (n = 6).

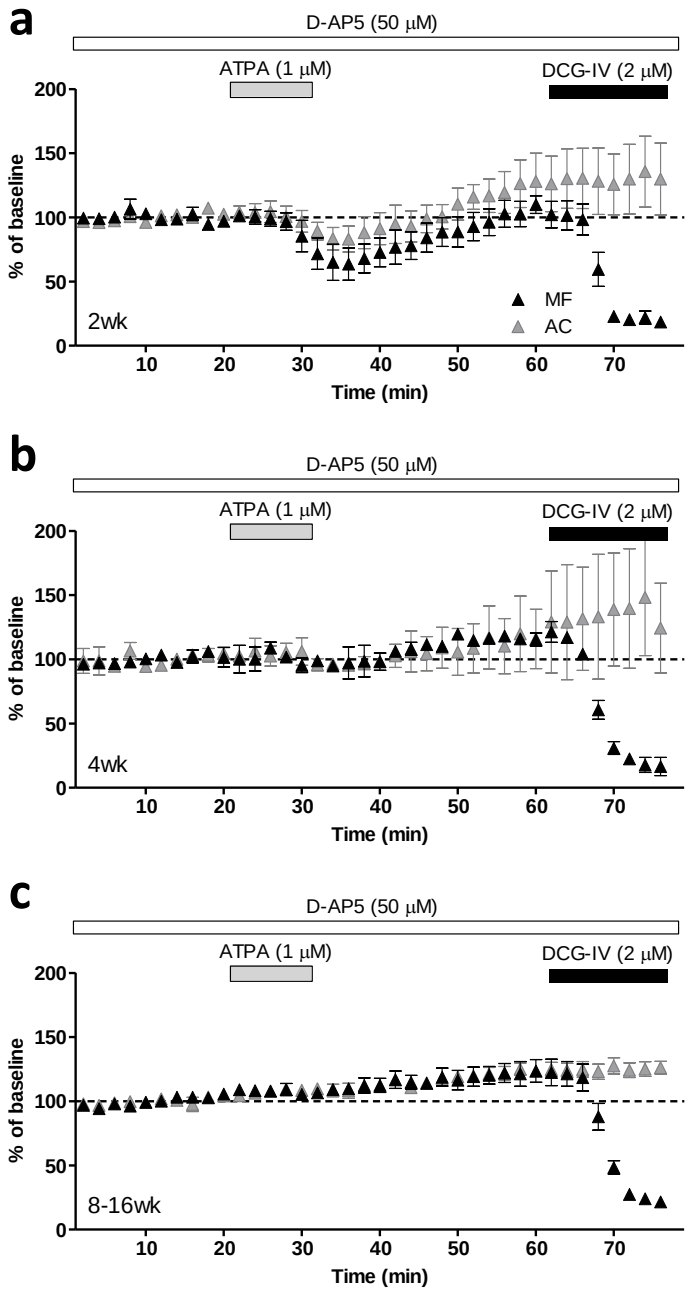

Figure 6-3. Validation of DG-specific GluK1 KO mice using ATPA in POMC-Cre; Grik1$^{wt/wt}$ mice

a. Depressant effect of ATPA in 2 week old mice (n = 4).

b. Depressant effect of ATPA in 4 week old mice (n = 3).

c. Depressant effect of ATPA in 8-16 week old mice (n = 4).

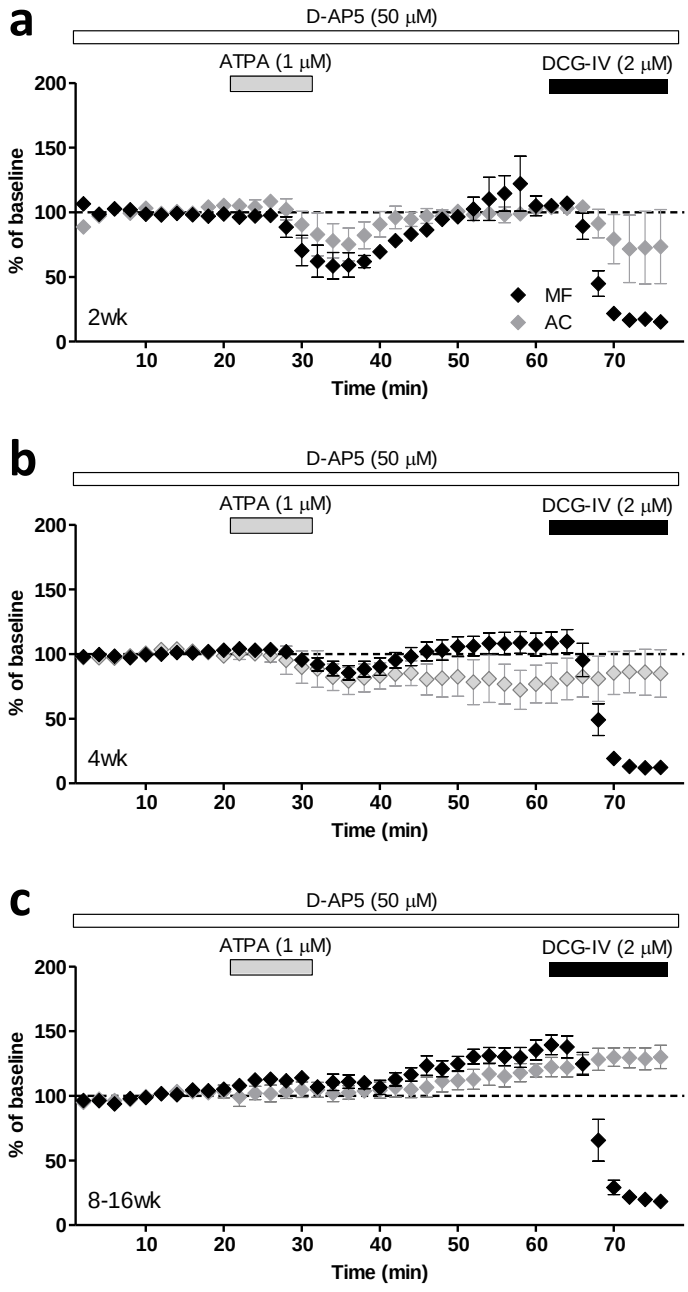

Figure 6-4. Validation of DG-specific GluK1 KO mice using ATPA in POMC-Cre; Grik1$^{flx/flx}$ mice

a. Depressant effect of ATPA in 2 weeks old mice (n = 3).

b. Depressant effect of ATPA in 4 weeks old mice (n = 6).

c. Depressant effect of ATPA in 8-16 weeks old mice (n = 5).

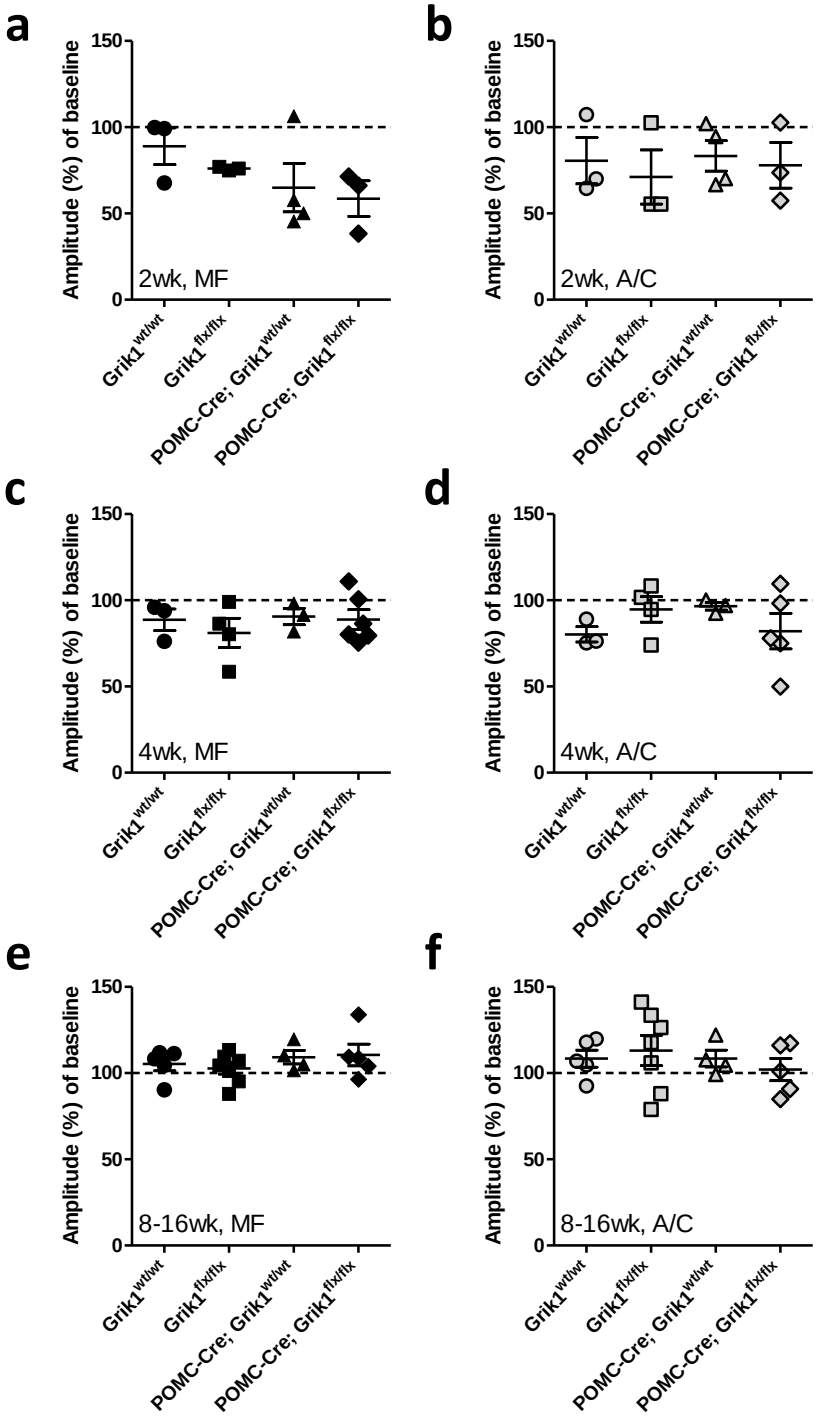

Figure 6-5. Summary chart showing degree of ATPA's depressant effect in 4 genotypes

a. ATPA reduces synaptic transmission in MF at 2 weeks.

b. ATPA reduces synaptic transmission in A/C at 2 weeks.

c. ATPA slightly reduces synaptic transmission in MF at 4 weeks.

d. ATPA slightly reduces synaptic transmission in A/C at 4 weeks.

e. ATPA does not reduces synaptic transmission in MF at 8-16 weeks.

f. ATPA does not reduces synaptic transmission in A/C at 8-16 weeks.

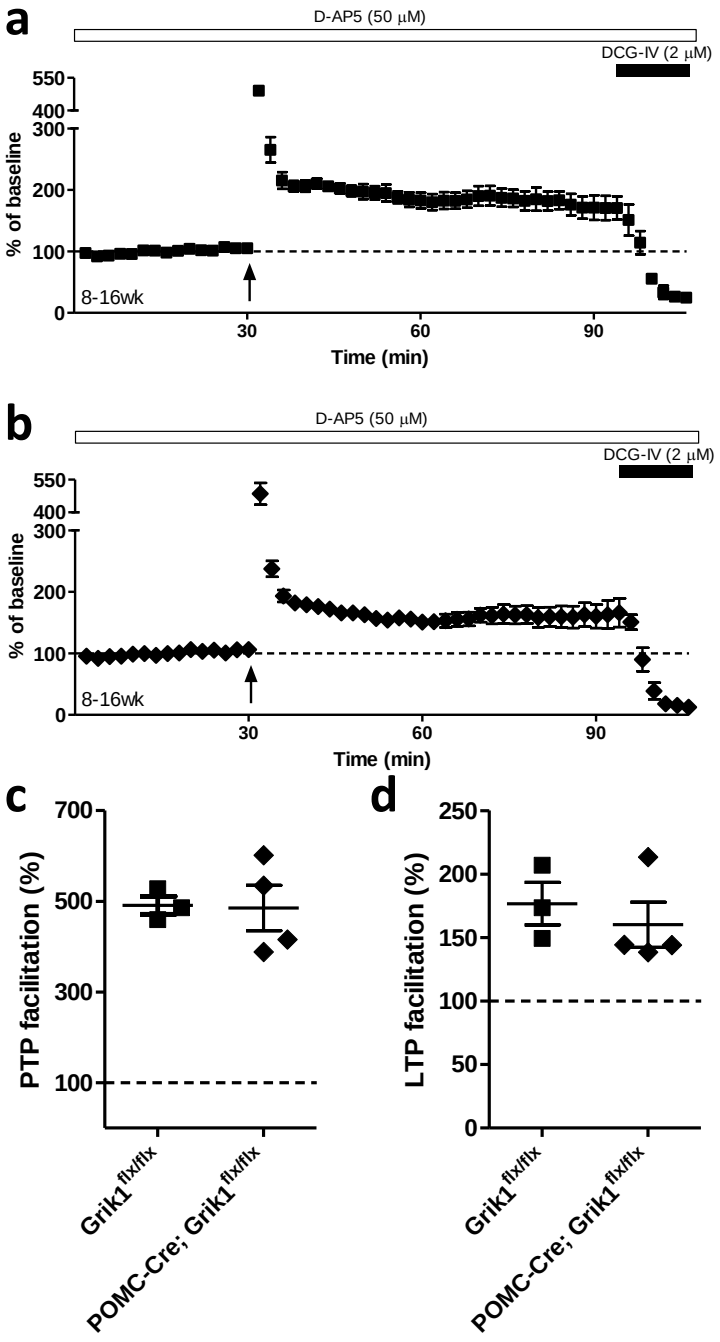

Figure 6-6. MF-LTP is intact in POMC-Cre; Grik1$^{flx/flx}$ mice compared to corresponding adult WT animals

a. MF-LTP is expressed in Grik1$^{flx/flx}$ mice (n = 3).

b. MF-LTP is expressed POMC-Cre; Grik1$^{flx/flx}$ mice (n = 4).

c. Degree of PTP is not different.

d. Magnitude of LTP is comparable.

Chapter 7. General discussion

7.1. Discussion

7.1.1. Discrepancy between pharmacological and genetic studies

The Aim of this study was to investigate the role of GluK1 antagonism on unique features of MF synapses and further investigate the role of GluK1 and GluK2 using a combination of genetic and pharmacological tools.

Firstly, we characterised MF synapses in our conditions. We consistently observed DCG-IV sensitive and insensitive responses regardless of slice orientation, however, in transverse slices a higher proportion of response were DCG-IV sensitive than in parasagittal slices (Sherwood et al 2012). Features that are thought to be characteristic of MF synapses, including pronounced PTP and HFF, were of greater magnitude in DCG-IV sensitive slices. This demonstrates that DCG-IV sensitive slices are more likely to contain MF synapses. We therefore used transverse slices for the remaining experiments in this study and furthermore defined the MF pathway as one that DCG-IV inhibits by ≥ 70%. In these conditions we found that GluK1 antagonism failed to block MF-LTP and did not alter the degree of PTP and LFF. These findings are consistent with the previous genetic studies that showed that genetic ablation of the GluK1 subunit did not change MF function (Breustedt & Schmitz 2004, Contractor et al 2001). In line with these studies, our global GluK1 KO mice exhibited a comparable level of MF-LTP, PTP and HFF to WT.

However, our results also partially agree with the pharmacological studies that directly contradict the results from the genetic studies. We observed that in WT animals, ACET reduces the amplitude of the 5th response during a HFF protocol, and in GluK1 KO mice this was not observed. As ACET is a specific antagonist for the GluK1 subunit (Dargan et al 2009), this confirms not only global GluK1 KO does not carry functional GluK1 but also suggests GluK1 plays a role in HFF, either by passing current at the post synapse or by triggering the facilitation. Therefore, it is reasonable to conclude that GluK1 contributes to HFF in normal conditions, but its role is easily compensated for in GluK1 KO animals.

Ca^{2+} permeable KARs have been reported to be important for MF-LTP (Andrade-Talavera et al 2012). During early developmental stages, ≥ 60 % of GluK1-KARs are expressed as the Ca^{2+} permeable form (GluK1 (Q)) whereas Ca^{2+} impermeable GluK1 (R)-KARs are more prevalent in adult animals (> 50%) (Bernard et al 1999). Therefore, development could diminish the importance of the GluK1 subunit. Consequently, the room for GluK1 antagonists to act would become smaller in adult animals and the blockade of MF-LTP would be more difficult to observe.

The previous pharmacological studies used juvenile animals (P12 - P35) (Bortolotto et al 1999, Dargan et al 2009, Lauri et al 2001a) and responses were DCG-IV insensitive (Sherwood et al 2012). In our study, we used adult Wistar rats (chapter 3) and DCG-IV sensitive transverse slices. Since the age of the animals and slice orientation could be of relevance, we tried to reproduce the conditions in which a role for GluK1 had been found in MF-LTP. However, ACET did not block MF-LTP in DCG-IV insensitive parasagittal slices obtained from P14 animals. There is an *in vivo* study that demonstrated blockade of mGluRs as well as GluK1 subunits were needed to block MF-LTP (Wallis et al 2015) and those responses were DCG-IV sensitive. Therefore, it may be of interest to test whether antagonism of mGluRs is also needed to block MF-LTP in parasagittal slices from P14 animals.

7.1.2. The role of the GluK2 subunit on MF function

Further investigation on the role of GluK2 subunits was carried out with the newly synthesised compounds UBP2002 and UBP2038. Both compounds show high potency toward GluK2, however, they also express antagonistic activity at GluK1 and GluA1 receptors. As both compounds showed minor selectivity for GluK2 over GluK1, we exploited global GluK1 KO animals to test these two compounds. GluK1 KO mice did not show significant deficits in MF function, therefore, it was the ideal condition to test the role of GluK2. As mentioned earlier, UBP2002 and UBP2038 exhibit antagonistic activity at GluA1. Therefore, we applied D-AP5 and GYKI 53655 during HFF and LFF experiments at all time and left only KAR-mediated responses. We found that UBP2002 and UBP2038 significantly reduce the amplitude of the 5^{th} response during HFF in reversible manner.

For MF-LTP, UBP2002 was chosen to be tested as UBP2002 has less potency towards GluA1 compared to UBP2038. The application of UBP2002 depressed synaptic transmission as expected. We did not observe MF-LTP in the presence of UBP2002 and the impairment of MF-LTP was not restored after washout. As synaptic transmission had not recovered to the baseline conditions after a period of extended washout, it is possible that UBP2002 was still present at a concentration high enough to block LTP. Lastly, in LFF experiments, the reduction caused by the application of UBP2002 or UBP2038 was not significant but washing out of compounds increased the degree of LFF significantly. Since the degree of LFF varied a lot, additional experiments will be needed to clearly address the role of GluK2 on LFF. Taken together, our results are consistent with the hypothesis that the GluK2 subunit plays a key role in MF function in our conditions.

7.1.3. DG-GluK1 mice

The same experimental scheme to validate the global GluK1 KOs (inhibition of MF-EPSPs with ATPA) was used to validate DG-GluK1 KO animals. In theory, Cre recombinase would be expressed from 2-3 postnatal weeks and by 8 postnatal weeks, Cre expression was expected to be sufficient to knock out GluK1. However, validation of DG-GluK1 KO by ATPA was unsuccessful. This is likely because the effect of ATPA is also age-dependent, in that adult animals no longer show an ATPA-induced depression in basal transmission. At 4 postnatal weeks when Cre recombinase is thought to have been expressed for up to 2 weeks, we did not see a difference in the degree of ATPA-induced depression compared to WT. This demonstrates that the expression of Cre recombinase was not sufficient within the effective time window for ATPA to be used. Additional validation will be needed to confirm that GluK1-containing KARs are indeed knocked out in these animals.

7.1.4. A suggested model for presynaptic mechanism at MF synapses

Here, we investigated the role of GluK1 and GluK2-containing KARs on MF functions. Although the downstream mechanism remains unclear, activation of KARs with a high dose of agonist has been shown to depress synaptic transmission in CA3 and CA1 synapses via presynaptic changes. In our study, the specific GluK1 agonist ATPA successfully depressed synaptic transmission at 2 and 4 weeks of age but not in adult animals. This indicates that the GluK1-mediated mechanism is present only during early developmental stages. This idea is supported by the observation that antagonism of GluK1 did not affect the degree of LFF, PTP and MF-LTP in adult rat slices and knock out of presynaptic GluK1 in adult DG-GluK1 KO mice did not impair MF-LTP. However, ACET reduced the degree of HFF in 4 weeks old WT mice and the effect of ACET was not seen in GluK1 KO mice. This confirms that GluK1 contribute to the degree of HFF. Therefore, it is reasonable to conclude that the role of GluK1 for MF function is present but minimal at 2 and 4 weeks and can be readily replaced by other subunit-containing KARs in adult animals. Genetic ablation of GluK1 can be substituted by other KARs so that functions of MF synapses in GluK1 KO remain intact.

In contrast to GluK1, the series of experiments carried out in 4 weeks old mice using UBP2002 and UBP2038 revealed that GluK2 antagonism robustly reduces the degree of LFF and HFF. Also, MF-LTP was not induced in the presence of UBP2002. This demonstrates that GluK2-containing KARs modulate both short term- and long term plasticity at MF synapses. Since expression of

GluK2 subunit increases with development and reaches its peak in DG and CA3 of adult animal (Bahn et al 1994), it is possible that the role of GluK1 is substituted by GluK2-containing KARs in the adult. The fact that we did not observe any deficit in MF function in GluK1 KO in our experiments also supports this notion.

It is worth noting that we did not test agonist and antagonists on pre- or postsynaptic KARs separately. Also, how KARs are distributed between the pre- and postsynaptic cell is still largely unknown. A few previous studies suggested that presynaptic KARs consist of homomeric GluK1 and GluK2/3 or GluK2/4 heteromers while postsynaptic KARs consist of GluK1-containing heteromers and GluK2/5 heteromers (Ball et al 2010, Darstein et al 2003, Vignes et al 1998). Further investigations are needed to determine if this is the case.

Taken together, we suggest a model to demonstrate how GluK1 and GluK2-containing KARs are responsible for short- and long-term plasticity at MF synapses (**Figure 7-1**). Upon repetitive stimulation such as a tetanus, HFS or LFS, presynaptic vesicles fuse with the presynaptic terminal to release neurotransmitter into the synaptic cleft. Released glutamate binds to the presynaptic KARs, for example homomeric GluK1-KARs and heteromeric GluK2-containing KARs. Activated KARs act as autoreceptors and allow Ca^{2+} to pass into the presynaptic cell increasing level of Ca^{2+} in presynaptic boutons. Elevated level of Ca^{2+} triggers activation of AC-cAMP-PKA pathway and recruitment of additional release sites (Chamberland et al 2014, Midorikawa & Sakaba 2017). As a result, release probability is increased and these presynaptic changes are observed as facilitation of synaptic responses.

On the other hand, activation of mGluR2/3 reduces glutamate release via down regulation of AC-cAMP-PKA pathway.

Future directions

In order to investigate the role of GluK1 and GluK2 subunits and their physiological importance in MF synapses, we exploited pharmacological tools to the greatest extent possible. A highly selective and potent GluK1 antagonist (ACET) and an agonist (ATPA) were used to examine the GluK1 subunit. We also obtained a newly developed GluK1 antagonist, UBP3000, but a calcium fluorescence assay revealed that UBP3000 is not as potent as ACET. Although ACET is highly selective to GluK1, it has also been reported to affect GluK3 homomers (Perrais et al 2009). For GluK2 subunit, UBP2002 and UBP2038 were developed and a series of experiments confirmed that the GluK2 subunit plays a critical role in MF function. However, both compounds exhibit

antagonistic activity at GluA1 and GluK1. Because of this, experiments had to be carried out in GluK1 KO animals in the presence of a specific antagonist of AMPARs (GYKI 53655). This restricts employment of these antagonists in physiological conditions, for example, an injection of GluK2 antagonist during a behavioural task would not be advisable and extra caution should be taken when designing experiments with these compounds. Taken together, it seems clear that we are still in need of a better antagonists that have greater selectivity and potency for each KAR subunit.

One of problems we encountered was that the technique used in this study (field potential recording) was restricted in that pre- or postsynaptic effects of antagonists (UBP2002 and UBP2038) was difficult to distinguish. GluK2 subunits are expressed both pre- and postsynaptically and the bath application of compounds would affect GluK2 subunit at both sites. For this reason, patch recording from a presynaptic terminal or postsynapatic CA3 neurons would be a more direct measure to demonstrate the role of pre- or postsynaptic GluK2 subunit.

One of aims of this study was to find the role of presynaptic GluK1 in the MF function by investigating DG-GluK1 KO animals. DG-GluK1 KOs were generated but we were unable to validate these animals due to the narrow time window of ATPA's depressant effect. For future investigation, validation of the animals is necessary. To detect if an adequate level of Cre recombinase has been reached and if GluK1 is knocked out in DG-GluK1 KO, other approaches need to be taken. *In situ* hybridization to look at mRNA of GluK1 subunit could be one way or western blotting of Cre recombinase could be another way. Alternatively, direct visualization of GluK1 with presynaptic marker could be checked.

It has been reported that interneurons in CA3 region express the GluK1 subunit (Paternain et al 2000). In addition, there is evidence which indicates KARs may not be directly involved in MF function but regulate network excitability in CA3 (Kwon & Castillo 2008b, Schmitz et al 2003). Therefore, investigation on this possibility could be an interesting next step. Since we already possess Cre-inducible GluK1 KO animals, crossing this line with GAD-Cre line would be the first step.

Concluding remarks

Here, we demonstrated the role of GluK1 and GluK2 subunit at MF synapses using a combination of genetic and pharmacological tools to shed some light on their functional role. Our results

indicate that GluK1 contributes to features of the MF at a minor level whereas GluK2 play an important role.

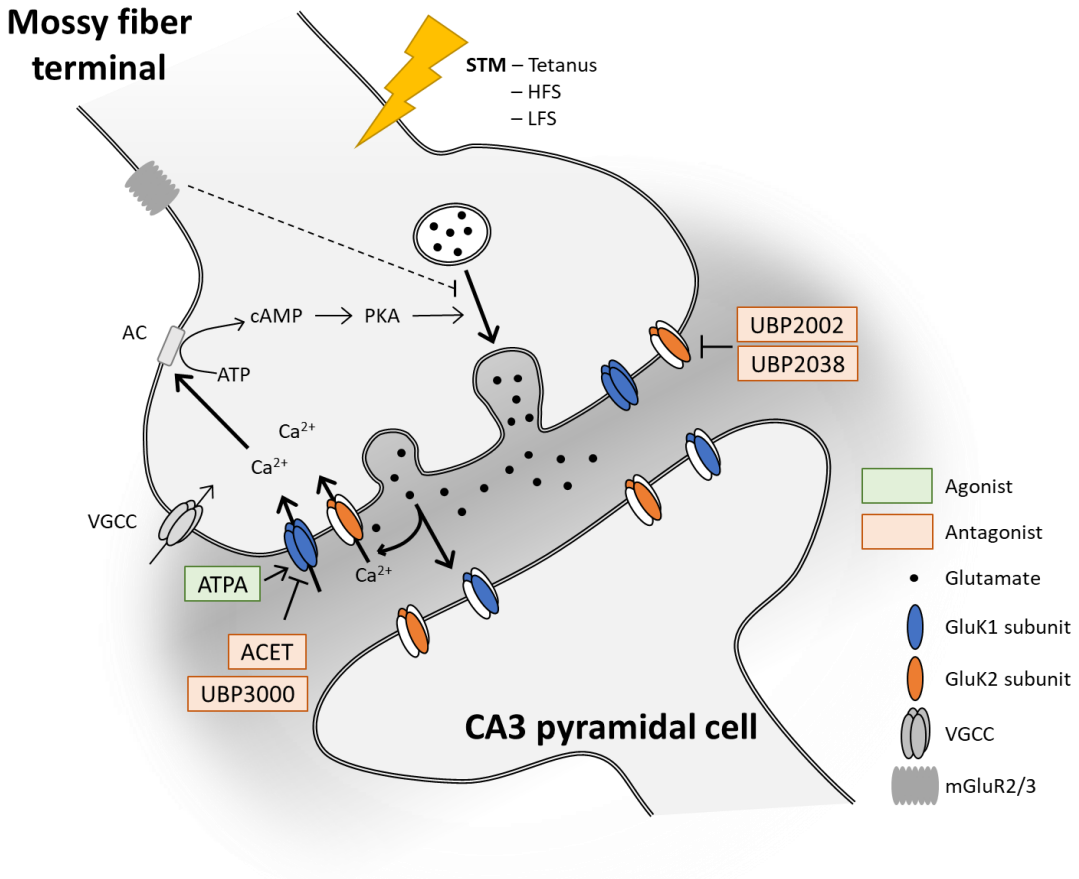

Figure 7-1. A schematic drawing of a mechanism that underlies presynaptic changes at MF synapses.

Presynaptic KARs such as homomeric GluK1 and heteromeric GluK2-KARs are responsible for increased glutamate release from the presynaptic terminal at early developmental stages.

References

Acsady L, Kamondi A, Sik A, Freund T, Buzsaki G. 1998. GABAergic cells are the major postsynaptic targets of mossy fibers in the rat hippocampus. J Neurosci 18: 3386-403

Aller MI, Pecoraro V, Paternain AV, Canals S, Lerma J. 2015. Increased Dosage of High-Affinity Kainate Receptor Gene grik4 Alters Synaptic Transmission and Reproduces Autism Spectrum Disorders Features. J Neurosci 35: 13619-28

Alt A, Weiss B, Ogden AM, Knauss JL, Oler J, et al. 2004. Pharmacological characterization of glutamatergic agonists and antagonists at recombinant human homomeric and heteromeric kainate receptors in vitro. Neuropharmacology 46: 793-806

Amaral DG, Dent JA. 1981. Development of the mossy fibers of the dentate gyrus: I. A light and electron microscopic study of the mossy fibers and their expansions. J Comp Neurol 195: 51-86

Amaral DG, Ishizuka N, Claiborne B. 1990. Neurons, numbers and the hippocampal network. Prog Brain Res 83: 1-11

Amaral DG, Scharfman HE, Lavenex P. 2007. The dentate gyrus: fundamental neuroanatomical organization (dentate gyrus for dummies). Prog Brain Res 163: 3-22

Amaral DG, Witter MP. 1989. The three-dimensional organization of the hippocampal formation: a review of anatomical data. Neuroscience 31: 571-91

Andersen P, Bliss TV, Skrede KK. 1971. Lamellar organization of hippocampal pathways. Exp Brain Res 13: 222-38

Andersen P, Morris R, Amaral D, Bliss T, O'Keefe J. 2007. The hippocampus book. Oxford University Press, Inc.

Anderson WW, Collingridge GL. 2007. Capabilities of the WinLTP data acquisition program extending beyond basic LTP experimental functions. J Neurosci Methods 162: 346-56

Ando M, Oku N, Takeda A. 2010. Zinc-mediated attenuation of hippocampal mossy fiber long-term potentiation induced by forskolin. Neurochem Int 57: 608-14

Andrade-Talavera Y, Duque-Feria P, Negrete-Diaz JV, Sihra TS, Flores G, Rodriguez-Moreno A. 2012. Presynaptic kainate receptor-mediated facilitation of glutamate release involves Ca2+ -calmodulin at mossy fiber-CA3 synapses. J Neurochem 122: 891-9

Andrade-Talavera Y, Duque-Feria P, Sihra TS, Rodriguez-Moreno A. 2013. Pre-synaptic kainate receptor-mediated facilitation of glutamate release involves PKA and Ca(2+) -calmodulin at thalamocortical synapses. J Neurochem 126: 565-78

Artinian J, Peret A, Marti G, Epsztein J, Crepel V. 2011. Synaptic kainate receptors in interplay with INaP shift the sparse firing of dentate granule cells to a sustained rhythmic mode in temporal lobe epilepsy. J Neurosci 31: 10811-8

Atar D, Backx PH, Appel MM, Gao WD, Marban E. 1995. Excitation-transcription coupling mediated by zinc influx through voltage-dependent calcium channels. J Biol Chem 270: 2473-7

Bahn S, Volk B, Wisden W. 1994. Kainate receptor gene expression in the developing rat brain. J Neurosci 14: 5525-47

Bahn S, Volk B, Wisden W. 1994. Kainate receptor gene expression in the developing rat brain. J Neurosci 14: 5525-47

Ball SM, Atlason PT, Shittu-Balogun OO, Molnar E. 2010. Assembly and intracellular distribution of kainate receptors is determined by RNA editing and subunit composition. J Neurochem 114: 1805-18

Balthasar N, Coppari R, McMinn J, Liu SM, Lee CE, et al. 2004. Leptin receptor signaling in POMC neurons is required for normal body weight homeostasis. Neuron 42: 983-91

Bannister NJ, Benke TA, Mellor J, Scott H, Gurdal E, et al. 2005. Developmental changes in AMPA and kainate receptor-mediated quantal transmission at thalamocortical synapses in the barrel cortex. J Neurosci 25: 5259-71

Barberis A, Sachidhanandam S, Mulle C. 2008. GluR6/KA2 kainate receptors mediate slow-deactivating currents. J Neurosci 28: 6402-6

Barbon A, Vallini I, Barlati S. 2001. Genomic organization of the human GRIK2 gene and evidence for multiple splicing variants. Gene 274: 187-97

Barnes SJ, Opitz T, Merkens M, Kelly T, von der Brelie C, et al. 2010. Stable mossy fiber long-term potentiation requires calcium influx at the granule cell soma, protein synthesis, and microtubule-dependent axonal transport. J Neurosci 30: 12996-3004

Bartesaghi R, Ravasi L. 1999. Pyramidal neuron types in field CA2 of the guinea pig. Brain Res Bull 50: 263-73

Bashir ZI, Bortolotto ZA, Davies CH, Berretta N, Irving AJ, et al. 1993. Induction of LTP in the hippocampus needs synaptic activation of glutamate metabotropic receptors. Nature 363: 347-50

Battistin T, Cherubini E. 1994. Developmental shift from long-term depression to long-term potentiation at the mossy fibre synapses in the rat hippocampus. Eur J Neurosci 6: 1750-5

Ben-Ari Y. 1985. Limbic seizure and brain damage produced by kainic acid: mechanisms and relevance to human temporal lobe epilepsy. Neuroscience 14: 375-403

Bernard A, Ferhat L, Dessi F, Charton G, Represa A, et al. 1999. Q/R editing of the rat GluR5 and GluR6 kainate receptors in vivo and in vitro: evidence for independent developmental, pathological and cellular regulation. Eur J Neurosci 11: 604-16

Bettler B, Boulter J, Hermans-Borgmeyer I, O'Shea-Greenfield A, Deneris ES, et al. 1990. Cloning of a novel glutamate receptor subunit, GluR5: expression in the nervous system during development. Neuron 5: 583-95

Birch PJ, Grossman CJ, Hayes AG. 1988. Kynurenic acid antagonises responses to NMDA via an action at the strychnine-insensitive glycine receptor. Eur J Pharmacol 154: 85-7

Blackstad TW, Kjaerheim A. 1961. Special axo-dendritic synapses in the hippocampal cortex: electron and light microscopic studies on the layer of mossy fibers. J Comp Neurol 117: 133-59

Blakemore LJ, Corthell JT, Trombley PQ. 2018. Kainate Receptors Play a Role in Modulating Synaptic Transmission in the Olfactory Bulb. Neuroscience 391: 25-49

Bleakman D, Ballyk BA, Schoepp DD, Palmer AJ, Bath CP, et al. 1996. Activity of 2,3-benzodiazepines at native rat and recombinant human glutamate receptors in vitro: stereospecificity and selectivity profiles. Neuropharmacology 35: 1689-702

Bortolotto ZA, Clarke VR, Delany CM, Parry MC, Smolders I, et al. 1999. Kainate receptors are involved in synaptic plasticity. Nature 402: 297-301

Bortolotto ZA, Lauri S, Isaac JT, Collingridge GL. 2003. Kainate receptors and the induction of mossy fibre long-term potentiation. Philos Trans R Soc Lond B Biol Sci 358: 657-66

Bortolotto ZA, Nistico R, More JC, Jane DE, Collingridge GL. 2005. Kainate receptors and mossy fiber LTP. Neurotoxicology 26: 769-77

Boss BD, Peterson GM, Cowan WM. 1985. On the number of neurons in the dentate gyrus of the rat. Brain Res 338: 144-50

Boulter J, Hollmann M, O'Shea-Greenfield A, Hartley M, Deneris E, et al. 1990. Molecular cloning and functional expression of glutamate receptor subunit genes. Science 249: 1033-7

Bowie D, Garcia EP, Marshall J, Traynelis SF, Lange GD. 2003. Allosteric regulation and spatial distribution of kainate receptors bound to ancillary proteins. J Physiol 547: 373-85

Braithwaite SP, Xia H, Malenka RC. 2002. Differential roles for NSF and GRIP/ABP in AMPA receptor cycling. Proc Natl Acad Sci U S A 99: 7096-101

Bredt DS, Nicoll RA. 2003. AMPA receptor trafficking at excitatory synapses. Neuron 40: 361-79

Breustedt J, Schmitz D. 2004. Assessing the role of GLUK5 and GLUK6 at hippocampal mossy fiber synapses. J Neurosci 24: 10093-8

Breustedt J, Vogt KE, Miller RJ, Nicoll RA, Schmitz D. 2003. Alpha1E-containing Ca2+ channels are involved in synaptic plasticity. Proc Natl Acad Sci U S A 100: 12450-5

Brusa R, Zimmermann F, Koh DS, Feldmeyer D, Gass P, et al. 1995. Early-onset epilepsy and postnatal lethality associated with an editing-deficient GluR-B allele in mice. Science 270: 1677-80

Bureau I, Bischoff S, Heinemann SF, Mulle C. 1999. Kainate receptor-mediated responses in the CA1 field of wild-type and GluR6-deficient mice. J Neurosci 19: 653-63

Bureau I, Dieudonne S, Coussen F, Mulle C. 2000. Kainate receptor-mediated synaptic currents in cerebellar Golgi cells are not shaped by diffusion of glutamate. Proc Natl Acad Sci U S A 97: 6838-43

Burnashev N, Zhou Z, Neher E, Sakmann B. 1995. Fractional calcium currents through recombinant GluR channels of the NMDA, AMPA and kainate receptor subtypes. J Physiol 485 (Pt 2): 403-18

Caiati MD, Sivakumaran S, Cherubini E. 2010. In the developing rat hippocampus, endogenous activation of presynaptic kainate receptors reduces GABA release from mossy fiber terminals. J Neurosci 30: 1750-9

Campbell SL, Mathew SS, Hablitz JJ. 2007. Pre- and postsynaptic effects of kainate on layer II/III pyramidal cells in rat neocortex. Neuropharmacology 53: 37-47

Carter AG, Vogt KE, Foster KA, Regehr WG. 2002. Assessing the role of calcium-induced calcium release in short-term presynaptic plasticity at excitatory central synapses. J Neurosci 22: 21-8

Castillo PE, Janz R, Sudhof TC, Tzounopoulos T, Malenka RC, Nicoll RA. 1997a. Rab3A is essential for mossy fibre long-term potentiation in the hippocampus. Nature 388: 590-3

Castillo PE, Malenka RC, Nicoll RA. 1997b. Kainate receptors mediate a slow postsynaptic current in hippocampal CA3 neurons. Nature 388: 182-6

Castillo PE, Schoch S, Schmitz F, Sudhof TC, Malenka RC. 2002. RIM1alpha is required for presynaptic long-term potentiation. Nature 415: 327-30

Castillo PE, Weisskopf MG, Nicoll RA. 1994. The role of Ca2+ channels in hippocampal mossy fiber synaptic transmission and long-term potentiation. Neuron 12: 261-9

Catches JS, Xu J, Contractor A. 2012. Genetic ablation of the GluK4 kainate receptor subunit causes anxiolytic and antidepressant-like behavior in mice. Behav Brain Res 228: 406-14

Chamberland S, Evstratova A, Toth K. 2014. Interplay between synchronization of multivesicular release and recruitment of additional release sites support short-term facilitation at hippocampal mossy fiber to CA3 pyramidal cells synapses. J Neurosci 34: 11032-47

Chatterton JE, Awobuluyi M, Premkumar LS, Takahashi H, Talantova M, et al. 2002. Excitatory glycine receptors containing the NR3 family of NMDA receptor subunits. Nature 415: 793-8

Chen YL, Huang CC, Hsu KS. 2001. Time-dependent reversal of long-term potentiation by low-frequency stimulation at the hippocampal mossy fiber-CA3 synapses. J Neurosci 21: 3705-14

Chergui K, Bouron A, Normand E, Mulle C. 2000. Functional GluR6 kainate receptors in the striatum: indirect downregulation of synaptic transmission. J Neurosci 20: 2175-82

Chicurel ME, Harris KM. 1992. Three-dimensional analysis of the structure and composition of CA3 branched dendritic spines and their synaptic relationships with mossy fiber boutons in the rat hippocampus. J Comp Neurol 325: 169-82

Chittajallu R, Vignes M, Dev KK, Barnes JM, Collingridge GL, Henley JM. 1996. Regulation of glutamate release by presynaptic kainate receptors in the hippocampus. Nature 379: 78-81

Christensen JK, Paternain AV, Selak S, Ahring PK, Lerma J. 2004. A mosaic of functional kainate receptors in hippocampal interneurons. J Neurosci 24: 8986-93

Chung HJ, Xia J, Scannevin RH, Zhang X, Huganir RL. 2000. Phosphorylation of the AMPA receptor subunit GluR2 differentially regulates its interaction with PDZ domain-containing proteins. J Neurosci 20: 7258-67

Ciabarra AM, Sullivan JM, Gahn LG, Pecht G, Heinemann S, Sevarino KA. 1995. Cloning and characterization of chi-1: a developmentally regulated member of a novel class of the ionotropic glutamate receptor family. J Neurosci 15: 6498-508

Claiborne BJ, Amaral DG, Cowan WM. 1986. A light and electron microscopic analysis of the mossy fibers of the rat dentate gyrus. J Comp Neurol 246: 435-58

Clarke VR, Ballyk BA, Hoo KH, Mandelzys A, Pellizzari A, et al. 1997. A hippocampal GluR5 kainate receptor regulating inhibitory synaptic transmission. Nature 389: 599-603

Clarke VR, Collingridge GL. 2002. Characterisation of the effects of ATPA, a GLU(K5) receptor selective agonist, on excitatory synaptic transmission in area CA1 of rat hippocampal slices. Neuropharmacology 42: 889-902

Clarke VR, Collingridge GL. 2004. Characterisation of the effects of ATPA, a GLU(K5) kainate receptor agonist, on GABAergic synaptic transmission in the CA1 region of rat hippocampal slices. Neuropharmacology 47: 363-72

Clarke VR, Molchanova SM, Hirvonen T, Taira T, Lauri SE. 2014. Activity-dependent upregulation of presynaptic kainate receptors at immature CA3-CA1 synapses. J Neurosci 34: 16902-16

Coleman PA, Massey SC, Miller RF. 1986. Kynurenic acid distinguishes kainate and quisqualate receptors in the vertebrate retina. Brain Res 381: 172-5

Collingridge GL, Isaac JT, Wang YT. 2004. Receptor trafficking and synaptic plasticity. Nat Rev Neurosci 5: 952-62

Collingridge GL, Kehl SJ, McLennan H. 1983. Excitatory amino acids in synaptic transmission in the Schaffer collateral-commissural pathway of the rat hippocampus. J Physiol 334: 33-46

Conquet F, Bashir ZI, Davies CH, Daniel H, Ferraguti F, et al. 1994. Motor deficit and impairment of synaptic plasticity in mice lacking mGluR1. Nature 372: 237-43

Contractor A, Mulle C, Swanson GT. 2011. Kainate receptors coming of age: milestones of two decades of research. Trends Neurosci 34: 154-63

Contractor A, Sailer AW, Darstein M, Maron C, Xu J, et al. 2003. Loss of kainate receptor-mediated heterosynaptic facilitation of mossy-fiber synapses in KA2-/- mice. J Neurosci 23: 422-9

Contractor A, Swanson G, Heinemann SF. 2001. Kainate receptors are involved in short- and long-term plasticity at mossy fiber synapses in the hippocampus. Neuron 29: 209-16

Contractor A, Swanson GT, Sailer A, O'Gorman S, Heinemann SF. 2000. Identification of the kainate receptor subunits underlying modulation of excitatory synaptic transmission in the CA3 region of the hippocampus. J Neurosci 20: 8269-78

Copits BA, Robbins JS, Frausto S, Swanson GT. 2011. Synaptic targeting and functional modulation of GluK1 kainate receptors by the auxiliary neuropilin and tolloid-like (NETO) proteins. J Neurosci 31: 7334-40

Copits BA, Swanson GT. 2012. Dancing partners at the synapse: auxiliary subunits that shape kainate receptor function. Nat Rev Neurosci 13: 675-86

Cossart R, Epsztein J, Tyzio R, Becq H, Hirsch J, et al. 2002. Quantal release of glutamate generates pure kainate and mixed AMPA/kainate EPSCs in hippocampal neurons. Neuron 35: 147-59

Cossart R, Esclapez M, Hirsch JC, Bernard C, Ben-Ari Y. 1998. GluR5 kainate receptor activation in interneurons increases tonic inhibition of pyramidal cells. Nat Neurosci 1: 470-8

Coussen F, Perrais D, Jaskolski F, Sachidhanandam S, Normand E, et al. 2005. Co-assembly of two GluR6 kainate receptor splice variants within a functional protein complex. Neuron 47: 555-66

Craig AM, Blackstone CD, Huganir RL, Banker G. 1993. The distribution of glutamate receptors in cultured rat hippocampal neurons: postsynaptic clustering of AMPA-selective subunits. Neuron 10: 1055-68

Crowder TL, Weiner JL. 2002. Functional characterization of kainate receptors in the rat nucleus accumbens core region. J Neurophysiol 88: 41-8

Cunha RA, Constantino MD, Ribeiro JA. 1997. Inhibition of [3H] gamma-aminobutyric acid release by kainate receptor activation in rat hippocampal synaptosomes. Eur J Pharmacol 323: 167-72

Cunha RA, Malva JO, Ribeiro JA. 1999. Kainate receptors coupled to G(i)/G(o) proteins in the rat hippocampus. Mol Pharmacol 56: 429-33

Cunha RA, Malva JO, Ribeiro JA. 2000. Pertussis toxin prevents presynaptic inhibition by kainate receptors of rat hippocampal [(3)H]GABA release. FEBS Lett 469: 159-62

Dargan SL, Clarke VR, Alushin GM, Sherwood JL, Nistico R, et al. 2009. ACET is a highly potent and specific kainate receptor antagonist: characterisation and effects on hippocampal mossy fibre function. Neuropharmacology 56: 121-30

Darstein M, Petralia RS, Swanson GT, Wenthold RJ, Heinemann SF. 2003. Distribution of kainate receptor subunits at hippocampal mossy fiber synapses. J Neurosci 23: 8013-9

Das A, Wallace GCt, Holmes C, McDowell ML, Smith JA, et al. 2012. Hippocampal tissue of patients with refractory temporal lobe epilepsy is associated with astrocyte activation, inflammation, and altered expression of channels and receptors. Neuroscience 220: 237-46

Davila NG, Houpt TA, Trombley PQ. 2007. Expression and function of kainate receptors in the rat olfactory bulb. Synapse 61: 320-34

Daw MI, Chittajallu R, Bortolotto ZA, Dev KK, Duprat F, et al. 2000. PDZ proteins interacting with C-terminal GluR2/3 are involved in a PKC-dependent regulation of AMPA receptors at hippocampal synapses. Neuron 28: 873-86

Delaney AJ, Jahr CE. 2002. Kainate receptors differentially regulate release at two parallel fiber synapses. Neuron 36: 475-82

Dev KK, Nishimune A, Henley JM, Nakanishi S. 1999. The protein kinase C alpha binding protein PICK1 interacts with short but not long form alternative splice variants of AMPA receptor subunits. Neuropharmacology 38: 635-44

Dietrich D, Kirschstein T, Kukley M, Pereverzev A, von der Brelie C, et al. 2003. Functional Specialization of Presynaptic Cav2.3 Ca2+ Channels. Neuron 39: 483-96

Doherty JJ, Alagarsamy S, Bough KJ, Conn PJ, Dingledine R, Mott DD. 2004. Metabotropic glutamate receptors modulate feedback inhibition in a developmentally regulated manner in rat dentate gyrus. J Physiol 561: 395-401

Dolman NP, More JC, Alt A, Knauss JL, Pentikainen OT, et al. 2007. Synthesis and pharmacological characterization of N3-substituted willardiine derivatives: role of the substituent at the 5-position of the uracil ring in the development of highly potent and selective GLUK5 kainate receptor antagonists. J Med Chem 50: 1558-70

Domenici MR, Berretta N, Cherubini E. 1998. Two distinct forms of long-term depression coexist at the mossy fiber-CA3 synapse in the hippocampus during development. Proc Natl Acad Sci U S A 95: 8310-5

Donevan SD, Beg A, Gunther JM, Twyman RE. 1998. The methylglutamate, SYM 2081, is a potent and highly selective agonist at kainate receptors. J Pharmacol Exp Ther 285: 539-45

Donevan SD, Rogawski MA. 1998. Allosteric regulation of alpha-amino-3-hydroxy-5-methyl-4-isoxazole-propionate receptors by thiocyanate and cyclothiazide at a common modulatory site distinct from that of 2,3-benzodiazepines. Neuroscience 87: 615-29

Dong H, O'Brien RJ, Fung ET, Lanahan AA, Worley PF, Huganir RL. 1997. GRIP: a synaptic PDZ domain-containing protein that interacts with AMPA receptors. Nature 386: 279-84

Duan GF, Ye Y, Xu S, Tao W, Zhao S, et al. 2018. Signal peptide represses GluK1 surface and synaptic trafficking through binding to amino-terminal domain. Nat Commun 9: 4879

Egebjerg J, Bettler B, Hermans-Borgmeyer I, Heinemann S. 1991. Cloning of a cDNA for a glutamate receptor subunit activated by kainate but not AMPA. Nature 351: 745-8

Falcon-Moya R, Losada-Ruiz P, Sihra TS, Rodriguez-Moreno A. 2018. Cerebellar Kainate Receptor-Mediated Facilitation of Glutamate Release Requires Ca(2+)-Calmodulin and PKA. Front Mol Neurosci 11: 195

Fernandes HB, Catches JS, Petralia RS, Copits BA, Xu J, et al. 2009. High-affinity kainate receptor subunits are necessary for ionotropic but not metabotropic signaling. Neuron 63: 818-29

Fisahn A, Heinemann SF, McBain CJ. 2005. The kainate receptor subunit GluR6 mediates metabotropic regulation of the slow and medium AHP currents in mouse hippocampal neurones. J Physiol 562: 199-203

Fisher JL, Mott DD. 2013. Modulation of homomeric and heteromeric kainate receptors by the auxiliary subunit Neto1. J Physiol 591: 4711-24

Fisher JL. 2015. The auxiliary subunits Neto1 and Neto2 have distinct, subunit-dependent effects at recombinant GluK1- and GluK2-containing kainate receptors. Neuropharmacology 99: 471-80

Frerking M, Malenka RC, Nicoll RA. 1998. Synaptic activation of kainate receptors on hippocampal interneurons. Nat Neurosci 1: 479-86

Frerking M, Ohliger-Frerking P. 2002. AMPA receptors and kainate receptors encode different features of afferent activity. J Neurosci 22: 7434-43

Frerking M, Schmitz D, Zhou Q, Johansen J, Nicoll RA. 2001. Kainate receptors depress excitatory synaptic transmission at CA3-->CA1 synapses in the hippocampus via a direct presynaptic action. J Neurosci 21: 2958-66

Gaarskjaer FB. 1978. Organization of the mossy fiber system of the rat studied in extended hippocampi. I. Terminal area related to number of granule and pyramidal cells. J Comp Neurol 178: 49-72

Gallyas F, Ball SM, Molnar E. 2003. Assembly and cell surface expression of KA-2 subunit-containing kainate receptors. Journal of Neurochemistry 86: 1414-27

Ganong AH, Lanthorn TH, Cotman CW. 1983. Kynurenic acid inhibits synaptic and acidic amino acid-induced responses in the rat hippocampus and spinal cord. Brain Res 273: 170-4

Garcia EP, Mehta S, Blair LA, Wells DG, Shang J, et al. 1998. SAP90 binds and clusters kainate receptors causing incomplete desensitization. Neuron 21: 727-39

Glatt CE, Snyder SH. 1993. Cloning and expression of an adenylyl cyclase localized to the corpus striatum. Nature 361: 536-8

Greger IH, Khatri L, Ziff EB. 2002. RNA editing at arg607 controls AMPA receptor exit from the endoplasmic reticulum. Neuron 34: 759-72

Gregor P, O'Hara BF, Yang X, Uhl GR. 1993. Expression and novel subunit isoforms of glutamate receptor genes GluR5 and GluR6. Neuroreport 4: 1343-6
Griffith WH. 1990. Voltage-clamp analysis of posttetanic potentiation of the mossy fiber to CA3 synapse in hippocampus. J Neurophysiol 63: 491-501
Hagena H, Manahan-Vaughan D. 2011. Learning-facilitated synaptic plasticity at CA3 mossy fiber and commissural-associational synapses reveals different roles in information processing. Cereb Cortex 21: 2442-9
Hagena H, Manahan-Vaughan D. 2015. mGlu5 acts as a switch for opposing forms of synaptic plasticity at mossy fiber-CA3 and commissural associational-CA3 synapses. J Neurosci 35: 4999-5006
Hamlyn LH. 1962. The fine structure of the mossy fibre endings in the hippocampus of the rabbit. J Anat 96: 112-20
Harris EW, Cotman CW. 1986. Long-term potentiation of guinea pig mossy fiber responses is not blocked by N-methyl D-aspartate antagonists. Neurosci Lett 70: 132-7
Haug FM. 1967. Electron microscopical localization of the zinc in hippocampal mossy fibre synapses by a modified sulfide silver procedure. Histochemie 8: 355-68
Hayes DM, Braud S, Hurtado DE, McCallum J, Standley S, et al. 2003. Trafficking and surface expression of the glutamate receptor subunit, KA2. Biochemical and Biophysical Research Communications 310: 8-13
Heckmann M, Bufler J, Franke C, Dudel J. 1996. Kinetics of homomeric GluR6 glutamate receptor channels. Biophys J 71: 1743-50
Henze DA, Urban NN, Barrionuevo G. 1997. Origin of the apparent asynchronous activity of hippocampal mossy fibers. J Neurophysiol 78: 24-30
Henze DA, Urban NN, Barrionuevo G. 2000. The multifarious hippocampal mossy fiber pathway: a review. Neuroscience 98: 407-27
Herb A, Burnashev N, Werner P, Sakmann B, Wisden W, Seeburg PH. 1992. The KA-2 subunit of excitatory amino acid receptors shows widespread expression in brain and forms ion channels with distantly related subunits. Neuron 8: 775-85
Hollmann M, Boulter J, Maron C, Beasley L, Sullivan J, et al. 1993. Zinc potentiates agonist-induced currents at certain splice variants of the NMDA receptor. Neuron 10: 943-54
Hollmann M, O'Shea-Greenfield A, Rogers SW, Heinemann S. 1989. Cloning by functional expression of a member of the glutamate receptor family. Nature 342: 643-8
Hsia AY, Salin PA, Castillo PE, Aiba A, Abeliovich A, et al. 1995. Evidence against a role for metabotropic glutamate receptors in mossy fiber LTP: the use of mutant mice and pharmacological antagonists. Neuropharmacology 34: 1567-72
Huang YY, Kandel ER, Varshavsky L, Brandon EP, Qi M, et al. 1995. A genetic test of the effects of mutations in PKA on mossy fiber LTP and its relation to spatial and contextual learning. Cell 83: 1211-22
Huang YY, Li XC, Kandel ER. 1994. cAMP contributes to mossy fiber LTP by initiating both a covalently mediated early phase and macromolecular synthesis-dependent late phase. Cell 79: 69-79
Huang YZ, Pan E, Xiong ZQ, McNamara JO. 2008. Zinc-mediated transactivation of TrkB potentiates the hippocampal mossy fiber-CA3 pyramid synapse. Neuron 57: 546-58
Ibrahim HM, Hogg AJ, Jr., Healy DJ, Haroutunian V, Davis KL, Meador-Woodruff JH. 2000. Ionotropic glutamate receptor binding and subunit mRNA expression in thalamic nuclei in schizophrenia. Am J Psychiatry 157: 1811-23
Ishii T, Moriyoshi K, Sugihara H, Sakurada K, Kadotani H, et al. 1993. Molecular characterization of the family of the N-methyl-D-aspartate receptor subunits. J Biol Chem 268: 2836-43
Ishizuka N, Cowan WM, Amaral DG. 1995. A quantitative analysis of the dendritic organization of pyramidal cells in the rat hippocampus. J Comp Neurol 362: 17-45

Ishizuka N, Weber J, Amaral DG. 1990. Organization of intrahippocampal projections originating from CA3 pyramidal cells in the rat. J Comp Neurol 295: 580-623

Ito I, Sugiyama H. 1991. Roles of glutamate receptors in long-term potentiation at hippocampal mossy fiber synapses. Neuroreport 2: 333-6

Jaffe D, Johnston D. 1990. Induction of long-term potentiation at hippocampal mossy-fiber synapses follows a Hebbian rule. J Neurophysiol 64: 948-60

Jane DE, Hoo K, Kamboj R, Deverill M, Bleakman D, Mandelzys A. 1997. Synthesis of willardiine and 6-azawillardiine analogs: pharmacological characterization on cloned homomeric human AMPA and kainate receptor subtypes. J Med Chem 40: 3645-50

Jaskolski F, Coussen F, Nagarajan N, Normand E, Rosenmund C, Mulle C. 2004. Subunit composition and alternative splicing regulate membrane delivery of kainate receptors. J Neurosci 24: 2506-15

Jaskolski F, Normand E, Mulle C, Coussen F. 2005. Differential trafficking of GluR7 kainate receptor subunit splice variants. J Biol Chem 280: 22968-76

Jia Y, Jeng JM, Sensi SL, Weiss JH. 2002. Zn2+ currents are mediated by calcium-permeable AMPA/kainate channels in cultured murine hippocampal neurones. J Physiol 543: 35-48

Johnson JW, Ascher P. 1987. Glycine potentiates the NMDA response in cultured mouse brain neurons. Nature 325: 529-31

Jones KA, Wilding TJ, Huettner JE, Costa AM. 1997. Desensitization of kainate receptors by kainate, glutamate and diastereomers of 4-methylglutamate. Neuropharmacology 36: 853-63

Jouhanneau JS, Ball SM, Molnar E, Isaac JT. 2011. Mechanisms of bi-directional modulation of thalamocortical transmission in barrel cortex by presynaptic kainate receptors. Neuropharmacology 60: 832-41

Jung MW, McNaughton BL. 1993. Spatial selectivity of unit activity in the hippocampal granular layer. Hippocampus 3: 165-82

Kaczor AA, Wrobel T, Kronbach C, Unverferth K, Stachal T, Matosiuk D. 2015. Synthesis and molecular docking of novel non-competitive antagonists of GluK2 receptor. Med Chem Res 24: 810-17

Kakegawa W, Tsuzuki K, Yoshida Y, Kameyama K, Ozawa S. 2004. Input- and subunit-specific AMPA receptor trafficking underlying long-term potentiation at hippocampal CA3 synapses. Eur J Neurosci 20: 101-10

Kamiya H, Ozawa S, Manabe T. 2002. Kainate receptor-dependent short-term plasticity of presynaptic Ca2+ influx at the hippocampal mossy fiber synapses. J Neurosci 22: 9237-43

Kamiya H, Shinozaki H, Yamamoto C. 1996. Activation of metabotropic glutamate receptor type 2/3 suppresses transmission at rat hippocampal mossy fibre synapses. J Physiol 493 (Pt 2): 447-55

Kamiya H. 2002. Kainate receptor-dependent presynaptic modulation and plasticity. Neurosci Res 42: 1-6

Kapur A, Yeckel MF, Gray R, Johnston D. 1998. L-Type calcium channels are required for one form of hippocampal mossy fiber LTP. J Neurophysiol 79: 2181-90

Keinanen K, Wisden W, Sommer B, Werner P, Herb A, et al. 1990. A family of AMPA-selective glutamate receptors. Science 249: 556-60

Kessler M, Terramani T, Lynch G, Baudry M. 1989. A glycine site associated with N-methyl-D-aspartic acid receptors: characterization and identification of a new class of antagonists. J Neurochem 52: 1319-28

Kidd FL, Coumis U, Collingridge GL, Crabtree JW, Isaac JT. 2002. A presynaptic kainate receptor is involved in regulating the dynamic properties of thalamocortical synapses during development. Neuron 34: 635-46

Kidd FL, Isaac JT. 1999. Developmental and activity-dependent regulation of kainate receptors at thalamocortical synapses. Nature 400: 569-73

Kleckner NW, Dingledine R. 1988. Requirement for glycine in activation of NMDA-receptors expressed in Xenopus oocytes. Science 241: 835-7

Ko S, Zhao MG, Toyoda H, Qiu CS, Zhuo M. 2005. Altered behavioral responses to noxious stimuli and fear in glutamate receptor 5 (GluR5)- or GluR6-deficient mice. J Neurosci 25: 977-84

Kobayashi K, Manabe T, Takahashi T. 1996. Presynaptic long-term depression at the hippocampal mossy fiber-CA3 synapse. Science 273: 648-50

Kohler M, Burnashev N, Sakmann B, Seeburg PH. 1993. Determinants of Ca2+ permeability in both TM1 and TM2 of high affinity kainate receptor channels: diversity by RNA editing. Neuron 10: 491-500

Kohler M, Kornau HC, Seeburg PH. 1994. The organization of the gene for the functionally dominant alpha-amino-3-hydroxy-5-methylisoxazole-4-propionic acid receptor subunit GluR-B. J Biol Chem 269: 17367-70

Kolleker A, Zhu JJ, Schupp BJ, Qin Y, Mack V, et al. 2003. Glutamatergic plasticity by synaptic delivery of GluR-B(long)-containing AMPA receptors. Neuron 40: 1199-212

Krogsgaard-Larsen P, Hansen JJ, Lauridsen J, Peet MJ, Leah JD, Curtis DR. 1982. Glutamic acid agonists. Stereochemical and conformational studies of DL-alpha-amino-3-hydroxy-5-methyl-4-isoxazolepropionic acid (AMPA) and related compounds. Neurosci Lett 31: 313-7

Kwon HB, Castillo PE. 2008a. Long-term potentiation selectively expressed by NMDA receptors at hippocampal mossy fiber synapses. Neuron 57: 108-20

Kwon HB, Castillo PE. 2008b. Role of glutamate autoreceptors at hippocampal mossy fiber synapses. Neuron 60: 1082-94

Laezza F, Wilding TJ, Sequeira S, Coussen F, Zhang XZ, et al. 2007. KRIP6: a novel BTB/kelch protein regulating function of kainate receptors. Mol Cell Neurosci 34: 539-50

Langdon RB, Johnson JW, Barrionuevo G. 1993. Asynchrony of mossy fibre inputs and excitatory postsynaptic currents in rat hippocampus. J Physiol 472: 157-76

Langdon RB, Johnson JW, Barrionuevo G. 1995. Posttetanic potentiation and presynaptically induced long-term potentiation at the mossy fiber synapse in rat hippocampus. J Neurobiol 26: 370-85

Laube B, Hirai H, Sturgess M, Betz H, Kuhse J. 1997. Molecular determinants of agonist discrimination by NMDA receptor subunits: analysis of the glutamate binding site on the NR2B subunit. Neuron 18: 493-503

Lauri SE, Bortolotto ZA, Bleakman D, Ornstein PL, Lodge D, et al. 2001a. A critical role of a facilitatory presynaptic kainate receptor in mossy fiber LTP. Neuron 32: 697-709

Lauri SE, Bortolotto ZA, Nistico R, Bleakman D, Ornstein PL, et al. 2003. A Role for Ca2+ Stores in Kainate Receptor-Dependent Synaptic Facilitation and LTP at Mossy Fiber Synapses in the Hippocampus. Neuron 39: 327-41

Lauri SE, Delany C, VR JC, Bortolotto ZA, Ornstein PL, et al. 2001b. Synaptic activation of a presynaptic kainate receptor facilitates AMPA receptor-mediated synaptic transmission at hippocampal mossy fibre synapses. Neuropharmacology 41: 907-15

Lauri SE, Segerstrale M, Vesikansa A, Maingret F, Mulle C, et al. 2005. Endogenous activation of kainate receptors regulates glutamate release and network activity in the developing hippocampus. J Neurosci 25: 4473-84

Lauri SE, Vesikansa A, Segerstrale M, Collingridge GL, Isaac JT, Taira T. 2006. Functional maturation of CA1 synapses involves activity-dependent loss of tonic kainate receptor-mediated inhibition of glutamate release. Neuron 50: 415-29

Lauridsen J, Honore T, Krogsgaard-Larsen P. 1985. Ibotenic acid analogues. Synthesis, molecular flexibility, and in vitro activity of agonists and antagonists at central glutamic acid receptors. J Med Chem 28: 668-72

Lawrence JJ, McBain CJ. 2003. Interneuron diversity series: containing the detonation--feedforward inhibition in the CA3 hippocampus. Trends Neurosci 26: 631-40

Leeson PD, Baker R, Carling RW, Curtis NR, Moore KW, et al. 1991. Kynurenic acid derivatives. Structure-activity relationships for excitatory amino acid antagonism and identification of potent and selective antagonists at the glycine site on the N-methyl-D-aspartate receptor. J Med Chem 34: 1243-52

Lei S, Pelkey KA, Topolnik L, Congar P, Lacaille JC, McBain CJ. 2003. Depolarization-induced long-term depression at hippocampal mossy fiber-CA3 pyramidal neuron synapses. J Neurosci 23: 9786-95

Lein ES, Callaway EM, Albright TD, Gage FH. 2005. Redefining the boundaries of the hippocampal CA2 subfield in the mouse using gene expression and 3-dimensional reconstruction. J Comp Neurol 485: 1-10

Leonard AS, Davare MA, Horne MC, Garner CC, Hell JW. 1998. SAP97 is associated with the alpha-amino-3-hydroxy-5-methylisoxazole-4-propionic acid receptor GluR1 subunit. J Biol Chem 273: 19518-24

Lerma J, Marques JM. 2013. Kainate receptors in health and disease. Neuron 80: 292-311

Lerma J, Paternain AV, Naranjo JR, Mellstrom B. 1993. Functional kainate-selective glutamate receptors in cultured hippocampal neurons. Proc Natl Acad Sci U S A 90: 11688-92

Li H, Chen A, Xing G, Wei ML, Rogawski MA. 2001. Kainate receptor-mediated heterosynaptic facilitation in the amygdala. Nat Neurosci 4: 612-20

Li H, Rogawski MA. 1998. GluR5 kainate receptor mediated synaptic transmission in rat basolateral amygdala in vitro. Neuropharmacology 37: 1279-86

Li JM, Zeng YJ, Peng F, Li L, Yang TH, et al. 2010. Aberrant glutamate receptor 5 expression in temporal lobe epilepsy lesions. Brain Res 1311: 166-74

Li Y, Hough CJ, Frederickson CJ, Sarvey JM. 2001. Induction of mossy fiber --> Ca3 long-term potentiation requires translocation of synaptically released Zn2+. J Neurosci 21: 8015-25

Liang Y, Yuan LL, Johnston D, Gray R. 2002. Calcium signaling at single mossy fiber presynaptic terminals in the rat hippocampus. J Neurophysiol 87: 1132-7

Lisman JE. 1999. Relating hippocampal circuitry to function: recall of memory sequences by reciprocal dentate-CA3 interactions. Neuron 22: 233-42

Lomash RM, Sheng N, Li Y, Nicoll RA, Roche KW. 2017. Phosphorylation of the kainate receptor (KAR) auxiliary subunit Neto2 at serine 409 regulates synaptic targeting of the KAR subunit GluK1. J Biol Chem 292: 15369-77

Lorente De Nó R. 1934. Studies on the structure of the cerebral cortex. II. Continuation of the study of the ammonic system. Journal für Psychologie und Neurologie 46: 113-77

Loscher W, Lehmann H, Behl B, Seemann D, Teschendorf HJ, et al. 1999. A new pyrrolyl-quinoxalinedione series of non-NMDA glutamate receptor antagonists: pharmacological characterization and comparison with NBQX and valproate in the kindling model of epilepsy. Eur J Neurosci 11: 250-62

Lowry ER, Kruyer A, Norris EH, Cederroth CR, Strickland S. 2013. The GluK4 kainate receptor subunit regulates memory, mood, and excitotoxic neurodegeneration. Neuroscience 235: 215-25

Lu W, Ziff EB. 2005. PICK1 interacts with ABP/GRIP to regulate AMPA receptor trafficking. Neuron 47: 407-21

Lyon L, Borel M, Carrion M, Kew JN, Corti C, et al. 2011. Hippocampal mossy fiber long-term depression in Grm2/3 double knockout mice. Synapse 65: 945-54

Maccaferri G, Toth K, McBain CJ. 1998. Target-specific expression of presynaptic mossy fiber plasticity. Science 279: 1368-70

Maeda T, Kaneko S, Akaike A, Satoh M. 1997. Direct evidence for increase in excitatory amino acids release during mossy fiber LTP in rat hippocampal slices as revealed by the patch sensor methods. Neurosci Lett 224: 103-6

Mah SJ, Cornell E, Mitchell NA, Fleck MW. 2005. Glutamate receptor trafficking: endoplasmic reticulum quality control involves ligand binding and receptor function. J Neurosci 25: 2215-25

Malenka RC, Bear MF. 2004. LTP and LTD: an embarrassment of riches. Neuron 44: 5-21

Martoglio B, Dobberstein B. 1998. Signal sequences: more than just greasy peptides. Trends Cell Biol 8: 410-5

Matsuda K, Budisantoso T, Mitakidis N, Sugaya Y, Miura E, et al. 2016. Transsynaptic Modulation of Kainate Receptor Functions by C1q-like Proteins. Neuron 90: 752-67

Matsuda K, Kamiya Y, Matsuda S, Yuzaki M. 2002. Cloning and characterization of a novel NMDA receptor subunit NR3B: a dominant subunit that reduces calcium permeability. Brain Res Mol Brain Res 100: 43-52

Matsuda S, Mikawa S, Hirai H. 1999. Phosphorylation of serine-880 in GluR2 by protein kinase C prevents its C terminus from binding with glutamate receptor-interacting protein. J Neurochem 73: 1765-8

Mauceri D, Cattabeni F, Di Luca M, Gardoni F. 2004. Calcium/calmodulin-dependent protein kinase II phosphorylation drives synapse-associated protein 97 into spines. J Biol Chem 279: 23813-21

May AP, Whiteheart SW, Weis WI. 2001. Unraveling the mechanism of the vesicle transport ATPase NSF, the N-ethylmaleimide-sensitive factor. J Biol Chem 276: 21991-4

Mayer ML, Ghosal A, Dolman NP, Jane DE. 2006. Crystal structures of the kainate receptor GluR5 ligand binding core dimer with novel GluR5-selective antagonists. J Neurosci 26: 2852-61

Mayer ML, Westbrook GL. 1987. Permeation and block of N-methyl-D-aspartic acid receptor channels by divalent cations in mouse cultured central neurones. J Physiol 394: 501-27

McHugh TJ, Jones MW, Quinn JJ, Balthasar N, Coppari R, et al. 2007. Dentate gyrus NMDA receptors mediate rapid pattern separation in the hippocampal network. Science 317: 94-9

McIlhinney RA, Le Bourdelles B, Molnar E, Tricaud N, Streit P, Whiting PJ. 1998. Assembly intracellular targeting and cell surface expression of the human N-methyl-D-aspartate receptor subunits NR1a and NR2A in transfected cells. Neuropharmacology 37: 1355-67

McIlhinney RA, Molnar E, Atack JR, Whiting PJ. 1996. Cell surface expression of the human N-methyl-D-aspartate receptor subunit 1a requires the co-expression of the NR2A subunit in transfected cells. Neuroscience 70: 989-97

McNaughton BL, Morris RGM. 1987. Hippocampal synaptic enhancement and information storage within a distributed memory system. Elsevier Publications 10: 408-15

Mellor J, Nicoll RA. 2001. Hippocampal mossy fiber LTP is independent of postsynaptic calcium. Nat Neurosci 4: 125-6

Melyan Z, Lancaster B, Wheal HV. 2004. Metabotropic regulation of intrinsic excitability by synaptic activation of kainate receptors. J Neurosci 24: 4530-4

Melyan Z, Wheal HV, Lancaster B. 2002. Metabotropic-mediated kainate receptor regulation of IsAHP and excitability in pyramidal cells. Neuron 34: 107-14
Mercer A, Trigg HL, Thomson AM. 2007. Characterization of neurons in the CA2 subfield of the adult rat hippocampus. J Neurosci 27: 7329-38
Micheau J, Vimeney A, Normand E, Mulle C, Riedel G. 2014. Impaired hippocampus-dependent spatial flexibility and sociability represent autism-like phenotypes in GluK2 mice. Hippocampus 24: 1059-69
Michishita M, Ikeda T, Nakashiba T, Ogawa M, Tashiro K, et al. 2003. A novel gene, Btcl1, encoding CUB and LDLa domains is expressed in restricted areas of mouse brain. Biochemical and Biophysical Research Communications 306: 680-86
Michishita M, Ikeda T, Nakashiba T, Ogawa M, Tashiro K, et al. 2004. Expression of Btcl2, a novel member of Btcl gene family, during development of the central nervous system. Brain Res Dev Brain Res 153: 135-42
Midorikawa M, Sakaba T. 2017. Kinetics of Releasable Synaptic Vesicles and Their Plastic Changes at Hippocampal Mossy Fiber Synapses. Neuron 96: 1033-40 e3
Milanesi E, Bonvicini C, Congiu C, Bortolomasi M, Gainelli G, et al. 2015. The role of GRIK4 gene in treatment-resistant depression. Genet Res (Camb) 97: e14
Miller LP, Johnson AE, Gelhard RE, Insel TR. 1990. The ontogeny of excitatory amino acid receptors in the rat forebrain--II. Kainic acid receptors. Neuroscience 35: 45-51
Min MY, Rusakov DA, Kullmann DM. 1998. Activation of AMPA, kainate, and metabotropic receptors at hippocampal mossy fiber synapses: role of glutamate diffusion. Neuron 21: 561-70
Mistry R, Dennis S, Frerking M, Mellor JR. 2011. Dentate gyrus granule cell firing patterns can induce mossy fiber long-term potentiation in vitro. Hippocampus 21: 1157-68
Moloney MG. 1998. Excitatory amino acids. Nat Prod Rep 15: 205-19
Monaghan DT, Cotman CW. 1982. The distribution of [3H]kainic acid binding sites in rat CNS as determined by autoradiography. Brain Res 252: 91-100
Monaghan DT, Cotman CW. 1985. Distribution of N-methyl-D-aspartate-sensitive L-[3H]glutamate-binding sites in rat brain. J Neurosci 5: 2909-19
Monyer H, Burnashev N, Laurie DJ, Sakmann B, Seeburg PH. 1994. Developmental and regional expression in the rat brain and functional properties of four NMDA receptors. Neuron 12: 529-40
Monyer H, Sprengel R, Schoepfer R, Herb A, Higuchi M, et al. 1992. Heteromeric NMDA receptors: molecular and functional distinction of subtypes. Science 256: 1217-21
Moore KA, Nicoll RA, Schmitz D. 2003. Adenosine gates synaptic plasticity at hippocampal mossy fiber synapses. Proc Natl Acad Sci U S A 100: 14397-402
More JC, Nistico R, Dolman NP, Clarke VR, Alt AJ, et al. 2004. Characterisation of UBP296: a novel, potent and selective kainate receptor antagonist. Neuropharmacology 47: 46-64
Moriyoshi K, Masu M, Ishii T, Shigemoto R, Mizuno N, Nakanishi S. 1991. Molecular cloning and characterization of the rat NMDA receptor. Nature 354: 31-7
Mosbacher J, Schoepfer R, Monyer H, Burnashev N, Seeburg PH, Ruppersberg JP. 1994. A molecular determinant for submillisecond desensitization in glutamate receptors. Science 266: 1059-62
Mothet JP, Parent AT, Wolosker H, Brady RO, Jr., Linden DJ, et al. 2000. D-serine is an endogenous ligand for the glycine site of the N-methyl-D-aspartate receptor. Proc Natl Acad Sci U S A 97: 4926-31
Mukherjee S, Manahan-Vaughan D. 2013. Role of metabotropic glutamate receptors in persistent forms of hippocampal plasticity and learning. Neuropharmacology 66: 65-81

Mulle C, Sailer A, Perez-Otano I, Dickinson-Anson H, Castillo PE, et al. 1998. Altered synaptic physiology and reduced susceptibility to kainate-induced seizures in GluR6-deficient mice. Nature 392: 601-5

Mulle C, Sailer A, Swanson GT, Brana C, O'Gorman S, et al. 2000. Subunit composition of kainate receptors in hippocampal interneurons. Neuron 28: 475-84

Nadler JV. 1981. Minireview. Kainic acid as a tool for the study of temporal lobe epilepsy. Life Sci 29: 2031-42

Negrete-Diaz JV, Duque-Feria P, Andrade-Talavera Y, Carrion M, Flores G, Rodriguez-Moreno A. 2012. Kainate receptor-mediated depression of glutamatergic transmission involving protein kinase A in the lateral amygdala. J Neurochem 121: 36-43

Ng D, Pitcher GM, Szilard RK, Sertie A, Kanisek M, et al. 2009. Neto1 is a novel CUB-domain NMDA receptor-interacting protein required for synaptic plasticity and learning. PLoS Biol 7: e41

Nicholls RE, Zhang XL, Bailey CP, Conklin BR, Kandel ER, Stanton PK. 2006. mGluR2 acts through inhibitory Galpha subunits to regulate transmission and long-term plasticity at hippocampal mossy fiber-CA3 synapses. Proc Natl Acad Sci U S A 103: 6380-5

Nicoll RA, Schmitz D. 2005. Synaptic plasticity at hippocampal mossy fibre synapses. Nat Rev Neurosci 6: 863-76

Nistico R, Dargan SL, Amici M, Collingridge GL, Bortolotto ZA. 2011. Synergistic interactions between kainate and mGlu receptors regulate bouton Ca signalling and mossy fibre LTP. Sci Rep 1: 103

Orav E, Atanasova T, Shintyapina A, Kesaf S, Kokko M, et al. 2017. NETO1 Guides Development of Glutamatergic Connectivity in the Hippocampus by Regulating Axonal Kainate Receptors. eNeuro 4

Pachernegg S, Strutz-Seebohm N, Hollmann M. 2012. GluN3 subunit-containing NMDA receptors: not just one-trick ponies. Trends Neurosci 35: 240-9

Paddock S, Laje G, Charney D, Rush AJ, Wilson AF, et al. 2007. Association of GRIK4 with outcome of antidepressant treatment in the STAR*D cohort. Am J Psychiatry 164: 1181-8

Palay SL, Chan-Palay V. 1974. Cerebellar Cortex. Springer-Verlag Berlin Heidelberg

Pan E, Zhang XA, Huang Z, Krezel A, Zhao M, et al. 2011. Vesicular zinc promotes presynaptic and inhibits postsynaptic long-term potentiation of mossy fiber-CA3 synapse. Neuron 71: 1116-26

Papouin T, Ladepeche L, Ruel J, Sacchi S, Labasque M, et al. 2012. Synaptic and extrasynaptic NMDA receptors are gated by different endogenous coagonists. Cell 150: 633-46

Park P, Sanderson TM, Amici M, Choi SL, Bortolotto ZA, et al. 2016. Calcium-Permeable AMPA Receptors Mediate the Induction of the Protein Kinase A-Dependent Component of Long-Term Potentiation in the Hippocampus. J Neurosci 36: 622-31

Partin KM, Bowie D, Mayer ML. 1995. Structural determinants of allosteric regulation in alternatively spliced AMPA receptors. Neuron 14: 833-43

Paschen W, Schmitt J, Dux E, Djuricic B. 1995. Temporal analysis of the upregulation of GluR5 mRNA editing with age: regional evaluation. Brain Res Dev Brain Res 86: 359-63

Paternain AV, Herrera MT, Nieto MA, Lerma J. 2000. GluR5 and GluR6 kainate receptor subunits coexist in hippocampal neurons and coassemble to form functional receptors. J Neurosci 20: 196-205

Paternain AV, Morales M, Lerma J. 1995. Selective antagonism of AMPA receptors unmasks kainate receptor-mediated responses in hippocampal neurons. Neuron 14: 185-9

Pei W, Huang Z, Wang C, Han Y, Park JS, Niu L. 2009. Flip and flop: a molecular determinant for AMPA receptor channel opening. Biochemistry 48: 3767-77

Perkins MN, Stone TW. 1982. An iontophoretic investigation of the actions of convulsant kynurenines and their interaction with the endogenous excitant quinolinic acid. Brain Res 247: 184-7

Perrais D, Pinheiro PS, Jane DE, Mulle C. 2009. Antagonism of recombinant and native GluK3-containing kainate receptors. Neuropharmacology 56: 131-40

Petralia RS, Wang YX, Niedzielski AS, Wenthold RJ. 1996. The metabotropic glutamate receptors, mGluR2 and mGluR3, show unique postsynaptic, presynaptic and glial localizations. Neuroscience 71: 949-76

Petralia RS, Wang YX, Wenthold RJ. 1994. Histological and ultrastructural localization of the kainate receptor subunits, KA2 and GluR6/7, in the rat nervous system using selective antipeptide antibodies. J Comp Neurol 349: 85-110

Pickard BS, Malloy MP, Christoforou A, Thomson PA, Evans KL, et al. 2006. Cytogenetic and genetic evidence supports a role for the kainate-type glutamate receptor gene, GRIK4, in schizophrenia and bipolar disorder. Mol Psychiatry 11: 847-57

Pinheiro PS, Lanore F, Veran J, Artinian J, Blanchet C, et al. 2013. Selective block of postsynaptic kainate receptors reveals their function at hippocampal mossy fiber synapses. Cereb Cortex 23: 323-31

Pinheiro PS, Perrais D, Coussen F, Barhanin J, Bettler B, et al. 2007. GluR7 is an essential subunit of presynaptic kainate autoreceptors at hippocampal mossy fiber synapses. Proc Natl Acad Sci U S A 104: 12181-6

Pinheiro PS, Rodrigues RJ, Rebola N, Xapelli S, Oliveira CR, Malva JO. 2005. Presynaptic kainate receptors are localized close to release sites in rat hippocampal synapses. Neurochem Int 47: 309-16

Qian J, Noebels JL. 2005. Visualization of transmitter release with zinc fluorescence detection at the mouse hippocampal mossy fibre synapse. J Physiol 566: 747-58

Ramón y Cajal S, Swanson N, Swanson LW. 1909, 1911, 1995. Histology of the nervous system of man and vertebrates. Oxford University Press

Randle JC, Guet T, Bobichon C, Moreau C, Curutchet P, et al. 1992. Quinoxaline derivatives: structure-activity relationships and physiological implications of inhibition of N-methyl-D-aspartate and non-N-methyl-D-aspartate receptor-mediated currents and synaptic potentials. Mol Pharmacol 41: 337-45

Rapp PR, Gallagher M. 1996. Preserved neuron number in the hippocampus of aged rats with spatial learning deficits. Proc Natl Acad Sci U S A 93: 9926-30

Rebola N, Carta M, Lanore F, Blanchet C, Mulle C. 2011. NMDA receptor-dependent metaplasticity at hippocampal mossy fiber synapses. Nat Neurosci 14: 691-3

Rebola N, Lujan R, Cunha RA, Mulle C. 2008. Adenosine A2A receptors are essential for long-term potentiation of NMDA-EPSCs at hippocampal mossy fiber synapses. Neuron 57: 121-34

Regehr WG, Delaney KR, Tank DW. 1994. The role of presynaptic calcium in short-term enhancement at the hippocampal mossy fiber synapse. J Neurosci 14: 523-37

Reid CA, Dixon DB, Takahashi M, Bliss TV, Fine A. 2004. Optical quantal analysis indicates that long-term potentiation at single hippocampal mossy fiber synapses is expressed through increased release probability, recruitment of new release sites, and activation of silent synapses. J Neurosci 24: 3618-26

Ren Z, Riley NJ, Garcia EP, Sanders JM, Swanson GT, Marshall J. 2003. Multiple trafficking signals regulate kainate receptor KA2 subunit surface expression. J Neurosci 23: 6608-16

Represa A, Dessi F, Beaudoin M, Ben-Ari Y. 1991. Effects of neonatal gamma-ray irradiation on rat hippocampus--I. Postnatal maturation of hippocampal cells. Neuroscience 42: 137-50

Represa A, Tremblay E, Ben-Ari Y. 1987. Kainate binding sites in the hippocampal mossy fibers: localization and plasticity. Neuroscience 20: 739-48

Robain O, Barbin G, Billette de Villemeur T, Jardin L, Jahchan T, Ben-Ari Y. 1994. Development of mossy fiber synapses in hippocampal slice culture. Brain Res Dev Brain Res 80: 244-50

Rodriguez-Moreno A, Lerma J. 1998. Kainate receptor modulation of GABA release involves a metabotropic function. Neuron 20: 1211-8

Rodriguez-Moreno A, Sihra TS. 2004. Presynaptic kainate receptor facilitation of glutamate release involves protein kinase A in the rat hippocampus. J Physiol 557: 733-45

Rodriguez-Moreno A, Sihra TS. 2013. Presynaptic kainate receptor-mediated facilitation of glutamate release involves Ca2+-calmodulin and PKA in cerebrocortical synaptosomes. FEBS Lett 587: 788-92

Ruiz A, Sachidhanandam S, Utvik JK, Coussen F, Mulle C. 2005. Distinct subunits in heteromeric kainate receptors mediate ionotropic and metabotropic function at hippocampal mossy fiber synapses. J Neurosci 25: 11710-8

Sailer A, Swanson GT, Perez-Otano I, O'Leary L, Malkmus SA, et al. 1999. Generation and analysis of GluR5(Q636R) kainate receptor mutant mice. J Neurosci 19: 8757-64

Salin PA, Scanziani M, Malenka RC, Nicoll RA. 1996. Distinct short-term plasticity at two excitatory synapses in the hippocampus. Proc Natl Acad Sci U S A 93: 13304-9

Sallert M, Malkki H, Segerstrale M, Taira T, Lauri SE. 2007. Effects of the kainate receptor agonist ATPA on glutamatergic synaptic transmission and plasticity during early postnatal development. Neuropharmacology 52: 1354-65

San Antonio A, Liban K, Ikrar T, Tsyganovskiy E, Xu X. 2014. Distinct physiological and developmental properties of hippocampal CA2 subfield revealed by using anti-Purkinje cell protein 4 (PCP4) immunostaining. J Comp Neurol 522: 1333-54

Sans N, Racca C, Petralia RS, Wang YX, McCallum J, Wenthold RJ. 2001. Synapse-associated protein 97 selectively associates with a subset of AMPA receptors early in their biosynthetic pathway. J Neurosci 21: 7506-16

Sasaki YF, Rothe T, Premkumar LS, Das S, Cui J, et al. 2002. Characterization and comparison of the NR3A subunit of the NMDA receptor in recombinant systems and primary cortical neurons. J Neurophysiol 87: 2052-63

Scanziani M, Salin PA, Vogt KE, Malenka RC, Nicoll RA. 1997. Use-dependent increases in glutamate concentration activate presynaptic metabotropic glutamate receptors. Nature 385: 630-4

Schiavini P, Dawe GB, Bowie D, Moitessier N. 2015. Discovery of novel small-molecule antagonists for GluK2. Bioorg Med Chem Lett 25: 2416-20

Schiffer HH, Swanson GT, Heinemann SF. 1997. Rat GluR7 and a carboxy-terminal splice variant, GluR7b, are functional kainate receptor subunits with a low sensitivity to glutamate. Neuron 19: 1141-6

Schmitt J, Dux E, Gissel C, Paschen W. 1996. Regional analysis of developmental changes in the extent of GluR6 mRNA editing in rat brain. Brain Res Dev Brain Res 91: 153-7

Schmitz D, Frerking M, Nicoll RA. 2000. Synaptic activation of presynaptic kainate receptors on hippocampal mossy fiber synapses. Neuron 27: 327-38

Schmitz D, Mellor J, Breustedt J, Nicoll RA. 2003. Presynaptic kainate receptors impart an associative property to hippocampal mossy fiber long-term potentiation. Nat Neurosci 6: 1058-63

Schmitz D, Mellor J, Frerking M, Nicoll RA. 2001a. Presynaptic kainate receptors at hippocampal mossy fiber synapses. Proc Natl Acad Sci U S A 98: 11003-8

Schmitz D, Mellor J, Nicoll RA. 2001b. Presynaptic kainate receptor mediation of frequency facilitation at hippocampal mossy fiber synapses. Science 291: 1972-6

Schoppa NE. 2006. AMPA/kainate receptors drive rapid output and precise synchrony in olfactory bulb granule cells. J Neurosci 26: 12996-3006

Scott R, Lalic T, Kullmann DM, Capogna M, Rusakov DA. 2008. Target-cell specificity of kainate autoreceptor and Ca2+-store-dependent short-term plasticity at hippocampal mossy fiber synapses. J Neurosci 28: 13139-49

Scoville WB, Milner B. 1957. Loss of recent memory after bilateral hippocampal lesions. J Neurol Neurosurg Psychiatry 20: 11-21

Sensi SL, Canzoniero LM, Yu SP, Ying HS, Koh JY, et al. 1997. Measurement of intracellular free zinc in living cortical neurons: routes of entry. J Neurosci 17: 9554-64

Sheng M, Cummings J, Roldan LA, Jan YN, Jan LY. 1994. Changing subunit composition of heteromeric NMDA receptors during development of rat cortex. Nature 368: 144-7

Sheng N, Shi YS, Lomash RM, Roche KW, Nicoll RA. 2015. Neto auxiliary proteins control both the trafficking and biophysical properties of the kainate receptor GluK1. Elife 4

Sheng N, Shi YS, Nicoll RA. 2017. Amino-terminal domains of kainate receptors determine the differential dependence on Neto auxiliary subunits for trafficking. Proc Natl Acad Sci U S A 114: 1159-64

Sherwood JL, Amici M, Dargan SL, Culley GR, Fitzjohn SM, et al. 2012. Differences in kainate receptor involvement in hippocampal mossy fibre long-term potentiation depending on slice orientation. Neurochem Int 61: 482-9

Shigemoto R, Kinoshita A, Wada E, Nomura S, Ohishi H, et al. 1997. Differential presynaptic localization of metabotropic glutamate receptor subtypes in the rat hippocampus. J Neurosci 17: 7503-22

Shin RM, Tully K, Li Y, Cho JH, Higuchi M, et al. 2010. Hierarchical order of coexisting pre- and postsynaptic forms of long-term potentiation at synapses in amygdala. Proc Natl Acad Sci U S A 107: 19073-8

Slomianka L. 1992. Neurons of origin of zinc-containing pathways and the distribution of zinc-containing boutons in the hippocampal region of the rat. Neuroscience 48: 325-52

Small B, Thomas J, Kemp M, Hoo K, Ballyk B, et al. 1998. LY339434, a GluR5 kainate receptor agonist. Neuropharmacology 37: 1261-7

Sobolevsky AI. 2013. Structure and gating of tetrameric glutamate receptors. J Physiol 593: 29-38

Sommer B, Burnashev N, Verdoorn TA, Keinanen K, Sakmann B, Seeburg PH. 1992. A glutamate receptor channel with high affinity for domoate and kainate. EMBO J 11: 1651-6

Sommer B, Keinanen K, Verdoorn TA, Wisden W, Burnashev N, et al. 1990. Flip and flop: a cell-specific functional switch in glutamate-operated channels of the CNS. Science 249: 1580-5

Soriano E, Frotscher M. 1994. Mossy cells of the rat fascia dentata are glutamate-immunoreactive. Hippocampus 4: 65-9

Srivastava S, Osten P, Vilim FS, Khatri L, Inman G, et al. 1998. Novel anchorage of GluR2/3 to the postsynaptic density by the AMPA receptor-binding protein ABP. Neuron 21: 581-91

Stensbol TB, Borre L, Johansen TN, Egebjerg J, Madsen U, et al. 1999. Resolution, absolute stereochemistry and molecular pharmacology of the enantiomers of ATPA. Eur J Pharmacol 380: 153-62

Stone TW. 2000. Development and therapeutic potential of kynurenic acid and kynurenine derivatives for neuroprotection. Trends Pharmacol Sci 21: 149-54

Straub C, Hunt DL, Yamasaki M, Kim KS, Watanabe M, et al. 2011. Distinct functions of kainate receptors in the brain are determined by the auxiliary subunit Neto1. Nat Neurosci 14: 866-73

Suzuki E, Okada T. 2010. Group I metabotropic glutamate receptors are involved in TEA-induced long-term potentiation at mossy fiber-CA3 synapses in the rat hippocampus. Brain Res 1313: 45-52

Swanson GT, Feldmeyer D, Kaneda M, Cull-Candy SG. 1996. Effect of RNA editing and subunit co-assembly single-channel properties of recombinant kainate receptors. J Physiol 492 (Pt 1): 129-42

Swanson GT, Gereau RWt, Green T, Heinemann SF. 1997a. Identification of amino acid residues that control functional behavior in GluR5 and GluR6 kainate receptors. Neuron 19: 913-26

Swanson GT, Green T, Heinemann SF. 1998. Kainate receptors exhibit differential sensitivities to (S)-5-iodowillardiine. Mol Pharmacol 53: 942-9

Swanson GT, Green T, Sakai R, Contractor A, Che W, et al. 2002. Differential activation of individual subunits in heteromeric kainate receptors. Neuron 34: 589-98

Swanson GT, Kamboj SK, Cull-Candy SG. 1997b. Single-channel properties of recombinant AMPA receptors depend on RNA editing, splice variation, and subunit composition. J Neurosci 17: 58-69

Swanson LW, Wyss JM, Cowan WM. 1978. An autoradiographic study of the organization of intrahippocampal association pathways in the rat. J Comp Neurol 181: 681-715

Takeda A, Kanno S, Sakurada N, Ando M, Oku N. 2008. Attenuation of hippocampal mossy fiber long-term potentiation by low micromolar concentrations of zinc. J Neurosci Res 86: 2906-11

Tanabe Y, Masu M, Ishii T, Shigemoto R, Nakanishi S. 1992. A family of metabotropic glutamate receptors. Neuron 8: 169-79

Tanabe Y, Nomura A, Masu M, Shigemoto R, Mizuno N, Nakanishi S. 1993. Signal transduction, pharmacological properties, and expression patterns of two rat metabotropic glutamate receptors, mGluR3 and mGluR4. J Neurosci 13: 1372-8

Tang M, Pelkey KA, Ng D, Ivakine E, McBain CJ, et al. 2011. Neto1 is an auxiliary subunit of native synaptic kainate receptors. J Neurosci 31: 10009-18

Tong G, Malenka RC, Nicoll RA. 1996. Long-term potentiation in cultures of single hippocampal granule cells: a presynaptic form of plasticity. Neuron 16: 1147-57

Toth K, Suares G, Lawrence JJ, Philips-Tansey E, McBain CJ. 2000. Differential mechanisms of transmission at three types of mossy fiber synapse. J Neurosci 20: 8279-89

Tzounopoulos T, Janz R, Sudhof TC, Nicoll RA, Malenka RC. 1998. A role for cAMP in long-term depression at hippocampal mossy fiber synapses. Neuron 21: 837-45

Urban NN, Barrionuevo G. 1996. Induction of hebbian and non-hebbian mossy fiber long-term potentiation by distinct patterns of high-frequency stimulation. J Neurosci 16: 4293-9

Valluru L, Xu J, Zhu Y, Yan S, Contractor A, Swanson GT. 2005. Ligand binding is a critical requirement for plasma membrane expression of heteromeric kainate receptors. J Biol Chem 280: 6085-93

Vesikansa A, Sakha P, Kuja-Panula J, Molchanova S, Rivera C, et al. 2012. Expression of GluK1c underlies the developmental switch in presynaptic kainate receptor function. Sci Rep 2: 310

Vignes M, Clarke VR, Parry MJ, Bleakman D, Lodge D, et al. 1998. The GluR5 subtype of kainate receptor regulates excitatory synaptic transmission in areas CA1 and CA3 of the rat hippocampus. Neuropharmacology 37: 1269-77

Vignes M, Collingridge GL. 1997. The synaptic activation of kainate receptors. Nature 388: 179-82

Villacres EC, Wong ST, Chavkin C, Storm DR. 1998. Type I adenylyl cyclase mutant mice have impaired mossy fiber long-term potentiation. J Neurosci 18: 3186-94

Vissel B, Royle GA, Christie BR, Schiffer HH, Ghetti A, et al. 2001. The role of RNA editing of kainate receptors in synaptic plasticity and seizures. Neuron 29: 217-27

Vogt K, Mellor J, Tong G, Nicoll R. 2000. The actions of synaptically released zinc at hippocampal mossy fiber synapses. Neuron 26: 187-96

Wafford KA, Kathoria M, Bain CJ, Marshall G, Le Bourdelles B, et al. 1995. Identification of amino acids in the N-methyl-D-aspartate receptor NR1 subunit that contribute to the glycine binding site. Mol Pharmacol 47: 374-80

Wallis JL, Irvine MW, Jane DE, Lodge D, Collingridge GL, Bortolotto ZA. 2015. An interchangeable role for kainate and metabotropic glutamate receptors in the induction of rat hippocampal mossy fiber long-term potentiation in vivo. Hippocampus 25: 1407-17

Wang H, Pineda VV, Chan GC, Wong ST, Muglia LJ, Storm DR. 2003. Type 8 adenylyl cyclase is targeted to excitatory synapses and required for mossy fiber long-term potentiation. J Neurosci 23: 9710-8

Wang H, Storm DR. 2003. Calmodulin-regulated adenylyl cyclases: cross-talk and plasticity in the central nervous system. Mol Pharmacol 63: 463-8

Wang J, Yeckel MF, Johnston D, Zucker RS. 2004. Photolysis of postsynaptic caged Ca2+ can potentiate and depress mossy fiber synaptic responses in rat hippocampal CA3 pyramidal neurons. J Neurophysiol 91: 1596-607

Watanabe M, Fukaya M, Sakimura K, Manabe T, Mishina M, Inoue Y. 1998. Selective scarcity of NMDA receptor channel subunits in the stratum lucidum (mossy fibre-recipient layer) of the mouse hippocampal CA3 subfield. Eur J Neurosci 10: 478-87

Watkins JC, Evans RH. 1981. Excitatory amino acid transmitters. Annu Rev Pharmacol Toxicol 21: 165-204

Weisskopf MG, Castillo PE, Zalutsky RA, Nicoll RA. 1994. Mediation of hippocampal mossy fiber long-term potentiation by cyclic AMP. Science 265: 1878-82

Weisskopf MG, Nicoll RA. 1995. Presynaptic changes during mossy fibre LTP revealed by NMDA receptor-mediated synaptic responses. Nature 376: 256-9

Wenthold RJ, Petralia RS, Blahos J, II, Niedzielski AS. 1996. Evidence for multiple AMPA receptor complexes in hippocampal CA1/CA2 neurons. J Neurosci 16: 1982-9

Wenthold RJ, Trumpy VA, Zhu WS, Petralia RS. 1994. Biochemical and assembly properties of GluR6 and KA2, two members of the kainate receptor family, determined with subunit-specific antibodies. J Biol Chem 269: 1332-9

Wenzel HJ, Buckmaster PS, Anderson NL, Wenzel ME, Schwartzkroin PA. 1997. Ultrastructural localization of neurotransmitter immunoreactivity in mossy cell axons and their synaptic targets in the rat dentate gyrus. Hippocampus 7: 559-70

Werner P, Voigt M, Keinanen K, Wisden W, Seeburg PH. 1991. Cloning of a putative high-affinity kainate receptor expressed predominantly in hippocampal CA3 cells. Nature 351: 742-4

West JR. 1983. Distal infrapyramidal and longitudinal mossy fibers at a midtemporal hippocampal level. Brain Res Bull 10: 137-46

West MJ, Slomianka L, Gundersen HJ. 1991. Unbiased stereological estimation of the total number of neurons in thesubdivisions of the rat hippocampus using the optical fractionator. Anat Rec 231: 482-97

Wilding TJ, Huettner JE. 1995. Differential antagonism of alpha-amino-3-hydroxy-5-methyl-4-isoxazolepropionic acid-preferring and kainate-preferring receptors by 2,3-benzodiazepines. Mol Pharmacol 47: 582-7

Wilding TJ, Huettner JE. 1997. Activation and desensitization of hippocampal kainate receptors. J Neurosci 17: 2713-21

Williams S, Johnston D. 1989. Long-term potentiation of hippocampal mossy fiber synapses is blocked by postsynaptic injection of calcium chelators. Neuron 3: 583-8

Wisden W, Seeburg PH. 1993. A complex mosaic of high-affinity kainate receptors in rat brain. J Neurosci 13: 3582-98

Wolosker H. 2007. NMDA receptor regulation by D-serine: new findings and perspectives. Mol Neurobiol 36: 152-64

Wong LA, Mayer ML, Jane DE, Watkins JC. 1994. Willardiines differentiate agonist binding sites for kainate- versus AMPA-preferring glutamate receptors in DRG and hippocampal neurons. J Neurosci 14: 3881-97

Wu H, Nash JE, Zamorano P, Garner CC. 2002. Interaction of SAP97 with minus-end-directed actin motor myosin VI. Implications for AMPA receptor trafficking. J Biol Chem 277: 30928-34

Wu ZL, Thomas SA, Villacres EC, Xia Z, Simmons ML, et al. 1995. Altered behavior and long-term potentiation in type I adenylyl cyclase mutant mice. Proc Natl Acad Sci U S A 92: 220-4

Wyeth MS, Pelkey KA, Petralia RS, Salter MW, McInnes RR, McBain CJ. 2014. Neto auxiliary protein interactions regulate kainate and NMDA receptor subunit localization at mossy fiber-CA3 pyramidal cell synapses. J Neurosci 34: 622-8

Xia J, Zhang X, Staudinger J, Huganir RL. 1999. Clustering of AMPA receptors by the synaptic PDZ domain-containing protein PICK1. Neuron 22: 179-87

Xia ZG, Refsdal CD, Merchant KM, Dorsa DM, Storm DR. 1991. Distribution of mRNA for the calmodulin-sensitive adenylate cyclase in rat brain: expression in areas associated with learning and memory. Neuron 6: 431-43

Xie X, Smart TG. 1994. Modulation of long-term potentiation in rat hippocampal pyramidal neurons by zinc. Pflugers Arch 427: 481-6

Yeckel MF, Kapur A, Johnston D. 1999. Multiple forms of LTP in hippocampal CA3 neurons use a common postsynaptic mechanism. Nat Neurosci 2: 625-33

Yokoi M, Kobayashi K, Manabe T, Takahashi T, Sakaguchi I, et al. 1996. Impairment of hippocampal mossy fiber LTD in mice lacking mGluR2. Science 273: 645-7

Yoshino M, Sawada S, Yamamoto C, Kamiya H. 1996. A metabotropic glutamate receptor agonist DCG-IV suppresses synaptic transmission at mossy fiber pathway of the guinea pig hippocampus. Neurosci Lett 207: 70-2

Zalutsky RA, Nicoll RA. 1990. Comparison of two forms of long-term potentiation in single hippocampal neurons. Science 248: 1619-24

Zhang W, St-Gelais F, Grabner CP, Trinidad JC, Sumioka A, et al. 2009. A transmembrane accessory subunit that modulates kainate-type glutamate receptors. Neuron 61: 385-96

Zukin RS, Bennett MV. 1995. Alternatively spliced isoforms of the NMDARI receptor subunit. Trends Neurosci 18: 306-13